Biochemical Characterization and Genetic Modeling of Glioma-Associated Mutations in Isocitrate Dehydrogenases

by

Giselle Y. López

Department of Pathology
Duke University

Date:_____

Approved:

_____
Hai Yan, Supervisor

_____
Roger McLendon

_____
Robin Bachelder

_____
Jeffrey Rathmell

_____
Salvatore Pizzo

Dissertation submitted in partial
fulfillment of the requirements for the degree
of Doctor of Philosophy in the Department of
Pathology in the Graduate School
of Duke University

2012

ABSTRACT

Biochemical Characterization and Genetic Modeling of Glioma-Associated Mutations in Isocitrate Dehydrogenases

by

Giselle Y. López

Department of Pathology
Duke University

Date:_____

Approved:

_____
Hai Yan, Supervisor

_____
Roger McLendon

_____
Robin Bachelder

_____
Jeffrey Rathmell

_____
Salvatore Pizzo

An abstract of a dissertation submitted in partial fulfillment of the requirements for the degree of Doctor of Philosophy in the Department of Pathology in the Graduate School of Duke University

2012

Abstract

Gliomas are the most common tumors of the central nervous system. Our lab recently identified mutations in *IDH1* and *IDH2* as occurring frequently in progressive gliomas. We applied a series of biochemical and genetic approaches to explore the roles of the mutations in tumors and generate models for study.

IDH1/2 normally function to convert isocitrate to α-ketoglutarate while simultaneously converting $NADP^+$ to NADPH. To assess changes in metabolism, we completed metabolic profiling and complementary studies in cell lines with and without mutant *IDH1* or mutant *IDH2*. We identified a decrease in hypoxia signaling and a decrease in global 5-hydroxymethylcytosine levels in cell lines with mutant *IDH1/2.*

Having observed mutations in *IDH1/2* in a large fraction of progressive gliomas, we asked if the mutations were either 1) advantageous for growth in brain parenchyma, or 2) advantageous in a particular cell-of-origin. Sequencing of a series of metastases to the brain from non-central nervous system tumors identified no mutations in *IDH1/2*, lending less credence to the first hypothesis. To elucidate whether mutations in *IDH1/2* can initiate glioma progression and explore the potential cell-of-origin for progressive gliomas, we generated mice in which we induced expression of mutant *IDH2* in various populations of cells in the brain, either alone or in combination with *TP53* deletion, another frequently altered gene in progressive gliomas. Mice with broad expression of mutant *IDH2* developed hydrocephalus and encephalomalacia early in life, but did not develop tumors. Therefore, we restricted expression, and two brain tumors were identified in mice with both *IDH2* mutation and *TP53* deletion. While this suggests that both mutations might be required for the development of tumors, this is too small a number to draw significant conclusions. Further research with an expanded cohort of

mice, utilization of additional drivers of expression, and further characterization of identified tumors will help in elucidating the role of mutant *IDH2* and the cell-of-origin for progressive gliomas.

Dedication

This thesis is dedicated in loving memory to Manuel López Reinante and Migdalia Mendez López.

Contents

List of Tables

List of Figures

Acknowledgements

Many people have played a critical role in generating the data shown in this paper. First and foremost, I need to thank Hai Yan for allowing me to join his lab and pursue, for his mentorship and guidance, and for allowing me to design and pursue projects of my own choosing.

A huge thanks is necessary for the entire Preston Robert Tisch Brain Tumor Center. They not only provided resources, but also mentorship, and assistance with developing projects. Many thanks to Lisa Ehringer and Diane Satterfield for their help with acquiring tumor samples for studies, and the use of the microtome so that I could generate my slides. Thanks for Scott Szafranski for his help in attempting to purify IDH1 for biochemical assays, and to Dr. Chien-Tsun Kuan for his assistance in setting up those studies. Thanks to Cathy Wang for tackling a number of new mouse studies head on and for being a source of cheeriness within the lab. And for free-food Fridays! Thanks to Patrick Killela for teaching me the premises of basic techniques for genetic studies and expression studies. Thanks to Matthew Wortham for teaching the basics of mouse techniques. Thanks to Zachary Reitman for his help in interpreting metabolic profiling studies. Thanks for Christopher Duncan for suggestions in the design of many of my experiments. Thanks to Genglin Jin to teaching me basic cell culture techniques and always being so polite and willing to share in both his space and his time. Thanks to Paula Greer for being such a key source of sanity in the last few months of my studies, and for tackling a large amount of the mouse work head-on so as to make my schedule easier. Thanks to Christopher Pirozzi for taking on half of the mouse work and ES cell work. Thanks to James Burchette for teaching me everything I know about

immunohistochemistry and antibody optimization. Thanks to Ling Wang for allowing me to use his imager for slides to generate an electronic record. Thanks to Yuki Kato for teaching me techniques of Western blotting, thus improving the techniques of the whole lab. Thanks also to Ivan Spasojevic and Ping Fan at the Duke University Cancer Center Clinical Pharmacology Lab for assistance with analysis of 2-HG in both cell lines and tissue samples.

Thanks to Gerard Smith for taking such exceedingly excellent care of my mice, and for making sure they stay spoiled with immaculate spaces and extra enrichment far beyond the requirements set by IACUC and DLAR, and for always bringing a smile to my day.

I also need to thank my entire Thesis Committee not only for their guidance on my thesis, but also for their help with both the design and completion of specific critical experiments. Thanks to Robin Bachelder for her help in setting up and designing studies involving hypoxia signaling. Thanks for Jeffrey Rathmell for help in planning studies for unexpected mouse phenotypes, and for finding new ways of utilizing my genetic mice for other studies. Thanks to Salvatore Pizzo for his unwavering support, mentorship, and feedback on both my studies and my career throughout my time at Duke. Thanks for Roger E. McLendon also for taking me under his wing, and for his critical assistance with interpreting histological results and planning further studies, and especially for revealing to me my true calling in life through both his example and his patience.

Thanks also goes to my entire family, and especially my parents Pablo and Vivian López, for their support of my decision to enter into a dual-degree program, and their patience while I continued to remain in school. I also would like to thank my sisters Jackelyn López-Roshwalb and Jeannette García for their unwavering support. My

thanks also belongs to my fiancé, Thomas Cowart, for being a source of emotional support and sanity throughout my grad school career. Thanks also to all my friends (you know who you are, and I apologize that I can't include everyone in here), but especially Erin Wilfong, Emma Neff, Loren Riskin, and Allison Betof for making sure that I remained healthy, happy, and well-fed.

All copyrighted material or published material was reproduced according to the policies laid out by the journal and rights retained by the authors for *Nature* (Koivunen et al., 2012[2]) and *Biochemical and Biophysical Research Communications* (Lopez et al., 2010[1]). Permission was received for inclusion of materials from the Encyclopedia of Life Sciences (Lopez et al., 2011[3]) Details are provided in Appendix A.

This research was supported by funding from the Duke Medical Scientist Training Program Training Grant T32-GM00717-34 and by the National Institutes of Health National Cancer Institute Grants R01CA118822-01 and R01CA140316-02S1 Supplement (Yan, H.), the James S. McDonnell Foundation, the Pediatric Brain Tumor Foundation Institute, the Intramural Research Programs of the National Human Genome Research Institute and the National Cancer Institute and National Institutes of Health.

1. Alterations in Gliomas (based in part of Brain Tumors, ELS 2011)[3]

1.1. Genetic Alterations in Astrocytomas

Astrocytomas are the most common neoplasms of the central nervous system. Their name is derived from their appearance to astrocytes, cells in the brain that serve a wide variety of functions, including regulating signaling molecules between neurons. Astrocytomas are categorized as grade I-IV tumors using the 2007 WHO classification system[4] based on histological appearance and historical survival. Histological grading is based on features such as the presence or absence of nuclear atypia, mitotic activity, vascular proliferation, endothelial hyperplasia, and necrosis. Genetic studies have identified a number of genetic alterations and mutations that correlate with various types and grades of tumors (Table 1).

Pilocytic astrocytomas are the lowest grade astrocytomas, and do not progress to higher-grade tumors. These tumors occur largely in children and adolescents. Pilocytic astrocytomas are genetically distinct from higher-grade tumors. Among the most frequent changes is gain of copy number at 7q34,[5] occurring in over two-thirds of pilocytic astrocytomas. Genetic studies have led to the identification of frequent gene rearrangement or mutation of *BRAF,*[6] leading to constitutive activation of BRAF.

Table 1: Common Genetic Abnormalities in Astrocytomas.

Tumor and WHO grade	Chromosomal abnormality	Genetic alteration
Grade I Pilocytic Astrocytoma	7q34 amplification	*BRAF/KIAA fusion*
Grade II Diffuse Astrocytoma	–17p13.1	*TP53* mutation
	Overexpression	*PDGFR*
	Mutation	*ATRX*
	Mutation	*IDH1/2*
Grade III Anaplastic Astrocytoma	–9p21	*CDKN2A* deletion
	–13q	*RB*1 mutation
	–17p	*TP53* mutation
	Overexpression	*EGFR*
	Mutation	*ATRX*
	Mutation	*IDH1/2*
Grade IV Secondary Glioblastoma	–17p	*TP53* mutation
	–10q23-25	*PTEN* mutation (rare)
	–19q	Unknown
	Mutation	*ATRX*
	Mutation	*IDH1/2*
Grade IV, Primary Glioblastoma	–9p21	*CDKN2A*/*B*, ARF deletion
	–10q23-25	*PTEN* mutation
	+7p	EGFR and/or EGFR variant III amplification, Sec61
	Protein hyperexpression	*EGFR* hyperexpression

PGDFR: platelet derived-growth factor receptor; EGFR: epidermal growth factor receptor

Unlike pilocytic astrocytomas, diffuse astrocytomas (WHO grade II) occur predominantly in adult patients in their third to fourth decades of life. Diffuse astrocytomas are slow-growing, diffusely infiltrating neoplasms. Histologically, diffuse astrocytomas comprise cells with an astrocytic appearance, which exhibit well-formed fibrillar processes and mild nuclear atypia.[7] Unlike higher-grade gliomas, diffuse astrocytomas do not contain features associated with aggressive tumors, such as mitotic figures, endothelial hyperplasia, and necrosis. Anaplastic astrocytomas (WHO grade III) are diffusely infiltrative tumors. Over time anaplastic astrocytomas almost universally progress to a higher grade tumor.

Grade IV astrocytoma is the highest grade astrocytoma and also referred to as glioblastoma multiforme (GBM). GBMs can be subdivided into primary and secondary GBM. Primary GBM appears *de novo*, with no prior history of a lower grade astrocytoma. It is the most common form of GBM, representing over 90% of GBMs.[7] Secondary GBM develops following a prior diagnosis of a lower grade astrocytoma, which progressed over time to GBM.[7] Despite a similar histopathology, primary and secondary GBM each comprise a distinct combination of genetic changes and tend to occur in distinct populations. While patients with primary GBM are usually over 60 years old, patients with secondary GBM average 45 years of age at diagnosis.[8] Combined, Grade II, Grade III, and secondary Grade IV astrocytomas are collectively referred to as progressive astrocytomas, and are distinct from primary GBM.

The importance of understanding the genetic differences in GBM tumors from different patients is becoming increasingly clear, as genetic differences between tumors may more accurately predict prognosis than histological differences alone.[9,10]

Genetically, a series of mutations are commonly associated with progressive astrocytomas, the most common being mutations in isocitrate dehydrogenase 1 (IDH1) at residue 132 or isocitrate dehydrogenase 2 (IDH2) at the analogous residue R172; 60-90% of diffuse astrocytomas have mutations in one of these genes.[11-19] As with Grade II astrocytomas, mutations in $IDH1^{R132}$ or $IDH2^{R172}$ are identified in 60-90% of Grade III astrocytomas, making this the most common genetic abnormality identified in these tumors. These mutations will be discussed in further detail later.

In progressive astrocytomas, the number of mutations increases as tumor grade increases. This may be associated with increased aggressiveness and the observed lower survival rates as tumor grade increases. Mutations or alterations in the Rb1 pathway (Figure 1) increase with tumor grade.[20-22] Although rare in Grade II astrocytomas, homozygous deletion of *CDKN2A*, homozygous deletion of *RB1*, or amplification of *CDK4* is present in one third of Grade III astrocytomas and two thirds of Grade IV astrocytomas (GBM).[21]

The *CDKN2A* locus is frequently deleted in a homozygous manner in progressive astrocytomas. 10-25% of anaplastic astrocytomas[20,21,23] and 38-52% of GBM tumors (not divided by type) have homozygous deletion of this locus.[20,21,23,24] Tumors with heterozygous deletion often have a mutation on the remaining *CDKN2A* locus, thus still inactivating the gene.[20,21,23,24] Frequently, secondary GBMs with deletion of this locus do not demonstrate the deletion in the corresponding lower grade tumor.[25] These results suggest that there is a strong selective pressure for deletion or inactivation of this region, and that this inactivation may be associated with tumor progression.

Rates of loss of heterozygosity (LOH) at the *RB1* locus increase with tumor grade and are associated with Grade IV glioblastomas,[20,21] being present in

approximately 45% of all GBMs.[21,26] However, other alterations are observed more frequently in lower grade tumors; *CDK4* amplification is present in 8% of anaplastic astrocytomas[20] and 6-34% of GBM tumors.[20,22,24,27,28] Amplification of *CDK4* occurs in about half of GBM samples without *CDKN2A* deletion.[22] Mutations of *RB1* or *CDKN2A*, and amplification of *CDK4* are often mutually exclusive.[20,27]

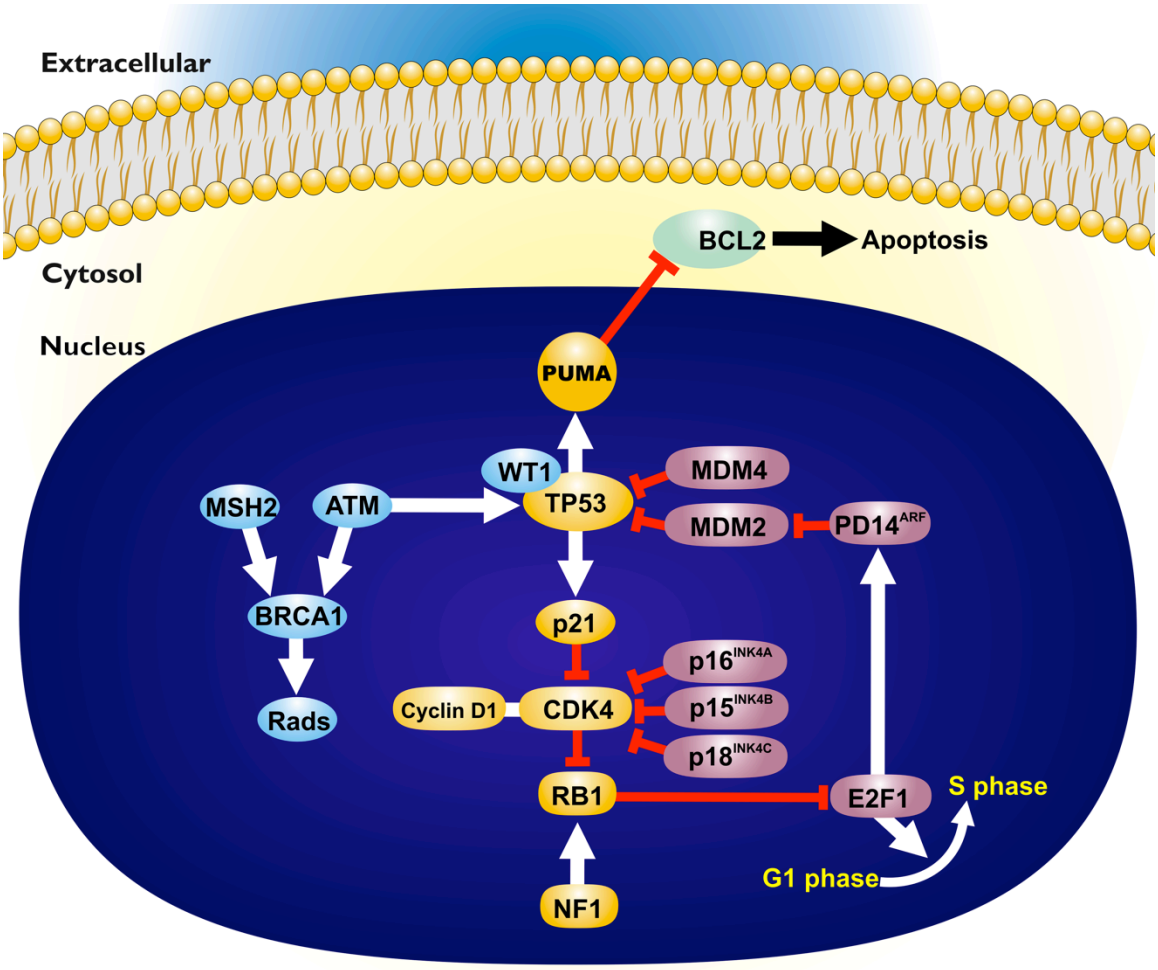

Figure 1: TP53 and Rb pathways (reprinted with permission)[3]

Other mutations commonly identified in progressive gliomas include mutation and/or deletion of *tumor protein p53* (*Li–Fraumeni syndrome*) (*TP53*).[29] Mutations in *TP53* tend to cluster around the DNA binding domain[24] and appear to be an early event in secondary GBM; a study of low-grade astrocytomas identified *TP53* mutations in 65%-75% of low-grade astrocytoma (Grade II) samples.[20,30] In addition, one study found that for each secondary GBM containing *TP53* mutations, the corresponding lower grade astrocytoma also contained the same mutation.[25] Interestingly, although mutations in *TP53* occur in approximately 60% of secondary GBM,[8,31] their frequency is much lower in primary GBM, occurring in approximately 30% of primary GBMs.[8,20,24,31-35] Although primary GBMs do not frequently have mutations in *TP53*, they often have mutations in other genes in the same pathway, with 60-70% of GBM having mutations somewhere in the p53 pathway[24,32] (Figure 1).

In various studies of brain tumor samples, up to 27% of Grade III astrocytomas or GBMs contained mutations in *PIK3CA.*[24,32,36-39] PIK3CA is a subunit of PI3K, and its activation leads to increased cell proliferation, survival, and migration. Activating *PIK3CA* mutations have been found to occur more often in younger patients with high-grade astrocytomas; this population also has a higher frequency of secondary than primary GBM.[37] It is likely that *PIK3CA* mutations tend to occur secondarily in the development of glioblastoma, rather than as an initiating factor.[37] Additionally, although *PTEN* loss is identified in a significant fraction of primary GBMs, it is rarely seen in lower grade astrocytomas.[40,41]

Mutations in *alpha-thalassemia/mental retardation X-linked* (*ATRX*) were recently identified in approximately 7% of GBM.[42] Further studies identified mutation in *ATRX* in over half of progressive astrocytomas of all grades,[43,44] suggesting that this

may be a key feature of progressive gliomas. Interestingly, a majority of oligoastrocytomas (tumors with a mixed histology sharing features of both astrocytomas and oligodendrogliomas) also demonstrate mutations in *ATRX*, although oligodendrogliomas do not.[43,44] Mutations in *ATRX* occur largely in tumors with *IDH1/2* mutations and *TP53* mutations.[43,44] ATRX was first found to play a role in pancreatic tumors and, in these tumors, led to alternative lengthening of telomeres.[42] It appears that *ATRX* may play a similar role in gliomas.[43,45]

Overexpression of platelet-derived growth factor A (PDGFA) and its receptor is also a common feature in progressive astrocytomas.[46] Although PDGF is only occasionally amplified,[24] PDGF and its receptors are upregulated in progressive gliomas and primary GBM at a high frequency, increasing with tumor grade.[47-50] Of note, overexpression of PDGFRα is correlated with *TP53* mutation.[30]

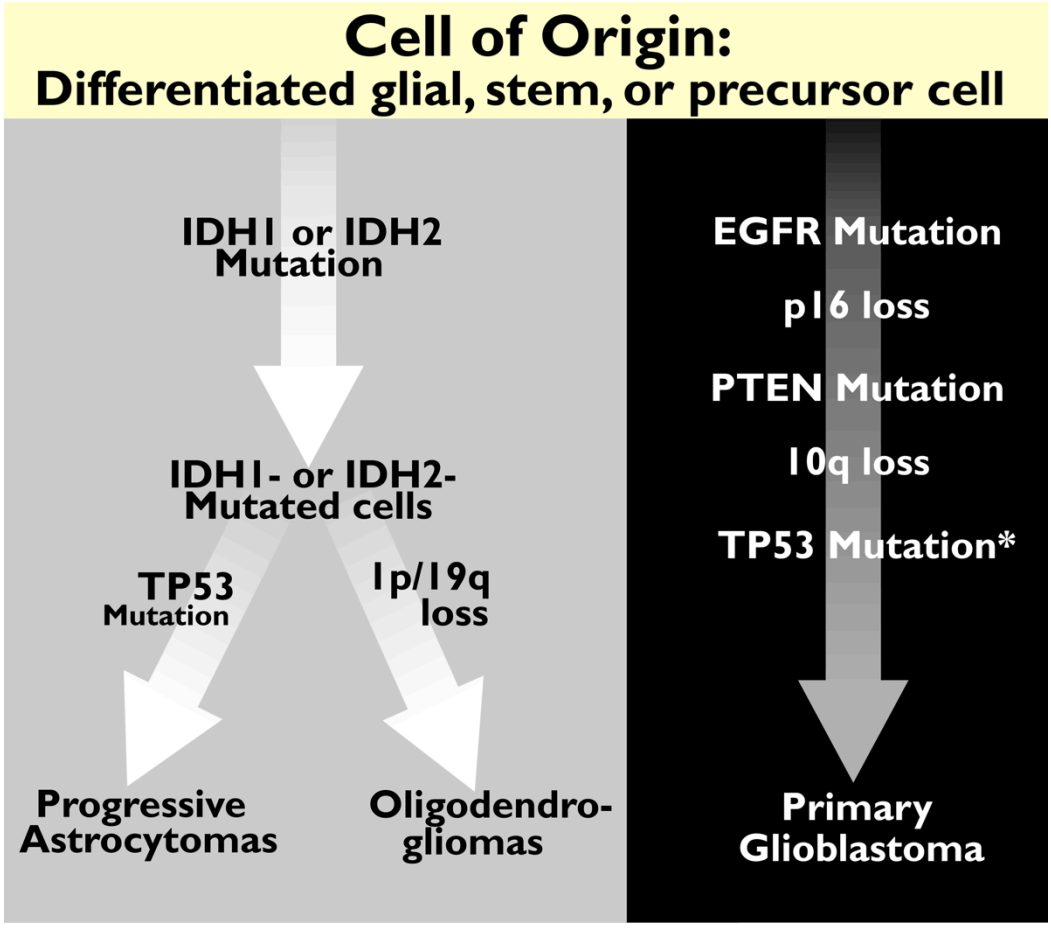

Figure 2: Proposed progression of gliomas. (reprinted with permission)[3] *TP53 mutation is present in approximately 30% of primary GBM, but over 60% of progressive astrocytomas.

Although there is great heterogeneity in the individual genes mutated in different primary GBMs, the actually pathways affected by these mutations are actually rather limited, with most mutations occurring in genes involved in receptor tyrosine kinase, p53, and retinoblastoma pathways[24,32] (some common mutations are listed in Figure 2). While an individual tumor has multiple mutations, these mutations are often in different pathways, with over two-thirds of tumors demonstrating mutations in all three pathways.[24,32]

1.2. Expression Studies in Gliomas

Expression analyses have identified 3-6 distinct expression patterns in GBM.[51-53] These fall largely into three main groups: proneural, proliferative, and mesenchymal (referred to by different names in different articles). The proneural group is characterized by the upregulation of genes involved in either Notch signaling, platelet derived growth factor signaling, the ARF pathway, or the TEL pathway.[52] The proneural group also shows expression of genes associated with neural stem cells or transit-amplifying cells,[51] and tumors in this group have a high frequency of mutations in IDH1.[53] Lower grade tumors (not Grade IV) fall almost exclusively into the proneural group.[51,52] The proneural group also comprises patients of a younger age compared to the proliferative and mesenchymal groups.[51,52] Additionally, patients in the proneural group, regardless of grade, have an improved survival compared to patients with tumors characterized as proliferative or mesenchymal. Interestingly, in some cases, as tumors in the proliferative group progress, they gain a more mesenchymal profile.[51]

The proliferative group is characterized by the expression of genes involved in cell cycle regulation and proliferation.[51,52] The mesenchymal group is characterized by overexpression of genes involved in angiogenesis, the NF-κB pathway, and the tumor necrosis factor pathway.[51-53] Both the proliferative and the mesenchymal groups have decreased PTEN expression and increased AKT compared to the proneural group.[51]

These expression signatures may provide some insight into the tumor cell of origin based on their similarities to the expression signatures of normal tissues. The proneural group shares similarity to some neural stem cell lines,[51,52] while proliferative tumors shared similar profiles with hematopoietic stem cells and the Jurkat cell line,

while the mesenchymal group shared features with a host of normal tissues, including endothelial and dendritic cells.[51]

1.3. Genetic Alterations in Oligodendrogliomas

Oligodendrogliomas are a form of progressive glioma and histologically comprise cells resembling oligodendrocytes. Oligodendrogliomas are divided up by grade into well-differentiated oligodendrogliomas (WHO grade II) and anaplastic oligodendrogliomas (WHO grade III).[7] Like progressive astrocytomas, over 80% of oligodendrogliomas contain mutations in either *IDH1* or *IDH2*.[12] Oligodendrogliomas also have characteristic losses of chromosomes 1p and 19q in over two-thirds of samples.[54-57] This distinguishes them from astrocytomas genetically (Table 2). Correspondingly, oligodendrogliomas generally do not contain mutations in *TP53*.[58]

Until recently, it was unclear which genes were the key drivers for the exceedingly frequent loss of chromosome arms 1p and 19q in oligodendrogliomas. Recent research suggests that the genes may be *homolog of capicua* (*CIC*) and *far-upstream element binding protein 1* (*FUBP1*).[58] Over two-thirds of tumors with 19q deletion had mutations in *CIC,*[58-60] and over half of oligodendrogliomas as a group had mutations in *CIC*.[43] *CIC* appears to play a role in receptor tyrosine kinase signaling.[61,62] While *FUBP1* mutations were not as frequent as *CIC* alterations, mutations in *FUBP1* were identified in over 10% of oligodendrogliomas in multiple studies.[43,58-60] *FUBP1* appears to play a role in *myc* signaling.[63] However, more research is needed to better understand the roles mutations in these genes may be playing in oligodendrogliomas. Of note, all tumors with mutations in *CIC* or *FUBP1* had mutations in *IDH1* or *IDH2*.[43]

Recently, *ATRX* was also identified as mutated in a fraction of central nervous system tumors, as described previously.[64] Interestingly, 7-14% of oligodendrogliomas contained mutations in *ATRX*.[42,43]

The exceedingly high rate of mutations in *IDH1/2* in both progressive gliomas and oligodendrogliomas strongly suggests that mutations in these genes may be among the earliest changes in a common precursor cell that gives rise to both tumor types (Figure 2).

Table 2: Summary of Genetic Alterations in Oligodendrogliomas

Tumor and WHO grade	Chromosomal abnormality	Genetic alteration
Grade II Oligodendroglioma	Mutation	*IDH1/2*
	–1p	*FUBP1*
	–19q	*CIC*
Grade III Anaplastic Oligodendroglioma	Mutation	*IDH1/2*
	Mutation	*PIK3CA/PIK3R1*
	–1p	*FUBP1*
	–19q	*CIC*
	–9p	*CDKN2A* deletion
	–4, –14, –15, –18	Unknown
	–10q	*PTEN* (rare)

Chromosome 9p losses in oligodendrogliomas correlate with grade. *PTEN* gene mutations and homozygous deletions of *CDKN2A*/*B* are not found in well-differentiated oligodendrogliomas but are found in up to half of anaplastic oligodendrogliomas.[65] Studies have also identified frequent mutations in either *PIK3CA* or *PIK3R1* in a significant fraction of anaplastic oligodendrogliomas.[37,58]

1.4. Mouse Models of Progressive Gliomas

Models in mice have begun exploring the interplay between genes, and which mutations are sufficient alone or in combination with others to form gliomas. For example, *TP53* null mice do not form spontaneous brain tumors.[66-68] Interestingly, sometimes a targeted deletion leads to tumor formation. In one study 17% of GFAP-Cre/*TP53*$^{fl/fl}$ mice developed gliomas resembling Grade III astrocytomas.[34] Additionally, when *TP53* deletion is combined with other mutations, this often either leads to tumor formation or accelerates it. For example, when GFAP-Cre/*TP53*$^{fl/fl}$ mice also had *PTEN*$^{fl/wt}$, tumors formed at a much higher rate than with *TP53* deletion alone.[34]

Interestingly, the driver used for different mutations is critical to whether or not tumors form. Mice overexpressing PDGFB driven by GFAP do not develop GBM,[66] although PDGFB overexpression driven retrovirally often leads to the formation of brain tumors.[68,69] The combination of a *TP53* null mice with either PDGFB overexpression retrovirally or PDGFB overexpression driven by a GFAP driver led to high rates of tumor formation.[68] Interestingly, PDGFB injected retrovirally and activated in cells with Nestin promoters generated oligodendrogliomas, whereas the same gene driven by GFAP promoters also generated oligoastrocytomas,[68] thus emphasizing the importance of the cell-of-origin in the type of tumors which form, even with the same genetic mutations. The aforementioned model is one of the few models to incorporate mutations/alterations frequently observed in progressive gliomas, as opposed to mutations/alterations frequently observed in primary GBM.

Models of low-grade gliomas have been developed, utilizing mice with heterozygous germline deletion of both *TP53* and *NF1*.[70] Both these mice and mice with heterozygous germline *TP53* deletion and GFAP driven *NF1* deletion demonstrate

GFAP+ astrocytomas of all grades.[70,71] These tumors occurred in locations throughout the brain, including the olfactory bulb, cortex, and brainstem.[70,71] An additional study that added heterozygous PTEN deletion to the *NF1*/*TP53* deficient mouse model found faster formation of GBM tumors and survival of one week vs. the eight weeks seen in the original study with intact PTEN.[72]

These studies provide an insight into the complexities of studying gliomas utilizing genetically-engineered mouse models. Different combinations of mutations can lead to tumors that are histologically identical. On the other hand, the same mutations, induced using a different driver impacting a slightly different population of cells, can lead to the development of a different type of tumor. In some cases, the same mutation may lead to tumors when present in one type of cell, and not lead to any tumors when driven in another type of cell. While this may be perceived as a challenge of using mouse models, it is also an opportunity; studying multiple models may allow us to better understand the conditions that promote the growth of tumors.

2. Isocitrate Dehydrogenase and Human Disease

2.1. Isocitrate Dehydrogenase and Progressive Gliomas

Our understanding of progressive gliomas was radically altered with the discovery of mutations in *IHD1* and *IDH2.*[32] These mutations were first identified in a study sequencing over 20,000 protein-coding genes in a series of glioblastoma samples, which revealed the presence of mutations in *IDH1* at the codon for amino acid residue 132 in 12% of GBMs.[32] These mutations were striking because they all occurred in the same amino acid residue, arginine 132, and were associated with younger patients who had a longer survival.[12] A series of follow-up studies of gliomas led to the discovery of the presence of mutations in *IDH1* in 60-90% of progressive gliomas, including grade II and grade III astrocytomas, oligodendrogliomas, and oligoastrocytomas, as well as secondary glioblastomas.[11-13,15,16,73,74] In addition, progressive gliomas that did not have mutations in *IDH1* were often found to have mutations in *IDH2* at the analogous amino acid residue R172.[12] On the contrary, primary GBM only rarely had mutated IDH1/2.[12]

IDH1 and IDH2 are homologous enzymes that function to catalyze the conversion of isocitrate to α-ketoglutarate while concomitantly reducing $NADP^+$ to NADPH (Figure 4). To complete this reaction, isocitrate is first oxidized to oxalosuccinate, while reducing $NADP^+$ to NADPH. Subsequently, oxalosuccinate is decarboxylated to generate α-ketoglutarate. Whereas IDH1 localizes to the cytosol and peroxisomes,[75-77] IDH2 localizes to the mitochondria (Figure 3).[78]

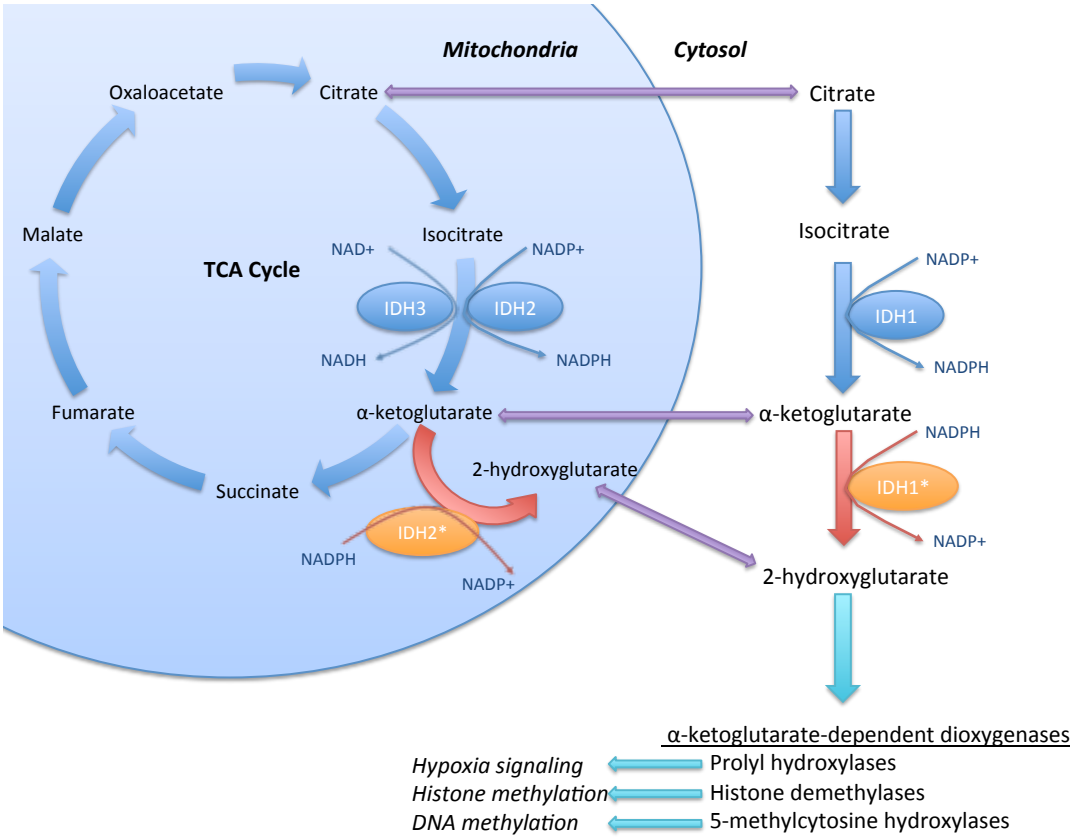

Figure 3: IDH mutations and cellular pathways.

IDH1 and IDH2 normally function as homodimers in both humans and other organisms.[79-81] Normally the arginines located at these mutation hotspot sites in IDH1/2 interact with the β-carboxyl group of isocitrate;[82,83] these mutations lead to a change in the active site of the proteins.[84] The consequences of IDH1/2 mutations are two-fold. First, mutations in $IDH1^{R132}$ and $IDH2^{R172}$ lead to abrogation of wild-type activity, with a dominant negative effect on normal IDH1 or IDH2 activity.[12,13,82] Secondly, these mutations lead to a novel function- namely, the conversion of α-ketoglutarate to D-2-hydroxyglutarate (2-HG) and the oxidation of NADPH to $NADP^+$ (Figure 4).[83-85] Subsequent studies have only found mutations in a single other amino acid, $IDH2^{R140}$,[83]

which is also predicted to normally interact with the β-carboxyl group of isocitrate. When mutated, it also leads to accumulation of 2-HG.[83] Nonetheless, the ramifications for the cell and the roles these mutations and the resulting novel metabolite play in the development of tumors are still being elucidated.

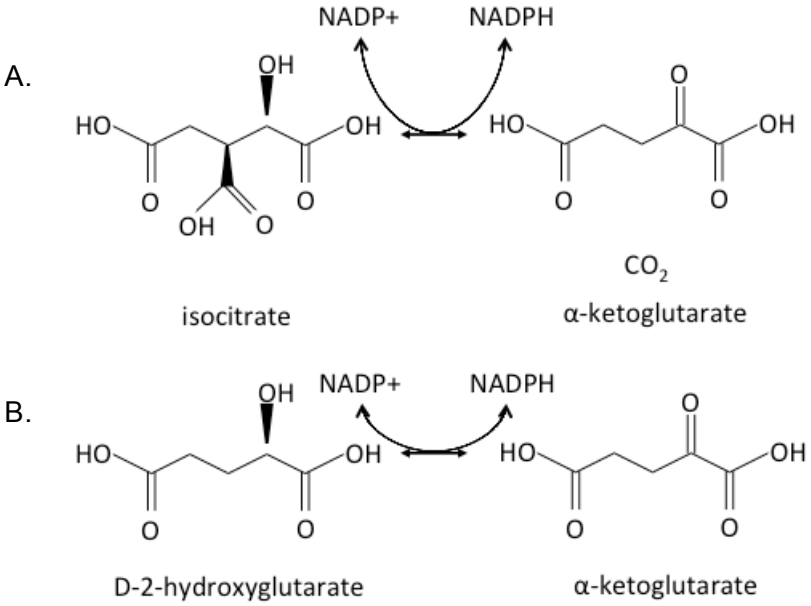

Figure 4: Normal and mutant function of IDH1/2. A) IDH1/2 normally function to convert isocitrate to α-ketoglutarate while generating NADPH from $NADP^+$. B) When mutated in gliomas, these enzymes are able to catalyze a new reaction, converting α-ketoglutarate to 2-HG while oxidizing NADPH to $NADP^+$.

2.2. IDH1/2 Mutations in Non-CNS Tumors

IDH1/2 were recently identified as frequently mutated in acute myelogenous leukemias.[86], and appear to inhibit hematopoietic differentiation and lead to a hypermethylation phenotype.[87,88] They have also been identified in central and periosteal cartilaginous neoplasms.[89] Less frequently, mutations have been identified in prostate cancer,[73] some myelodysplastic syndromes,[90] B-cell acute lymphoblastic leukemia,[73] blast phase chronic myelogenous leukemia,[91] colorectal cancer,[92] melanoma,[1] breast carcinoma,[93] and paraganglioma.[94]

2.3. Oxidative Stress

IDH1 has been shown to play a role in protection against reactive oxygen species (ROS) generated during metabolism or conditions of cellular stress in yeast and mammalian lines.[95,96] Normal functions of NADPH are numerous, including synthesis of fatty acids and cholesterol, and a role in nucleotide synthesis (reviewed in [97]). NADPH is also utilized by cells as a reducing equivalent for the generation of glutathione and thioredoxin, which help protect against oxidative damage.[98,99] The brain, compared to other tissues, consumes a large amount of oxygen (reviewed in Ballatori *et al*.[100]), and thus may have an increased sensitivity to oxidative damage. Studies have shown that in fibroblast, leukemia, and other cell lines, increased IDH1 leads to an increase in the ratio of reduced glutathione to total glutathione[101,102] and appears to provide protection against oxidative damage.[96,103,104]

Decreases in cellular IDH1 levels have been shown to lead to decreased survival

after oxidant exposure.[96] This is correlated with increased levels of peroxides, lipid peroxidation, and DNA damage.[96] Mutant IDH1/2, which actively utilizes NADPH to generate 2-HG, can thus potentially decrease levels of NADPH through its active depletion.

Interestingly, studies using the addition of 2-HG in vitro to cerebral cortex lysates from young rats demonstrate an increase in oxidative stress and lipid peroxidation following addition of 2-HG.[105] When taken in the context of the previous studies, it becomes apparent that there may be two different mechanisms through which mutant IDH1/2 may lead to increased oxidative stress- 1) a decrease in native IDH1/2 activity, reducing the capacity to respond to oxidative stress, and 2) an increase in 2-HG, which may inherently lead to increased oxidative stress.

2.4. Hypermethylation

Accumulation of 2-HG in tumors with mutant *IDH1/2* and a potential decrease in α-ketoglutarate may interfere with α-ketoglutarate-requiring enzymes. Recent research has shown that TET2 function may be impaired in the presence of 2-HG.[87,106] TET2 normally functions to hydroxylate 5-methylcytosine to 5-hydroxymethylcytosine, and may work to actively demethylate DNA.[107,108] In some leukemias, mutant IDH1/2 are correlated with a global hypermethylation phenotype and decrease in 5-hydroxymethylcytosine.[87] The same research on mutant IDH1/2 in leukemias has suggested that changes in methylation status correlate with a decrease in hematopoietic differentiation and the maintenance of a more undifferentiated state.[87] Interestingly, recent studies have also found a correlation between IDH mutation status and global

hypermethylation in glioma patient samples.[106,109,110] Studies are now beginning to elucidate genes for which there may be a correlation between promoter hypermethylation and presence of mutant IDH1, such as *RBP1,*[110,111] *GOS2,*[110] and *MGMT.*[112-114] It seems reasonable to hypothesize that hypermethylation may be caused by inhibition of α-ketoglutarate dependent dioxygenases, such as TET2.[87,106] However, one group has proposed the reverse; namely, that an initial hypermethylation phenotype (of unknown origin) may promote mutations in *IDH1/2*.[110]

Mouse ES cells have an interesting methylation pattern, with globally elevated 5-hydroxymethylcytosine levels, with 5-hydroxymethylcytosine primarily located at promoters with a high CpG content;[115] 5% of CpGs demonstrating hydroxymethylated cytosines.[116] However, the role of 5-hydroxymethylcytosine in development is still not clear, with research providing conflicting results. In one study in mouse ES cells, genes with promoters with high 5-hydroxymethylcytosine were expressed at higher levels than genes with promoters with either high 5-methylcytosine or unaltered cytosine.[116] As mouse ES cells were allowed to differentiate, the levels of 5-hydroxymethylcytosine decreased, and the expression of the genes associated with 5-hydroxymethylcytosine also decreased.[116] However, another study found low expression of genes with elevated levels of 5-hydroxymethylcytosine at their promoters, but that 5-hydroxymethylcytosine was preferentially located at the promoters of genes that were likely to become upregulated during differentiation.[115] This appeared to "prime" those genes for future activity.[115] Thus, although it appears that 5-hydroxymethylcytosine plays a critical role in ES cells and differentiation, more studies are needed to elucidate the exact role. It is possible that 5-hydroxymethylcytosine may play different roles on different promoters depending on other cues, such as histone methylation status. Of note, both TET1 and

TET2 are expressed in mouse ES cells, and appear to play a role in differentiation.[117] As these enzymes have been shown to be inhibited by 2-HG,[87] the presence of TET proteins in mouse ES cells means that mouse ES cell lines may have some utility for studies on the effect of mutant IDH1/2 on 5-hydroxymethylcytosine levels.

2.5. Hypoxia

Hypoxia is a common feature of the tumor microenvironment, and resistance to hypoxia is often considered a key feature of glial tumors. Hypoxia inducible factor-1α (HIF-1α), a key signaling molecule in hypoxia, plays a role in regulating apoptosis, metabolism, and angiogenesis (reviewed in[118]). Mutant IDH1/2, by modulating the HIF-1α pathway, may impact oxygen sensing in the cell. Levels of HIF-1α are regulated by HIF prolyl hydroxylases (PHDs), which ubiquitinate HIF-1α, leading to its degradation. PHDs use α-ketoglutarate as a substrate. Thus, low levels of α-ketoglutarate, as is theoretically possible in the setting of mutant IDH1/2, might lead to an increase in HIF-1α signaling.[119] Additionally, 2-HG has already been shown to inhibit TET2, an α-ketoglutarate-dependent dioxygenases, and may inhibit other α-ketoglutarate dioxygenases, such as HIF-1α.[82,106] Thus, mutant IDH1/2 have the potential to increase levels of HIF-1α via decreases in α-ketoglutarate or inhibition of PHD by 2-HG.

Nonetheless, studies regarding the effect of mutant IDH1/2 on both α-ketoglutarate and HIF-1α are conflicting in their results. While some studies have observed a decrease in α-ketoglutarate and an increase in HIF-1α in cell lines over-expressing mutant IDH1,[82,106] other studies have found no correlation between mutant IDH1 status and HIF-1α expression levels.[120] Studies in patient tumors have also yielded

conflicting results.[82,120] More studies are needed to better understand the impact of these mutations on hypoxia signaling.

2.6. Mouse Models of Mutant IDH

Recently, a mouse model was generated allowing for conditional expression of mutant IDH1^{R132H} under the control of Cre.[88,121] These mice were crossed with mice allowing for expression of Cre in either all hematopoietic progenitors or only myeloid progenitors.[88] The researchers identified an increase over time in hematopoietic stem cells and myeloid progenitors in the bone marrow and spleen of both mouse models, and an increase in histone methylation.[88] They then expressed IDH1^{R132H} in the brain using either Nestin-Cre or GFAP-Cre.[121] Both drivers led to broad expression within the brain in a large fraction of the cells. Nestin-Cre/IDH1$^{R132H/wt}$ mice died shortly after birth, and developed massive hemorrhage within the brain.[121] These mice also demonstrated "cavitation" and significant cell death throughout the brain.[121] GFAP-Cre led to a greater variability in degree of expression of mutant IDH1.[122] Interestingly, in these mice, the degree of hemorrhage correlated with levels of 2-HG in the brain.[121] Additionally, although neural stem cell and glial progenitor cells from these mice did not demonstrate an increase in histone methylation, they did demonstrate a decrease in presence of 5-hydroxymethylcytosine.[121] However, although these mice developed a wide variety of symptoms correlated with expression of mutant IDH1, these mice did not develop brain tumors.[121] Further studies may yet identify a model in which mutant IDH1 may, either alone or in concert with other mutations, lead to the development of gliomas. To date, no genetically-engineered mouse models have been developed utilizing mutant IDH2.

2.7. Mutant IDH2 and 2-hydroxyglutaric Acidurias

Patients with a rare disease known as D-2-hydroxyglutaric aciduria have elevated levels of D-2-HG in their urine[123-126] and serum.[124,125] Patients with D-2-hydroxyglutaric aciduria have developmental delay and often develop an epileptic encephalopathy, in addition to hypotonia and dysmorphic features.[123,127,128] MRI studies in various cases show decreased white matter and bilateral symmetrical lesions, sometimes referred to as subependymal cysts, adjacent to the lateral ventricles.[123,125,129] MRI studies have also shown dilated ventricles and cortical atrophy.[124-126,129] Interestingly, both macrocephaly[124] and microcephaly[125] have been noted. Post-mortem histological analyses were completed on one patient with 2-hydroxyglutaric aciduria. These studies confirmed bilateral white matter atrophy and corresponding enlargement of the lateral ventricles.[126] There was loss of white matter fibers and mild gliosis.[126] Studies in model systems have attempted to begin to explore the mechanism behind this striking phenotype. When 2-HG is applied to neuronal cultures from chick embryos, extensive neurotoxicity is noted.[130] These studies also identified an increase in intracellular calcium in neurons exposed to 2-HG, and that excitotoxicity from NMDA receptor activation and calcium influx may be a mechanism for neurotoxicity.[130] Of note, although patients with L-2-hydroxyglutaric aciduria (in which the other chiral form of 2-HG is elevated in urine and serum) have increased rates of a variety of brain tumors (reviewed in[131]), patients with D-2-hydroxyglutaric aciduria do not appear to be at increased risk of brain tumors.

It has been identified that IDH1 and IDH2 normally generate 2-HG at low levels during normal function.[132] About half of patients with D-2-hydroxyglutaric aciduria have

mutations in D-2-hydroxyglutaric acid dehydrogenase.[128] This gene normally functions to convert D-2-HG, which has no known function in the human body, to α-ketoglutarate. It appears that without this gene, 2-HG accumulates at least in part from the normal function of IDH1/2, leading to the aforementioned symptoms.[127] Although this provided an explanation for the source of D-2-hydroxyglutaric aciduria in approximately half of patients suffering from this disease, the cause of the increase in D-2-HG was unclear in the other half. Recently, a group identified mutations in IDH2 in the majority of these remaining patients.[133] As a result, patients with 2-hydroxyglutaric aciduria are now classified into two groups: Type I patients have mutations in D-2-hydroxyglutaric acid dehydrogenase, and a comparatively moderate increase in 2-HG, whereas Type II patients have mutations in $IDH2^{R140}$ and a higher increase in 2-HG in urine and serum compared to Type I patients.[134] However, due to the small number of patients that suffer from 2-hydroxyglutaric aciduria, there is still much that is not understood about this disease.

3. Role of IDH1 in Tumor Location versus Cell Type [1]

(based on Lopez, et al.[1])

3.1. Introduction

Although IDH mutations have been identified in gliomas and some leukemias, we attempted to address whether mutations in IDH may be present in other tumor types. In considering other tumors which might also harbor previously unknown mutations in *IDH1/2*, melanomas were considered, as they share some critical genetic features with progressive astrocytomas, such as a high rate of mutations in *TP53*.[135] Although a previous small-scale study had not identified any mutations in IDH1 in melanomas,[136] we decided to complete a larger and broader study utilizing 78 tumor samples and cell lines.

Additionally, we attempted to address a second hypothesis with this study. In noting that both oligodendrogliomas and astrocytomas have *IDH1/2* mutations while sharing very few other mutations in common between them, the hypothesis arose that there was potentially a characteristic of the brain parenchyma that placed a selective pressure for the presence of *IDH1/2* mutations for growth within the brain. We attempted to address this hypothesis by assessing whether *IDH1/2* mutations might be observed in metastases to the brain from non-central nervous system tumors. We sequenced $IDH1^{R132}$ and $IDH2^{R172}$ in 53 metastatic brain tumors, including melanomas.

3.2. Methods

We obtained a panel of cell lines derived from pathology-confirmed non-CNS metastatic melanoma tumor resections, with paired blood samples, from 78 patients enrolled in a clinical trial at the Surgery Branch of the National Cancer Institute at the

United States National Institutes of Health, and approved by the appropriate Institutional Review Board. Tumor resections were mechanically or enzymatically dispersed to generate the cell lines. We also obtained a panel of 53 frozen tumor resections from metastases to the brain through the Tissue Bank at the Preston Robert Tisch Brain Tumor Center at Duke University. Genomic DNA was isolated using the DNeasy Blood and Tissue Kit (Qiagen, Valencia, CA, USA). Primers for sequencing were synthesized by Integrated DNA Technologies (Coralville, IA, USA) and Invitrogen (Carlsbad, CA, USA). Primers were designed to amplify Exon 4 of IDH1 or IDH2 using Primer 3 (http://www-genome.wi.mit.edu/cgibin/primer/primer3_www.cgi), and generated products between 300-500 base pairs in length. Exon 4 contains the codon for the most frequently mutated amino acid residue in both IDH1 and IDH2 in gliomas. In one melanoma sample in which a mutation in *IDH1* was identified, all coding exons of *TP53*, *CDKN2A/B*, as well as hotspot exons of *BRAF* and *NRas*, were sequenced using the aforementioned techniques.

3.3. Results

78 melanoma samples from patients were sequenced for $IDH1^{R132}$ and $IDH2^{R172}$ mutations. A heterozygous *IDH1* c.C394T (p.R132C) mutation was identified in tissue derived from a melanoma lung metastasis from a 53-year-old female , and was not present in corresponding blood (Figure 5). No $IDH2^{R172}$ mutations were detected in any of these samples. *BRAF*, *NRas*, *TP53*, and *CDKN2A*/*CDKN2B* were sequenced in the sample with mutated *IDH1*. No mutations were identified in *NRas*, *TP53*, and

CDKN2A/*CDKN2B*. A *BRAF* c.T1799A (p.V600E) mutation, which is an activating mutation,[137,138] was identified in this sample.

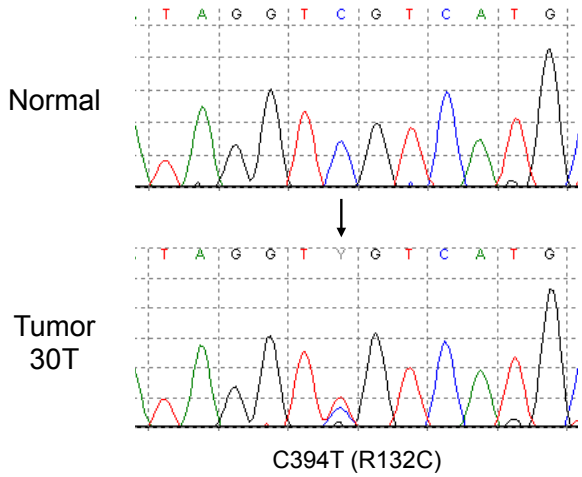

Figure 5: An IDH1^{R132C} mutation identified in a cell line derived from a melanoma metastasis to the lung. [1]

We sequenced Exon 4 of *IDH1* and *IDH2* in 9 melanoma metastases to the brain and 44 other metastases to the brain from other primary tumors, including lung, breast, renal, uterine, ovarian, esophageal, and urothelial cancers. No mutations were identified in any of the tumor metastases.

3.4. Discussion

Mutations in IDH1 or IDH2 occur at a high frequency in progressive gliomas, acute myelogenous leukemias, and central and periosteal cartilaginous neoplasms.[139] Mutations are present at a lower frequency in some myelodysplastic syndromes[90] and

blast phase chronic myelogenous leukemia[91] However, these mutations are very rare in other tumors.[73,91-94] Because melanomas share some similar genetic features to progressive astrocytomas, we decided to sequence a panel of melanomas in an attempt to evaluate the frequency of *IDH1/2* mutations in these tumors. We identified an *IDH1*^{R132C} mutation in one melanoma.[1] To our knowledge, this is the first *IDH1/2* mutation identified in a melanoma. However, sequencing of a panel of melanomas did not identify further mutations in *IDH1/2,* suggesting that mutant *IDH1/2* are unlikely to play a large role in the development of these tumors.

Noting that mutations in *IDH1/2* only occur at a high rate in progressive gliomas and acute myelogenous leukemias, we developed two potential hypotheses for this observation. Hypothesis 1: *IDH1/2* mutations are cell-lineage dependent. In other words, there is some shared characteristic of the cell-of-origin for progressive gliomas and acute myelogenous leukemias, and these cells are inherently predisposed to malignant transformation in the presence of mutant *IDH1/2*. Hypothesis 2: There is a selective pressure within different niches within the body, including the brain parenchyma, and *IDH1/2* mutations may promote growth in those tissues. If this second hypothesis were correct, then we would expect to see a higher rate of mutations in *IDH1/*2 in metastases to the brain from non-central nervous system tumors than in tumors at the site-of-origin.

In our study, we did not identify any mutations in Exon 4 of *IDH1/2* in a panel of metastases to the brain from non-CNS tumors. This would appear to disprove the second hypothesis, that *IDH1*^{R132} or *IDH2*^{R172} mutations provide a selective growth advantage in a general sense within brain tissue. Therefore, we conclude that of these two hypotheses, the first is more probable. In other words, we propose that mutations in IDH1/2 are likely advantageous in a cell-lineage dependent manner, and that there is a

selective pressure for mutations in the cell-of-origin for progressive gliomas and the cell-of-origin for acute myelogenous leukemias. However, the scope of these studies does not allow us to rule out other hypotheses. For example, an unknown mutation may initiate the tumor, and provide selective pressure for subsequent mutations in *IDH1/2.* Further studies are needed to better understand the features shared by tumors with these mutations, and to comprehend the role mutant *IDH1/2* may play in tumorigenesis.

4. Metabolic Profiling and Biochemical Characterization

4.1. Introduction

The Warburg effect,[140] in which there is an increased rate of aerobic glycolysis, has been proposed as a potential result of changes in metabolism resulting from mutations in IDH1/2.[141,142] The Warburg effect is particularly prominent in GBM, with one study finding that 90% of glucose and 60% of glutamine is converted into lactate and alanine in GBMs.[143] Increased glycolysis may provide an advantage to a dividing cancer cell by providing not only energy but also basic metabolites required by a rapidly dividing cell.[141] The effect of mutant IDH1/2 on the cellular metabolic and physiologic state is largely unknown. It is possible that mutations in IDH1 may provide a mechanism for initiating this shift in metabolism, by altering the levels of key metabolites needed in a rapidly growing cell, such as NADPH.[142] Because these are among the earliest changes in progressive gliomas, it is possible that these changes occur in a precursor cell that is common to both oligodendrogliomas and progressive astrocytomas. A cell that is in a more undifferentiated state may have unique responses to the changes induced by the presence of mutant IDH1/2 compared to a more differentiated cell. We utilized broad metabolomics profiling in mouse ES cells with and without mutant IDH1 or mutant IDH2 in hopes of identifying changes in metabolism and other pathways.

Studies in leukemias suggest that 2-HG may inhibit the function of TET2, which normally functions to convert 5-methylcytosine in DNA to 5-hydroxymethylcytosine.[87] The generation of stable mouse cell lines expressing mutant IDH1/2 allowed us to directly evaluate the relationship between mutant IDH1/2 and methylation status in undifferentiated cells, which demonstrate a unique methylation pattern compared to

terminally differentiated cells.[144] We addressed whether mutant IDH1/2 affects the methylation status of these cells.

4.2. Methods

4.2.1. Generation of Mouse ES Cell Lines with Conditional Heterozygous Expression of IDH1^{R132H} or IDH2^{R172K}

To study the effect of mutations in *IDH1/2* in undifferentiated cells, we utilized the UNC Animal Models Core to generate mouse ES cell lines with knock-in IDH1^{R132H} or IDH2^{R172K}. Plasmid-based gene targeting vectors were used. Following integration of homology regions into the vector, point mutations were inserted for IDH1^{R132H} (codon 132: CGA→CAC) and IDH2^{R172K} (codon 172 AGG→AAG). The constructs also contained 3' and 5' homology arms for homologous recombination within the appropriate gene, a neomycin selection marker flanked by Flp sites, and a stop cassette (adenovirus splice acceptor and three copies of an SV40 polyadenylation sequence) flanked by Cre sites (Figure 6). The plasmid was electroporated into mouse ES cells for homologous recombination. Successful homologous recombination was verified at UNC via PCR and Southern blot (not shown). Heterozygosity was also verified through genomic sequencing.

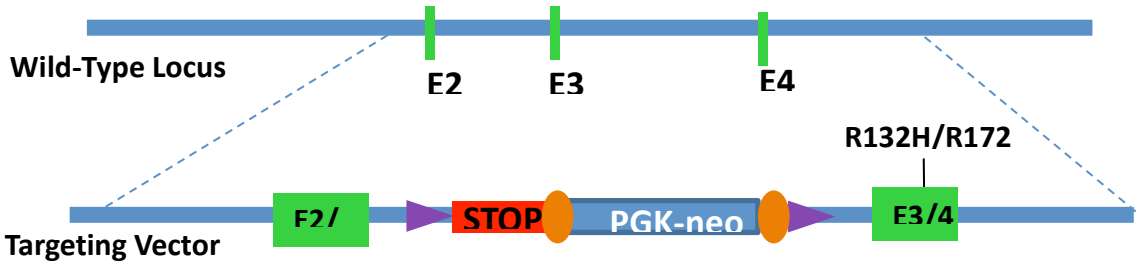

Figure 6: Targeting vector for homologous recombination allowing for expression of mutant IDH1/2. Note that the codon for $IDH1^{R132}$ is located in exon 3 of *IDH1,* whereas the codon for $IDH2^{R172}$ is located in exon 4 of *IDH2*. Loxp sites are denoted by purple triangles. Flp sites are denoted by orange ovals.

To generate mouse ES cells with stable endogenous expression of mutant IDH1/2, Cre-mediated deletion was used to remove the selection marker and stop codons.

Presence of the mutant alleles of IDH1/2 was verified through sequencing of genomic DNA (gDNA). Isolation of gDNA was accomplished using Lyse and Go PCR Reagent (Thermo Scientific, USA) per the manufacturer's protocols. The region of interest containing the mutation was amplified using KAPA Taq polymerase using the following primers. For IDH1: Forward: GTAAAACGACGGCCAGTTCACCAAAGATGCTGCAGAG, Reverse: GGGTGTAGATGCCCAAAGAA. For IDH2: Forward: GTAAAACGACGGCCAGTGTAGGGCTGTGGTGGGTCTA, Reverse: GAGAGGCAGTTCAAGCCAAG. The forward primers contained an M13 (-20) forward sequencing primer for subsequent Sanger sequencing analysis for the presence of wild-type and mutant alleles.

Expression of mutant IDH1/2 was verified via cDNA sequencing on two clones for each gene. RNA was extracted using the RNeasy Kit (Qiagen, CA, USA) per manufacturer's protocols. iScript cDNA Synthesis Kit (BioRad, CA, USA) was used to

generate cDNA for sequencing. KAPA Taq polymerase was used for amplification of the region of interest. DNA was amplified using the following primers for IDH1: Forward: GTAAAACGACGGCCAGTTCACCAAAGATGCTGCAGAG, Reverse: AGGCCCAGGAACAACAAAAT. For IDH2: Forward: GTAAAACGACGGCCAGTTGTCAAGTGTGCCACAATCA, Reverse: GGGGTGAAGACCAACTTGAA. The forward primers contained an M13 (-20) forward sequencing primer for subsequent Sanger sequencing for analysis of the presence of both wild-type and mutant alleles.

Expression was also verified through measurement of 2-HG generation. Cells were washed, pelleted, and stored at -80ºC. Cells were then thawed and lysed on ice with pre-chilled M-PER Mammalian Protein Extraction Reagent (Thermo Scientific) with complete protease inhibitor cocktail (Roche) for 15 minutes, then spun down at 4ºC for 10 minutes at 13,200 rpm. Protein concentration was measured in an aliquot of each sample using Protein Assay Buffer (BioRad). Concentrations were normalized to 5µg/µl through addition of M-PER to each sample. Samples were measured by LC-negative electrospray ionization-MS/MS as described previously.[145,146]

4.2.2. Mouse ES Cell Growth

Mouse ES cells were grown on standard cell-culture plates treated with 0.1% gelatin solution for 30 minutes prior to use. Cells were placed in these plates in ES Media (15% FBS, 50U/mL Penicillin/Streptomycin, 2mM L-glutamine, 0.1mM non-essential amino acids, 500U/mL leukocyte inhibitory factor, 0.1mM β-mercaptoethanol, 1mM sodium pyruvate, in GMEM, sterile-filtered) and grown at 37ºC, 6% CO_2. Media

was replaced with fresh media every 24 hours. Cells were passaged every 2-3 days when plates reached approximately 80% confluence. Fresh ES Media was exchanged for old media on plates 3 hours prior to passaging. For passaging, cells were washed with Phosphate-Buffered Saline (PBS) without bivalent cations (Gibco). 0.25% trypsin/EDTA was added, and immediately upon dissociation of colonies, medium was gently pipetted to dissociate colonies into single cells. Following dissociation, washing media (ES Media without leukocyte inhibitory factor) was added to inactivate trypsin, and cells were spun down at 1,000 rpm for 4 minutes. After removing the supernatant, cells were resuspended in fresh ES Media (usually at a 1:5 or 1:6 dilution), and plated on gelatin-treated cell culture dishes. Plates were gently rocked to achieve a uniform distribution.

4.2.3. Measurement of 2-HG in Mouse ES Cells

2-HG was measured in mouse ES cells with and without mutant IDH1/2. ES cells were plated as described in Section 4.2.2 in 60mm cell culture dishes. Following 2 days of growth, cells were removed with trypsin and washed as described in Section 4.2.2. Following the second wash with PBS, cells were spun down at 1,000 rpm for 4 minutes, supernatant was removed, and the pellet was stored at -80ºC. Pellets were thawed on ice and resuspended in cold M-PER. Cells were lysed on ice for 15 minutes, then spun down at 4ºC for 10 minutes at 13,200 rpm. Supernatant was saved, and protein concentration was measured using Protein Assay Buffer (BioRad) and compared to a Pre-diluted Protein Assay Standards BSA Set (Thermo). Protein concentration in samples was normalized using additional lysis buffer, with concentration normalized to

12µg/µL. Samples were measured by LC-negative electrospray ionization-MS/MS as described previously.[145,146]

4.2.4. Metabolic Profiling of Mouse ES Cells Expressing Mutant IDH1/2

To assess the changes occurring in mouse ES cells with mutant IDH1/2, we, in collaboration with Metabolon, completed metabolic profiling using three mass spectrometry platforms: liquid chromatography (LC)-MS/MS with electrospray ionization, (LC)-MS/MS without electrospray ionization and gas chromatography (GC)-MS to assess metabolic profiles as previously described.[147-150] Mouse ES cells were grown at 37ºC 6% CO_2 in 60mm plates as described in Section 4.2.2. Two plates were combined for each measured sample. Five biological replicates were generated for each cell line studied (ten plates total per line, as two 60mm cell culture plates were combined to collect 10^7 cells, as required for sampling). Cells lines utilized were: E14 parental, IDH1 Clone B9, IDH1 Clone C6, IDH2 Clone B8, and IDH2 Clone C5. Each plate was placed in a different location within the incubator so as to minimize variability in results from slight differences in temperature or humidity. Cells were washed with pre-warmed PBS. 0.25% pre-warmed trypsin was added to each plate, and plates were rotated gently to encourage cells to enter suspension. Following suspension of cells, washing media (ES cell media without growth factors) was added to each sample to inhibit trypsin, and plates were again gently rocked. Cells were spun down for 4 minutes at 1,000 rpm and resuspended in fresh PBS. Cells were counted using trypan blue and a haemocytometer. Values from three counts per sample were averaged to determine the concentration of cells. 10^7 cells were collected for each sample and spun down for 4

minutes at 1,000 rpm. PBS was removed, and cells were flash frozen on dry ice and stored at -80ºC until transfer to Metabolon.

4.2.5. Assessment of Oxidative Stress

We assessed the impact of mutant IDH1/2 on response to oxidative stress utilizing Hct116 cell lines. These lines were generated using homologous recombination to allow for expression of mutant IDH1. These lines were generated in the lab by Chris Duncan as described previously.[151] Studies were completed with parental Hct116 or Hct116 $IDH1^{R132H}$ clone 1D3. Oxidative stress was measured using -5-(and-6)-carboxy-2',7'-dichlorodihydrofluoroscein diacetate (H_2DCFDA) (Invitrogen). For visualization studies using a microscope, cells were grown in 24-well plates at 50,00 cells per well for 48 hours prior to the study. For FACS studies, cells were grown in 6-well plates at a concentration of 200,000 cells per well for 24 hours at 37ºC, 5% CO_2. For pseudo-hypoxia to generate oxidative stress, cells were treated with 200μM $CoCl_2$ for 18 hours. All procedures involving H_2DCFDA were completed in low light levels.

For direct microscopic visualization, wells were washed with DPBS and placed in fresh media. H_2DCFDA was then added to the media for a final concentration of 1μM, and plates were incubated at 37ºC, 5% CO_2 for 8 minutes. As a positive control, cells were stressed with 50μM H_2O_2 for 15 minutes for visualization studies using a microscope. Cells were visualized every 15-30 minutes with excitation at 465-495nm.

For FACS, one population of wells was treated with 5μM H_2O_2 for 10 minutes as a stressor. All wells were washed with PBS and treated with trypsin. Cells were resuspended in McCoy's medium, which inactivated the trypsin. Cells were spun for 3 minutes at 1,260 rpm. Cells were washed twice in fresh 1% bovine serum albumin (BSA)

in PBS, and spun between washes as previously described. 50µg of H_2DCFDA was dissolved in 17.3µL DMSO and, and 12.8µl was added to 16mL 1% BSA/PBS to yield a final carboxy-H_2DCFDA concentration of 1µM, or 580ng/µL. Cells from each well were resuspended in 2.5mL 1µM H_2DCFDA solution, placed in a fresh 6-well plate, and incubated at 37ºC, 5% CO_2 for 15 minutes. Cells were spun down for 3 minutes and resuspended in 2mL of 1% BSA in PBS, and analyzed by flow cytometry using a FACSCalibur flow cytometer (BD Biosciences, USA) using the FITC channel (approx. 492nm excitation/520nm emission). Cells were gated such that approximately 3-5% of parental cells were positive at baseline.

These same studies were also completed with our mouse ES cell lines. For mouse ES cells, studies were completed with parental, one mutant IDH1 clone, and one mutant IDH2 clone. Oxidative stress was measured using H_2DCFDA (Invitrogen). Cells were grown in 6-well plates at a concentration of 90,000 cells per well.

For pseudo-hypoxia to generate oxidative stress, cells were treated with 200µM $CoCl_2$ for 18 hours. All procedures involving H_2DCFDA were completed in low light levels. As a positive control, cells were stressed with 2.5µM H_2O_2 for 10 minutes. For direct microscopic visualization, wells were then immediately visualized with excitation at 465-495nm.

For FACS sorting, wells were washed with PBS. Wells were treated with trypsin, and cells resuspended in DMEM, which inactivated the trypsin. Cells were spun for 3 minutes at 1,260 rpm. Cells were washed twice in fresh 1% BSA in PBS, and spun between washes as previously described. 50µg of H_2DCFDA was dissolved in 17.3µL DMSO and, and 12.8µl was added to 16mL 1% BSA/PBS to yield a final H_2DCFDA concentration of 1µM, or 580ng/µL. Cells from each well were resuspended in 2.5mL

1μM H_2DCFDA solution, placed in a fresh 6-well plate, and incubated at 37ºC, 5% CO_2 for 15 minutes. Cells were spun down for 3 minutes, resuspended in 2mL of 1%BSA/PBS, and analyzed by flow cytometry using the FITC channel.

4.2.6. Analysis of Hypoxia Signaling in Hct116 Cells with Mutant IDH1/2

To evaluate the impact of mutant IDH1 on response to hypoxia, we and collaborators in the Kaelin laboratory compared HIF-1α protein levels in lines under normoxia and mild hypoxia by Western blot. Hct116 cell lines with or without mutant *IDH1* or mutant *IDH2* were grown for 48 hours at 37ºC, 5% CO_2, until they reached 50%-60% confluence. The appropriate plates were transferred to mild hypoxia of 7.5% O_2 for 16 hours, or normoxia with desferrioxamine (DFO) for 16 hours, while the remaining plates stayed in normoxia. Following exposure to mild hypoxia, cell culture dishes were placed on ice, and washed with cold PBS. Cells were dissociated with a cell scraper, gently suspended in PBS, and spun down at 4ºC, 1,000 rpm for 4 minutes. Cells were resuspended in lysis buffer (50mM Tris pH 7.5 150mM sodium chloride, 0.5% Nonidet P-40, complete protease inhibitor cocktail tablet [Roche], 5mM sodium fluoride, 1mM sodium pyrophosphate, 1mM β-glycerophosphate, 1mM dithiothreitol), allowed to sit for 15 minutes on ice, the spun down at 4ºC for 10 minutes at 13,200 rpm. Supernatant was saved, and protein concentration was measured using Protein Assay Buffer (BioRad) and compared to a Pre-diluted Protein Assay Standards BSA Set (Thermo). Protein concentration in samples was normalized using additional lysis buffer. Loading buffer (Laemmli Sample Buffer [BioRad] with β-mercaptoethanol) was added to samples, and was placed at 90ºC for 3 minutes. Samples were loaded onto NuPage 4-12% Bis-Tris

Gel (Invitrogen) and run at 150 volts for approximately 1 hour. Protein was transferred onto PVDF using semi-dry transfer, and blocked for one hour in washing buffer (10mM Tris, pH 7.5, 150mM sodium chloride, 0.05% TWEEN-20) with 5% powdered milk (weight/volume). Membrane was transferred to washing buffer with 5% BSA and anti-HIF-1α antibody (BD-Biosciences 610958) or blocking buffer and anti-PHD2 antibody (Cell Signaling D31E11). Membrane was placed at 4ºC overnight. Following exposure to primary antibody, membrane was washed in washing buffer with 5% powdered milk (weight/volume) 3x 10minutes with shaking at room temperature. The membrane was then placed in blocking buffer with secondary anti-mouse HRP-conjugated antibody diluted 1:10,000 (GE Healthcare NA9231V). This was placed at room temperature with shaking for 45 minutes, then washed 3x 15 minutes with shaking at room temperature in washing buffer. Detection was completed using Super Signal West Femto Maximum Sensitivity Substrate (Thermo), and detected using autoradiography film. The same procedure was completed with anti-GAPDH or anti-tubulin antibody as a control.

4.2.7. Measurement of 5-hydroxymethylcytosine in Mouse ES Cells Expressing Mutant IDH1/2

We, in collaboration with Dr. Lucy Godley at the University of Chicago, measured 5-hydroxymethylcytosine (5hMC) levels in the IDH1/2 mutant mouse ES cell lines as well as the parental line using a dot-blot assay to assess global levels of 5-hydroxymethylcytosine.[152] Briefly, labeled (for identification of 5-hydroxymethylcytosine) genomic DNA was blotted onto a membrane, blocked with BSA, and treated with avidin-HRP for measurement of chemiluminescence.[152] For further quantification, we and collaborators utilized LC/MS to assess changes in global levels between mutant and

wild-type cell lines. These studies allow us to see if there are large global changes in levels of 5-hydroxymethylcytosine.

4.3. Results

4.3.1. Verification of Mouse ES Cell Generation

Heterozygosity of mouse ES cells for mutant IDH1 or mutant IDH2 was verified by genomic sequencing (Figure 7). Subsequently, mRNA expression from both alleles was verified (Figure 8) We also verified 2-HG generation in mutant IDH1/2 lines (Figure 9).

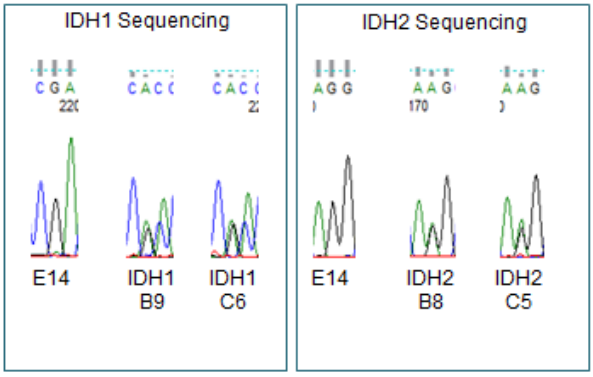

Figure 7: Heterozygous alleles for mutant IDH1 or mutant IDH2 in mouse ES cell clones as determined by gDNA sequencing. E14 represents the parental, wild-type line. Sequences: (at codon 132) wild-type IDH1:CGA, mutant IDH1:CAC; (at codon 172) wild-type IDH2:AGG, mutant IDH2:AAG.

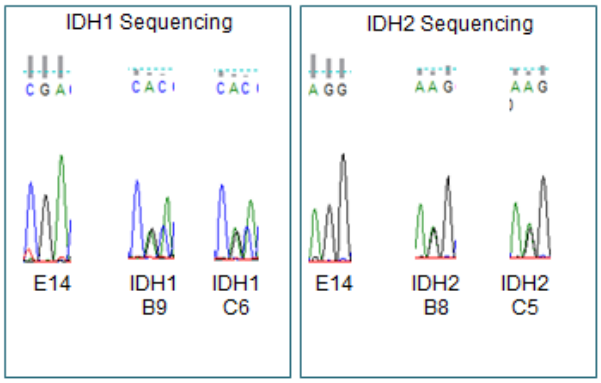

Figure 8: Heterozygous expression of mutant and wild-type IDH1 or IDH2 in mouse ES cells as determined by mRNA analysis. E14 represents the parental, wild-type line. Sequences: (at codon 132) wild-type IDH1:CGA, mutant IDH1:CAC; (at codon 172) wild-type IDH2:AGG, mutant IDH2:AAG.

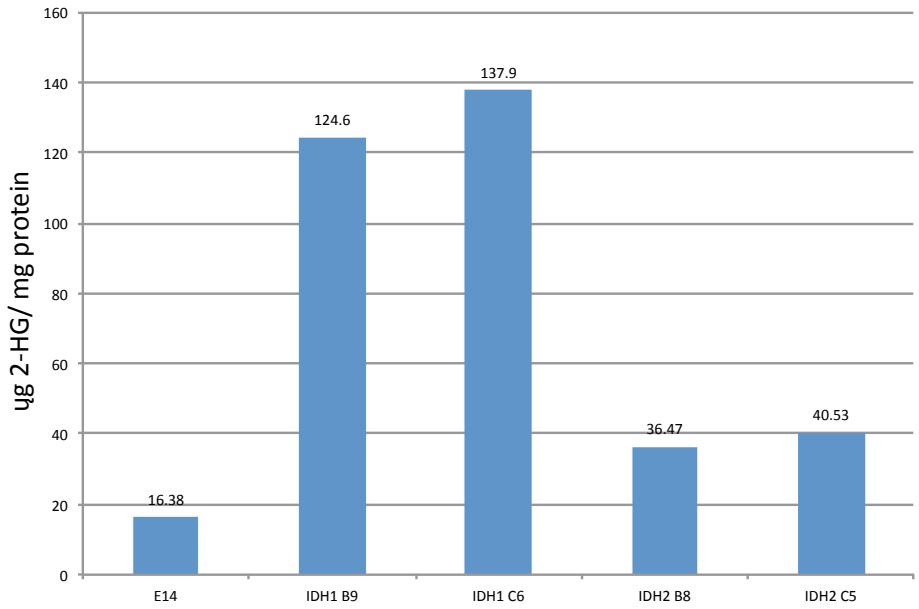

Figure 9: 2-HG generation in mouse ES cells with mutant IDH1/2. E14 represents the parental, wild-type line.

4.3.2. Metabolomic Profiling

Metabolic profiling was completed to assess changes in levels of various metabolites in mouse ES cells in the setting of mutant *IDH1* or mutant *IDH2*. These studies verified generation of 2-HG, with IDH1 mutants showing a 100-fold increase in levels and IDH2 mutants showing a 30-fold increase in levels compared to the parental line (Figure 10).

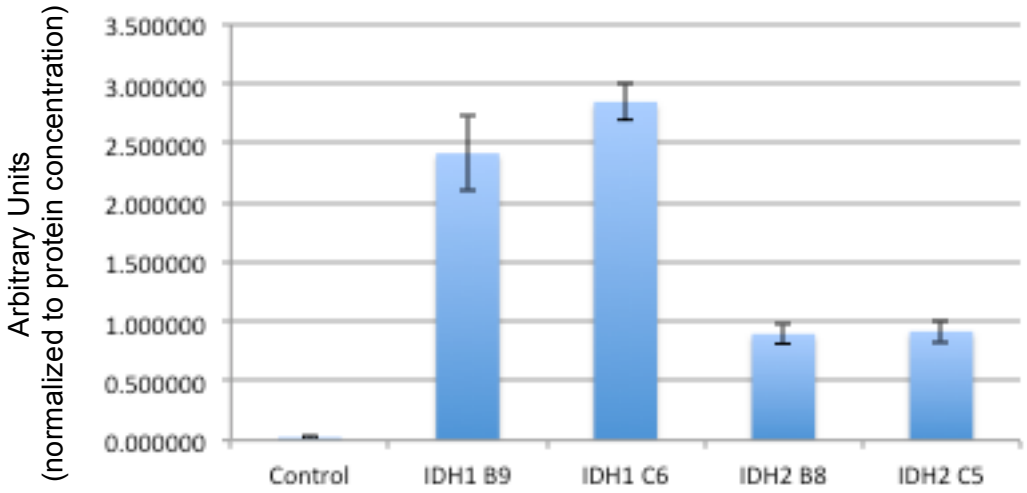

Figure 10: 2-HG generation in mouse ES cells with mutant IDH1/2. Each value represents measurements from five biological replicates. Error bars represent standard deviation. P<0.0005 for each mutant compared to control.

Results from metabolic profiling identified an increase in oxidized glutathione in mouse ES cell lines with mutant IDH1/2 compared to control (Figure 11). Correspondingly, there was an increased ratio of oxidized to reduced glutathione in mouse ES cell lines with mutant IDH1/2 compared to control (data not shown). We also

identified increased levels of 2-aminobutyrate and ophthalmate in these lines (Figure 12). Because of the findings of increased oxidized glutathione and increased ophthalmate, we assessed responses to oxidative stress in the setting of mutant IDH1/2.

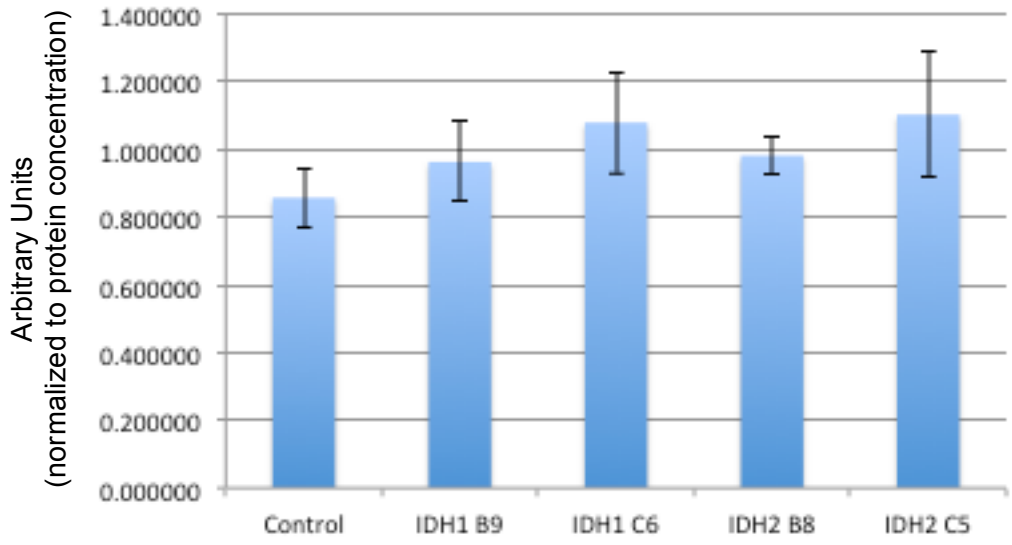

Figure 11: Levels of oxidized glutathione are increased in mouse ES cells with mutant IDH1/2. Each value represents measurements from five biological replicates. Error bars represent standard deviation. Difference from control was $P<0.05$ for IDH1 C6, IDH2 B8, and IDH2 C5.

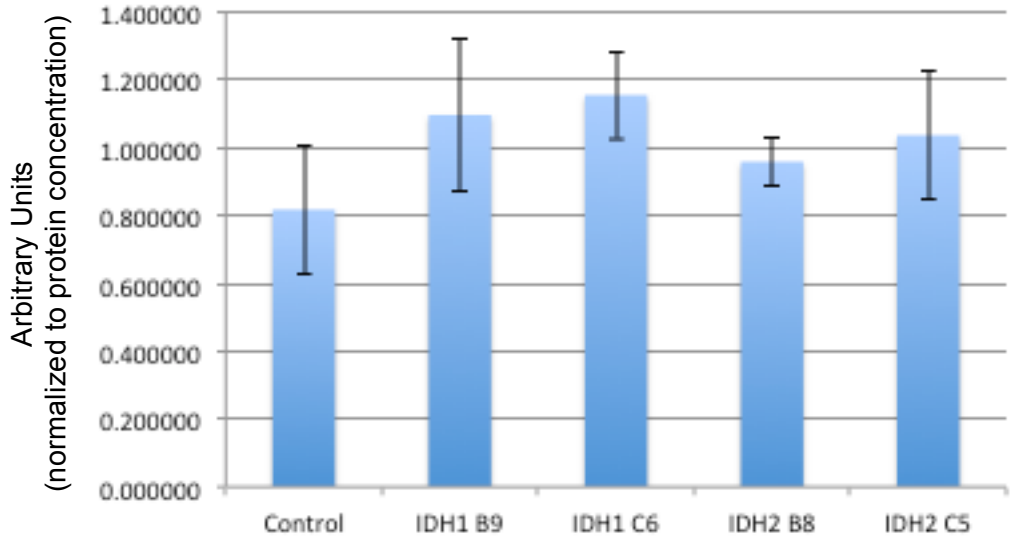

Figure 12: Ophthalmate levels are increased in mouse ES cells with mutant IDH1/2. Each value represents measurements from five biological replicates. Error bars represent standard deviation. Difference from control was $P<0.2$ for each mutant line compared to control, but did not reach statistical significance.

4.3.3. Effect of Mutant IDH1/2 on Response to Oxidative Stress

No gross changes or differences were noted visually either at baseline or in response to pseudo-hypoxia in Hct116 cells with mutant IDH1 compared to the parental line when treated with H_2DCFDA to detect reactive oxygen species (Figure 13). Likewise, no changes in response were noted in mouse ES cells with mutant IDH1 or mutant 2 (Figure 14).

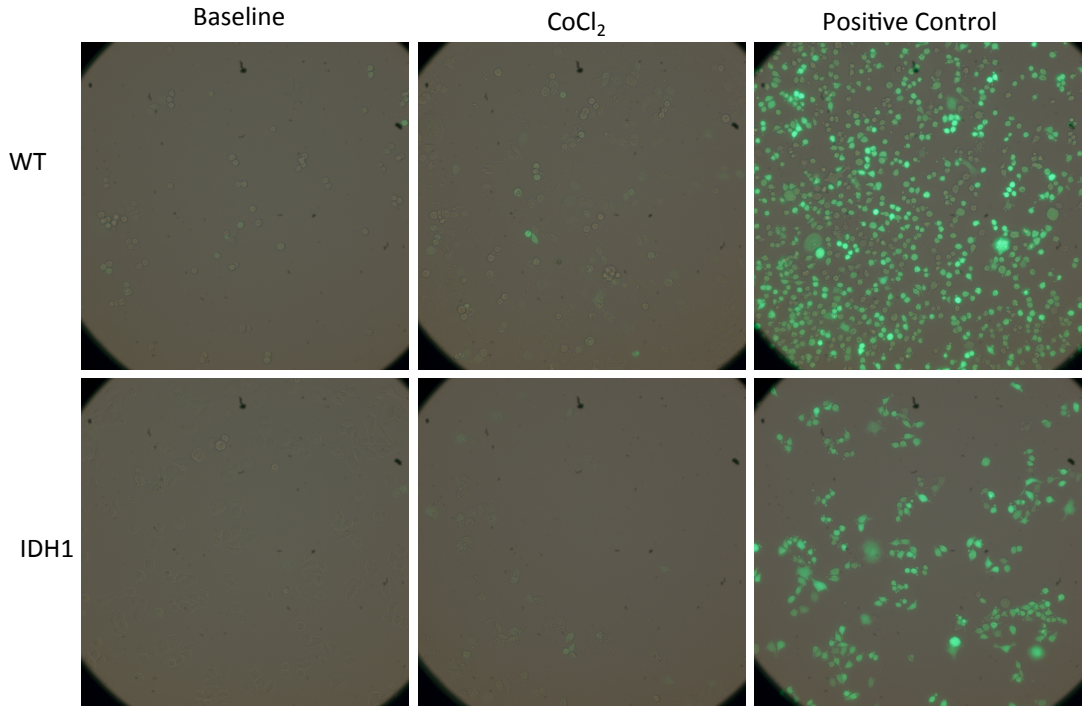

Figure 13: Mutant IDH1 and response to oxidative stress in Hct116. Oxidative stress measured via fluorescence in the presence of H_2DCFDA. Cells were treated with $CoCl_2$ for 18 hours to mimic hypoxia. H_2O_2 exposure was used as a positive control.

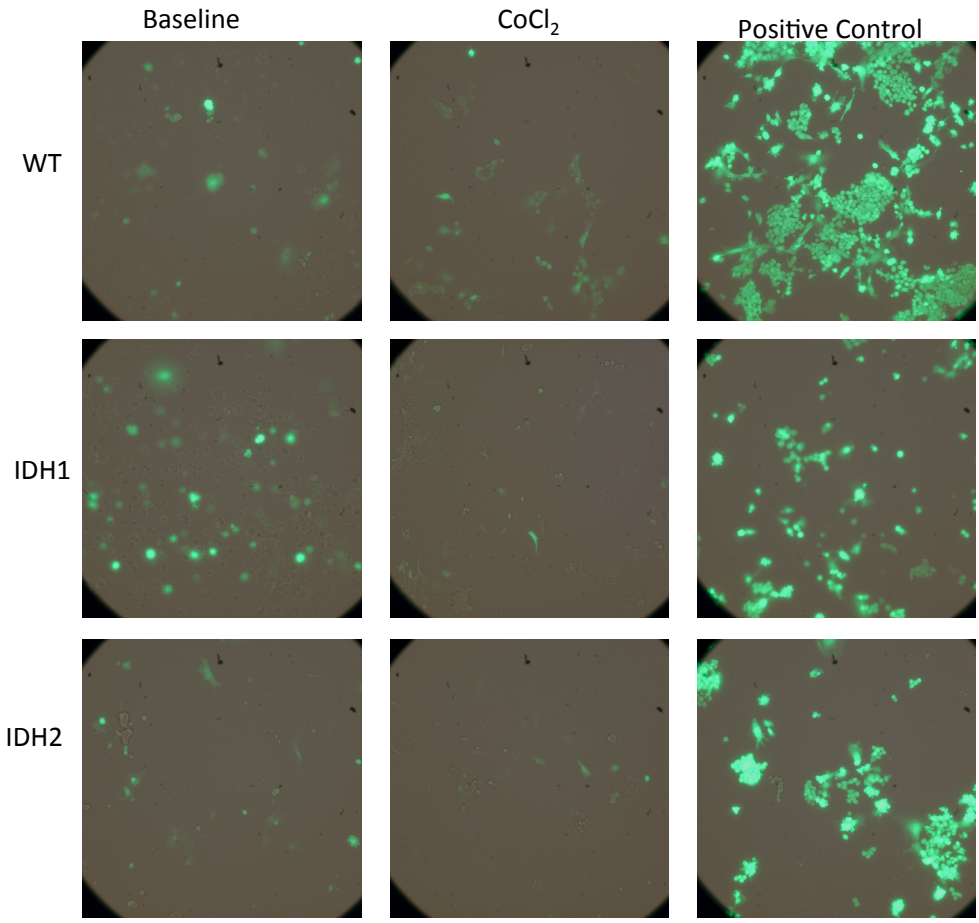

Figure 14: Mutant IDH1/2 and response to oxidative stress in mouse ES cells. Oxidative stress measured via fluorescence in the presence of H_2DCFDA. Cells were treated with $CoCl_2$ for 18 hours to mimic hypoxia. H_2O_2 exposure was used as a positive control.

We subsequently used a more quantitative approach to measure oxidative stress. Utilizing H_2DCFDA as a marker of oxidative stress, we measured baseline levels and levels following treatment with H_2O_2 using FACS. However, we did not detect significant changes in cell lines with mutant IDH1/2 as compared to the parental lines (Figure 15, Figure 16)

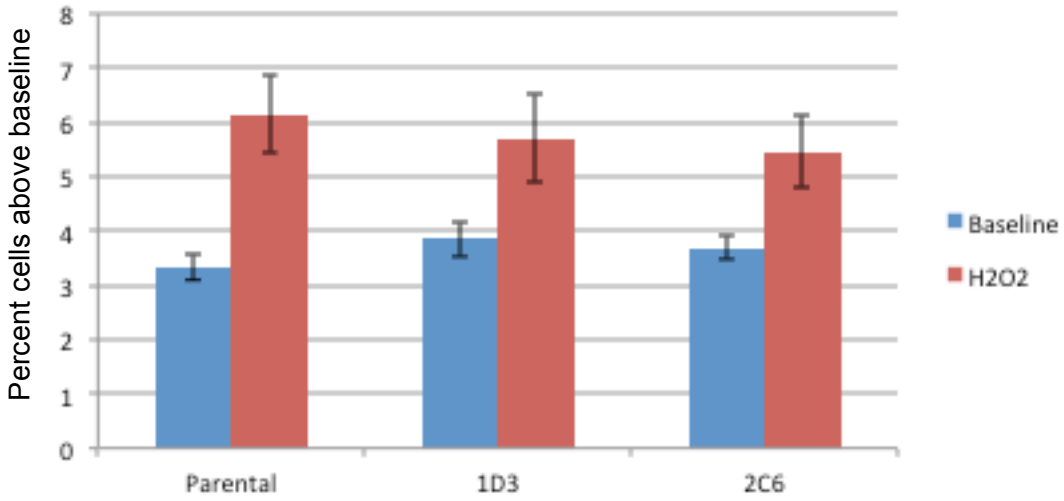

Figure 15: Response of Hct116 cells with mutant IDH1 (Clones 1D3 and 2D6) to oxidative stress as measured by FACS. Cutoff for positivity set to include 95% of parental cells at baseline. Error bars represent standard deviation of experiment completed in duplicate. P>0.05 for experimental lines compared to parental line under the same condition.

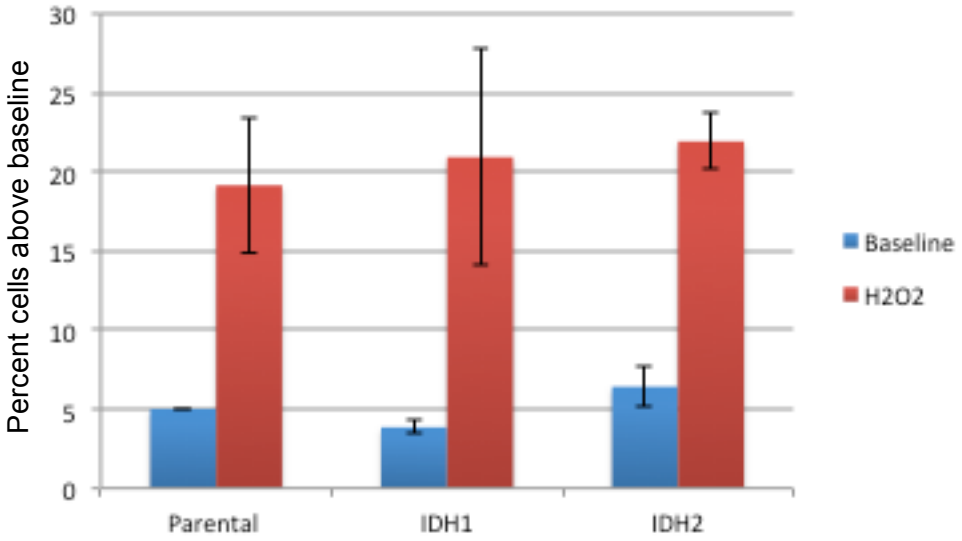

Figure 16: Response of mouse ES cells with mutant IDH1/2 to oxidative stress as measured by FACS. Cutoff for positivity set to include 95% of parental cells at baseline . Error bars represent standard deviation. P>0.05 for experimental lines compared to parental line under the same conditions.

4.3.4. Role of Mutant IDH1/2 in Hypoxia Signaling

To assess the response to hypoxia, we exposed Hct116 cell lines with either wild-type or mutant IDH1 to mild hypoxia for 24 hours. While levels of HIF-1α increase in the setting of hypoxia, the increase in protein is attenuated in mutant IDH1 cell lines compared to the wild-type parental cell line (Figure 17).[2] These studies were completed initially at Duke and replicated in the Kaelin lab with similar results.

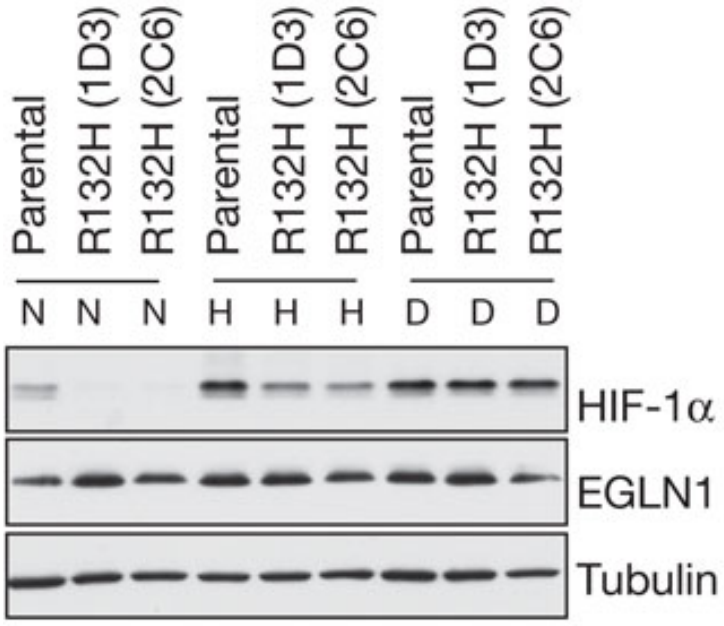

Figure 17: IDH1^{R132H} attenuates response to hypoxia in Hct116.[2] N= normoxia, H= 7.5% oxygen,, D= DFO. Exposure to hypoxia or DFA was for 16 hours.

4.3.5. 5-hydroxymethylcytosine Status in Mouse ES Cells with Mutant IDH1/2

To assess levels of 5-hydroxymethylcytosine in mouse ES cells, we first completed a dot-blot assay, in which the levels in experimental lines are measured as a

fraction of levels in the parental line. Compared to the parental line, levels of 5-hydroxymethylctyosine are decreased in cell lines containing mutant IDH1/2 (Figure 18).

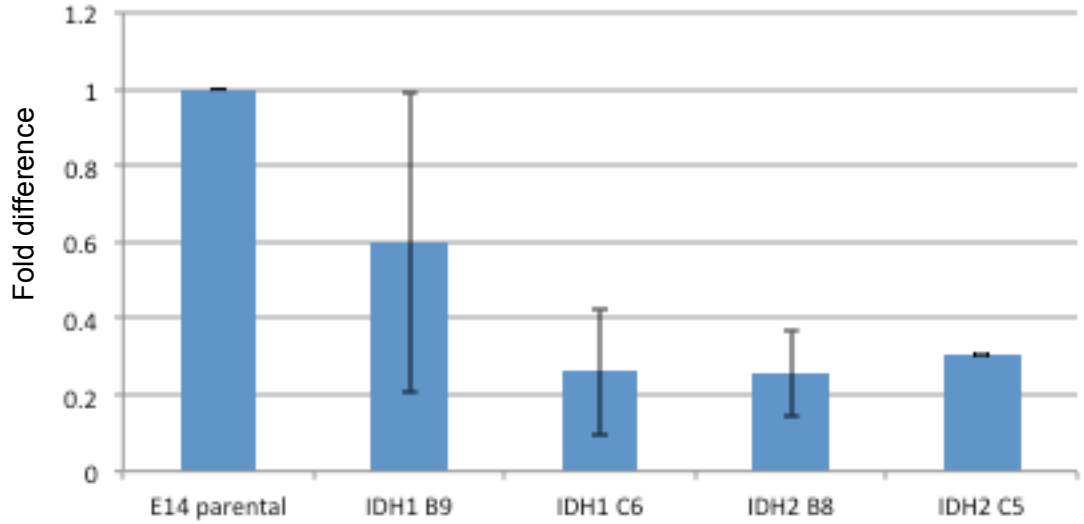

Figure 18: Global 5-hydroxymethylcytosine levels in mouse ES cells with mutant IDH1/2. Y axis = fold difference from levels in the parental E14 mouse ES cell line. Error bars represent standard deviation. Values represent average of two separate experiments completed on different days.

Following these initial studies, we quantitatively measured levels of 5-hydroxymethylcytosine. Levels of 5-hydroxymethylcytosine were measured as a fraction of total cytosines, and were decreased in cell lines with mutant IDH1 or mutant IDH2 compared to the parental line, although the decrease in 5-hmC did not reach statistical significance.

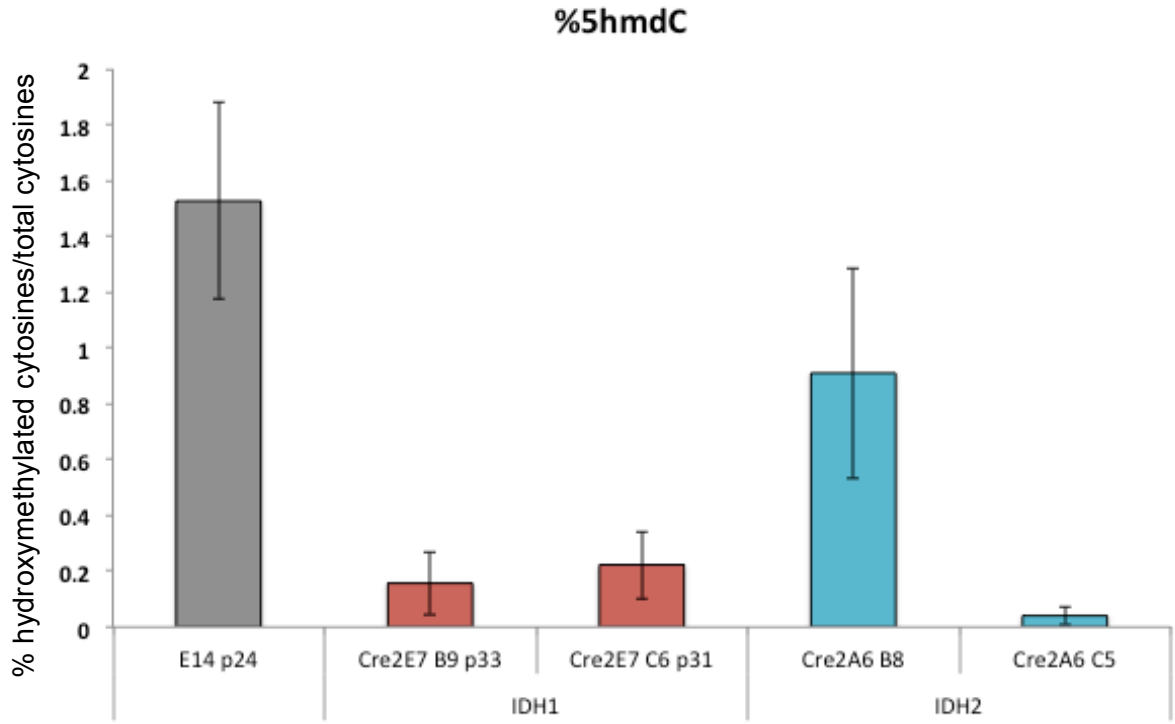

Figure 19: 5-hydroxymethylated cytosines as a percentage of total cytosines. Error bars represent standard deviation of two biological replicates.

4.4. Discussion

Mouse ES cells were successfully generated which had successful homologous recombination leading to the presence of either mutant IDH1^{R132H} or IDH2^{R172K}, as verified by genomic DNA sequencing of the appropriate region (Figure 7). Expression was verified through sequencing of mRNA expression from both wild-type and mutant alleles (Figure 8), and functional protein was verified through assessment of increases in levels of 2-HG (Figure 9).

4.4.1. Metabolic Profiling in Mouse ES Cells

We completed metabolic profiling in mouse ES cells in an attempt to understand the metabolic changes that occur in a cell with mutant IDH1/2. Over 200 chemicals were identified and analyzed in the study. In general, TCA cycle intermediates demonstrated only subtle differences in levels. This is in line with findings from metabolic profiles using other cell lines within the lab (data not shown). Glutamine was found to be decreased in mouse ES lines with mutant IDH1/2 (Figure B- 2). Glutamine has shown to be a source of substrate for eventual generation of 2-HG.[85] Therefore, if the cells are actively generating 2-HG, it is probable that these cells might be depleting glutamine in the process. In our own preliminary studies, increased glutamine in the media appeared to lead to increased levels of 2-HG (data not shown). However, in a larger sense, there were no large trends or changes detected in the levels of TCA cycle intermediates. A limitation of these studies is that they represent only one time point. It is possible that analyses of flux through the TCA cycle may reveal changes not obvious when looking at a metabolic snapshot. Futures studies analyzing flux through pathways, such as studies utilizing carbon-labeled substrates, may identify changes not identified through metabolic profiling alone.

However, there were some differences in metabolites that appeared to point to potential changes in other pathways. Of note, increases in oxidized glutathione, 2-aminobutyrate, and ophthalmate were identified (Figure 11, Figure 12, Figure B- 3), suggesting an increase in oxidative stress, as will be discussed in the subsequent section.

4.4.2. Mutant IDH1/2 and Oxidative Stress

The ramifications of mutant IDH1/2 on cellular behavior are still largely unknown. IDH1 and IDH2 produce NADPH, a reducing equivalent which confers cellular protection against oxidative damage. As GBM patients with IDH1/2 mutations have a longer survival than GBM patients with wild-type IDH1/2, we postulated that IDH1/2 mutants may provide tumor cells with sensitivity to oxidative stress, such as that conferred by chemotherapy or radiation therapy. Metabolic profiling identified an increase in oxidized glutathione and an increased ratio of oxidized glutathione to reduced glutathione in mouse ES cells with $IDH1^{R132H}$ or $IDH2^{R172K}$ compared to the parental lines (Figure 11). Additionally, there was an increase in ophthalmate (Figure 12), and 2-aminobutyrate (Figure B- 3), an intermediate in the synthesis of ophthalmate. Ophthalmate has been suggested to be a biomarker of oxidative stress.[153-155] These two intriguing results suggested a degree of increased oxidative stress within the cells even at baseline, since they implied the potential for increased flux through the glutathione biosynthesis pathway. To assess for baseline level of oxidative stress in cell lines with mutant IDH1/2, and the ability to respond to stressors, we measured stress in mouse ES cells and Hct116 cell lines with mutant IDH1/2, utilizing H_2DCFDA.

Initial studies using H_2DCFDA utilized light microscopy to assess for gross changes in fluorescence. These studies were completed in both mouse ES cell lines and Hct116 cell lines with mutant IDH1/2, comparing them to the respective parental lines either at baseline or under the setting of pseudo-hypoxia. Results were disappointing, as there were no clear gross differences in the presence of mutant IDH1/2 (Figure 13,Figure 14). Therefore, we proceeded to do a more quantitative assessment utilizing

FACS. Following exposure to H_2DCFDA, cell fluorescence was analyzed using flow cytometry, allowing for quantitative measurement of changes in reactive oxygen species levels both at baseline and in response to stress. This would allow us to assess if the cells were 1) more stressed at baseline or 2) able to compensate at baseline, but more sensitive to additional stressors. Again, despite multiple studies utilizing different cell lines with mutant IDH1/2, there were no significant differences in fluorescence between cell lines with mutant IDH1/2 and those without (Figure 15,Figure 16). This would suggest that if there is a difference in levels of oxidative stress, any differences are likely too small to be biologically relevant. Studies completed by collaborators in human astrocytes with mutant IDH1 utilizing H_2DCFDA also did not find significant differences in reactive oxygen species either at baseline or under the setting of increased oxidative stress.[2]

Results of studies by other groups on the implications of 2-HG or mutant IDH for cellular stress have yielded conflicting results. Sasaki et al. generated mice which expressed mutant IDH1 in a population of brain cells. They found decreased levels of reduced glutathione intracellularly in these mice,[121] consistent with our findings of increased oxidized glutathione in our mouse ES cells expressing mutant IDH1 or mutant IDH2. Again, this would appear to suggest increased levels of oxidative stress. However, in their in vivo system, they found a decrease in reactive oxygen species as measured by H_2DCFDA in various populations of brain cells in Nestin-Cre/IDH1^{R132H} mice.[121] On the other hand, in studies completed by another group, when 2-HG was added to the cerebral cortex of rats, there was an increase in oxidative stress.[156] Complicating things further, studies with mutant IDH1 in myeloid progenitors did not detect a significant change in ROS.[88] Further research is needed to better understand these paradoxical

findings and the specific contexts under which oxidative stress may be increased or decreased.

4.4.3. Hypoxia Signaling Impacted by Mutant IDH1

2-HG bears structural similarity to α-ketoglutarate, and studies have found inhibition of a number of α-ketoglutarate-dependent dioxygenases in the presence of 2-HG.[87,106,157] Prolyl hydroxylases (PHD), which are α-ketoglutarate-dependent dioxygenases, normally function to lead to the ubiquitination and degradation of HIF-1α. Because of findings by other labs of inhibition of a number of α-ketoglutarate-dependent dioxygenases by 2-HG, we hypothesized that introduction of mutant IDH1 into cell lines would lead to an increase in HIF-1α as a response to inhibition of PHDs. Quite to our surprise, we found that the presence of mutant IDH1 leads to an attenuated response to hypoxia in Hct116 with mutant IDH1 (Figure 17).[2] Work in our lab and with collaborators found that response to hypoxia as measured by HIF-1α was attenuated in a number of different cell lines with mutant IDH1, including human astrocytes and a human oligodendroglioma line.[2] Further studies with collaborators revealed that, although 2-HG is an antagonist of TET2, 2-HG appears to serve as an agonist of PHD2, being converted to α-ketoglutarate and serving as a substrate for generation of succinate and increased activity of PHD2.[2] Gene expression signatures from IDH-mutated astrocytomas appear to agree with these findings, suggesting an impaired HIF response compared to wild-type astrocytomas of similar grade.[2] Thus, whether 2-HG serves as an agonist or antagonist of an enzyme is likely dependent on the structure and active site of that particular enzyme.

Upregulation of hypoxia signaling is often described in cancers as pro-tumorigenic, as it can lead to increased angiogenesis and assist with growth of the tumors. Thus, we were initially surprised to identify a decrease in HIF-1α in our cell lines with mutant IDH1, and continued to be surprised as work with further cell lines only re-affirmed our initial findings.[2] However, there are scenarios in which a decrease in HIF-1α could be pro-tumorigenic. In one study, a group generated an astrocytoma line in which HIF-1α was knocked out.[158] This line grew more slowly than the same line with intact HIF-1α when injected subcutaneously in mice, but grew more quickly and more invasively when injected in the brain.[158] Thus, the surrounding parenchyma may impact whether the same mutations are pro-tumorigenic or not. This has serious implications for studies attempting to address the implications of hypoxia signaling in gliomas, as context is critical. Progressive gliomas are by their nature invasive tumors. The findings from this group suggest that changes in HIF-1α may be one factor that modulates that invasiveness.

Hypoxia signaling often leads to increased VEGF and angiogenesis. Yet, low grade gliomas are in part defined by a lack of endothelial hyperplasia and a lack of microvascular proliferation, features which are observed in and define GBMs.[7] An attenuation of hypoxia signaling in progressive gliomas by mutant IDH1/2 may be a reason why these features are only observed in higher grade tumors. Further research is needed to better understand the implications of the presence of mutant IDH1/2 for hypoxia signaling in the context of progressive gliomas. Research on other pathways have often revealed that different parts of a single pathway may react differently to different stimuli; it is not always simply “on” or “off.” Further research utilizing patient

samples and mouse models may help further elucidate some of these contradictory findings.

4.4.4. 5-hydroxymethylcytosine and Mouse ES Cells

Levels of 5-hydroxymethylcytosine have been shown to decrease in the absence of TET2.[117,159] 2-HG appears to inhibit TET2 function in acute myeloid leukemias, and may impair differentiation of hematopoietic precursors.[87] Recently, 5-hydroxymethylcytosine levels were found to increase in the brain throughout development into adulthood; the lowest levels of 5-hydroxymethylcytosine were identified in neural precursor-like cells and the developing brain.[160]

In mouse ES cells, levels of 5-hydroxymethylcytosine change during differentiation.[115,116] Thus it would be reasonable to assume that mutant IDH1/2 would have the potential to impact levels of 5-hydroxymethylcytosine in mouse ES cells. Indeed, we found a decrease in the levels of 5-hydroxymethylcytosine in mouse ES cells utilizing two different methods to detect 5-hydroxymethylcytosine (Figure 18,Figure 19). This is in concordance with what has been found in other cell lines within our lab, and in leukemias in other labs.[87] We did not detect significant changes in the levels of 5-methylcytosine (Figure B- 4). This trend appears to hold true in vivo. Recent studies by other groups utilizing Nestin-Cre/IDH1$^{R132H/wt}$ mice identified lower levels of 5-hydroxymethylcytosine in neural stem cells from these mice.[121] Studies are underway in our lab utilizing cell lines with mutant IDH1 to better understand these epigenetic changes.[151]

Mutant IDH1/2 appear to impair hematopoietic differentiation in mice, and this appears to be correlated with a decrease in 5-hydroxymethylcytosine.[87] These studies

have the potential to yield insights into leukemias with mutant IDH1/2. Similar studies are needed to better understand progressive gliomas. Isolation of neural stem cells in which mutant IDH1/2 could be induced would be of particular interest in exploring the ramifications of changes in methylation and differentiation. Methylation profiling and gene expression studies completed on these cell lines with and without mutant IDH1/2 both at baseline and after differentiation could provide new insights into which genes are turned on or turned off in the presence of mutant IDH1/2.

5. Mouse Models of Mutant IDH2

5.1. Introduction

While we and others have completed cell line studies and patient sample studies to explore mutant IDH1/2, there are limitations to these studies. A mouse model system allows for mutant IDH1/2 cells to interact with the surrounding brain parenchyma and immune system. Long-term, mice with mutant IDH2 would allow for assessment of the efficacy of novel therapies to treat these deadly cancers. We explored the ability of mutant IDH2 to lead to tumorigenesis when induced in neural stem cells in a mouse model system. We utilized a conditional mutant $IDH2^{R172K}$ with expression under the control of Cre. Utilizing a broad driver, GFAP+, which leads to expression of Cre throughout the brain, we were able to generate mice with mutant IDH2 expressed broadly throughout the brain. Using a narrower driver requiring induction, Nestin-CreER, we were able to induce mutant IDH2 expression in a much more restricted population of cells. We also attempted to see if combining the most common mutations seen in progressive gliomas, namely, IDH mutation and p53 deletion, would impact tumor formation in mice.

5.2. Methods

5.2.1. Generation of Mice with Conditional Expression of Knock-in IDH2^{R172K}

All studies completed with mice were approved by the Duke Institutional Animal Care and Use Committee. To assess the effects of mutant IDH2 in an in vivo modeling system, mouse ES cells with conditional expression of mutant IDH2 were generated as described previously. Cells that were not treated with Cre, and who thus still retained conditional expression of the mutant enzyme, were injected into blastocysts to allow for the development of chimeras. These chimeras were used to generate offspring which were genotyped for the presence of heterozygous mutant IDH2 (Figure 6). These mice were then crossed with mice expressing Cre recombinase in different populations of cells.

To generate heterozygous mutant knock-in mice in which we can study the phenotype in the brain, we crossed two types of mice: (a) animals in which one allele of the IDH2 gene has been replaced with a mutant allele preceded by a stop signal flanked by recombinase recognition sequences (loxp-stop-loxp-mutant exon 3/4) (Figure 4) and (b) one of two sets of animals that express the Cre recombinase. The first set is GFAP-Cre mice, which express Cre broadly in glial cells, particularly in astrocytes.[122] The second is Nestin-CreER^{T2} mice,[161] which express an inactive Cre in neural stem cells (Nestin-CreER mice graciously donated by Gordon Fishell). Following treatment with tamoxifen, the Cre relocates to the nucleus, where it is active. These cells with active Cre, and all future cells derived from them, including astrocytes and oligodendrocytes,

will express heterozygous mutant IDH2. These mice will be referred to as GFAP-Cre/IDH2$^{R172K/wt}$ and Nestin-CreER/IDH2$^{R172K/wt}$ mice.

5.2.2. Mice with Multiple Mutations from Progressive Astrocytomas.

The most common combination of mutations in progressive astrocytomas is mutant *IDH1/2* in combination with mutation/deletion of *TP53*. Therefore, we also crossed Nestin-CreER/IDH2$^{R172K/wt}$ mice with p53$^{fl/fl}$ mice to yield mutant *IDH1/2* mice also heterozygous or homozygous for *loxp-p53-loxp* (Figure 20). This will allow for the presence of mutant *IDH2* and deletion of *TP53* within the same cells in the brain.

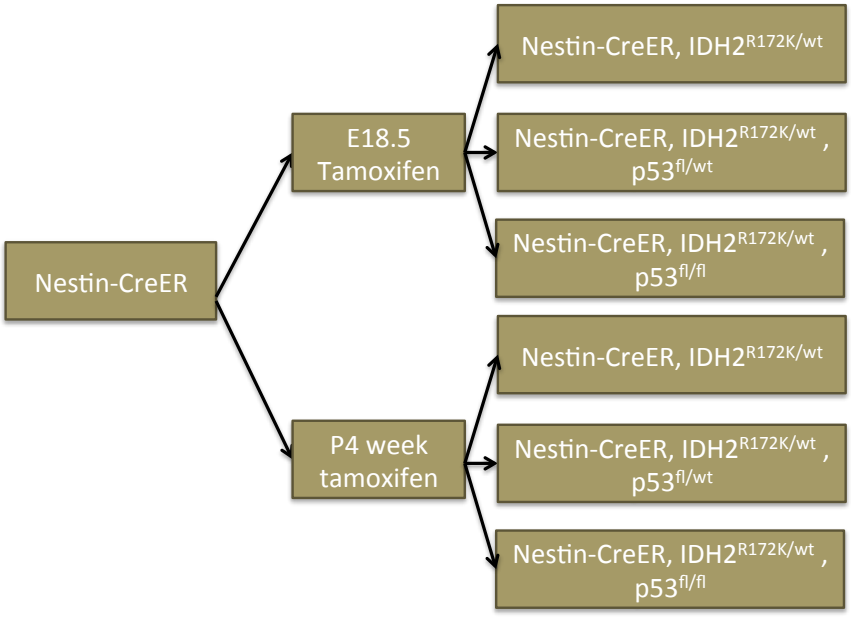

Figure 20: Schematic of Nestin-CreER mice. The same schematic was repeated with tamoxifen treated mice without Nestin-CreER as a control.

5.2.3. Induction of Mutant IDH2 in Populations of Cells.

Induction of expression of mutant IDH1 or mutant IDH2 will occur at two stages during development. Because human patients with oligodendrogliomas and progressive astrocytomas tend to be younger adults, we induced expression of $IDH1^{R132H}$ or $IDH2^{R172K}$ at 4 weeks of age, to approximate tumor onset in adults. This was done via administration of 200mg/kg of tamoxifen via oral gavage. Induction at 4 weeks of age also minimizes the number of non-tumor cells which will express the mutant protein, minimizing the chance of phenotypes resulting from expression of mutant IDH1/2 in normal tissues, which may confound results. However, because only a small fraction of cells will express mutant IDH1/2, this had the potential to be insufficient to allow for the formation of tumors. In addition, if tumors in humans form from mature astrocytes or oligodendrocytes rather than from stem cells, there is the potential to not see a phenotype following induction of mutations in adult mouse neural stem cells, since the majority of astrocytes and oligodendrocytes have already developed by this point and no longer express Nestin. Therefore, we also administered 3mg tamoxifen via oral gavage to pregnant female mice at E18.5 (treatments summarized in Figure 20). Studies with Nestin-CreER/EGFP have shown labeling of mature astrocytes and oligodendrocytes in mice when tamoxifen is administered at this stage of development.[162] This will provide two advantages. Because of the earlier induction, a larger population of cells will express mutant IDH1/2, thus increasing the odds of tumor formation. In addition, because this will lead to the presence of the mutation in both neural stem cells as well as mature astrocytes and oligodendrocytes derived from them, this increased the likelihood of the

mutation being present in the cell of origin for progressive gliomas, since the mutant protein will be expressed in a larger population of cells within the brain.

Experimental genotypes expressing the aforementioned combinations were generated in cohorts of approximately 15-20 mice for each experimental genotype and at least 4-20 mice for each control genotype. We included a cohort for each induction time (embryonic day 18.5 or postnatal week 4) and monitored for one year for the development of neurological symptoms or any signs of distress. Neurological dysfunction was checked at least every other day by assessing mice for difficulty with ambulation or posture, changes in hair coat, such as lack of grooming, and changes in activity level, such as pacing or reluctance to move. Mice that did not develop symptoms were sacrificed at 1 year of age to assess for presence of tumors or other abnormalities. Mice with symptoms were sacrificed either via intracardiac perfusion or CO_2 euthanasia. For intracardiac perfusion, mice were injected via intraperitoneal injection with a lethal dose of urethane, followed by intracardiac perfusion of at least 15mL of Dulbecco's Phosphate Buffered Saline and 15mL 4% paraformaldehyde to allow for fixation of tissues. Survival was calculated as overall survival rate between different genotypes. Statistics were completed using GraphPad Prism 6 (GraphPad), with log-rank tests to assess significance.

5.2.4. X-gal Staining Verification of Cre Activation Following Induction

For verification of successful Cre activation in the appropriate cells in mouse brains following treatment with tamoxifen, Nestin-CreER$^{+/-}$ mice were crossed with Rosa-(loxp-stop-loxp)-LacZ mice (Rosa-LacZ$^{+/-}$). In these mice, all cells in which Cre was activated, and the progeny of those cells, will stain blue in the presence of X-gal. Mice were treated with tamoxifen at either E18.5 or P4 weeks of age as described previously. At 7-9 weeks of age, mice were administered a lethal dose of urethane, followed by intracardiac perfusion with at least 15mL 0.1M phosphate buffer (PB). Following exsanguination, mice were perfused with at least 15mL fixation solution (0.1M PB, 2.5% glutaraldehyde. 2% paraformaldehyde). Brains were then dissected and placed in chilled post-fixation solution (0.1M PB, 2.5% glutaraldehyde) overnight with gentle rocking. Brains were washed in cold 0.1M PB for six washed of 10 minutes each with shaking. Using a vibratome, brains were sliced into 100µm slices and placed in chilled 0.1M PB. A stock K3 solution (100mM $K_3Fe(CN)_6$ in 0.1M PB), stock K4 solution (100mM $K_4Fe(CN)_6$ in 0.1M PB), and stock 5-bromo-4-chloro-3-indoyl-β-D-galacto-pyranoside (X-gal) solution (40mg/mL in dimethylformamide) were prepared, and used to make X-gal buffer (0.1M PB, 10mM $K_3Fe(CN)_6$, 10mM $K_4Fe(CN)_6$, 0.48mg/mL X-gal). Sections were placed in X-gal buffer overnight with gentle shaking at 37ºC in the dark. The reaction was stopped with cold Dulbecco's phosphate buffered saline with calcium and magnesium (DPBS) (Gibco, USA). Slices were washed several times in fresh DPBS, placed on positively charged slides and coverslipped using an aqueous mounting fluid.

5.2.5. 2-HG Measurement in Mice with Mutant IDH2

Mice that were either GFAP-Cre or GFAP-Cre/IDH2$^{R172K/wt}$ were euthanized via standard CO_2 euthanasia. Brains were dissected, cut into quarters (left hemisphere, right hemisphere, left cerebellum, right cerebellum), and immediately placed in storage at -80ºC. Samples were measured by LC-negative electrospray ionization-MS/MS as described previously.[145,146]

5.2.6. Histological Assessment of Tissues

Following fixation overnight in formalin, brains were transferred to 70% ethanol for paraffin-embedding. To allow for assessment for the presence of brain tumors, brains were sliced in horizontal sections. 5μm sections were obtained. A series of 12 sections were placed on positively charged slides, followed by 100μm steps, throughout the entire brain. The first and last section of each set was stained using haematoxylin and eosin (H&E) staining to assess for any histological changes in cellular organization or appearance, including increased cellular density, pleomorphic nuclei, and mitotic figures. Sections and stains of tumors and representative brains were reviewed by a neuropathologist. Stains were completed by the Research Histology Laboratory at Duke University. Cellular proliferation was assessed using Ki67 staining. Changes in structure and organization were assessed using H&E with Luxol Fast Blue (LFB). Brains with mucin-like material were stained with Periodic Acid Schiff (PAS). Brains with accumulations of cells of unclear type were stained with anti-GFAP and anti-S-100. Immunohistochemical staining was complete by Zuowei Su at the Duke Research Histology Lab. Tumors were additionally stained with anti-cytokeratin, anti-desmin, and anti-smooth muscle actin as needed.

5.3. Results

5.3.1. GFAP-Cre Mouse Model System

To assess whether functional IDH2 could be activated in cells within the brain, we measured levels of 2-HG following activation by Cre. Because GFAP-Cre leads to a broader expression of Cre throughout the brain, we assessed for generation of 2-HG in symptomatic GFAP-Cre/IDH2$^{R172K/wt}$ mice.

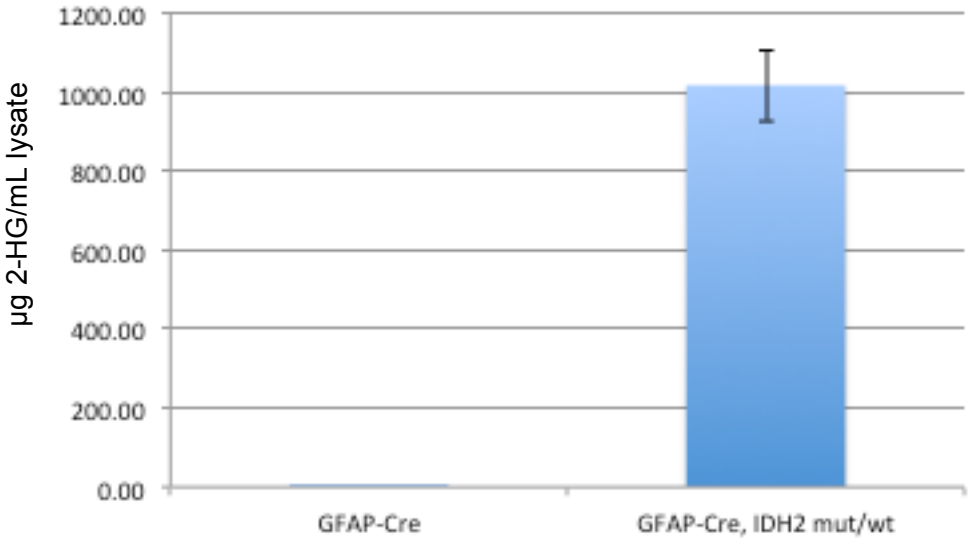

Figure 21: GFAP-Cre/IDH2$^{R172K/wt}$ mice generate 2-HG. P<0.005. Error bar represents standard deviation for four GFAP-Cre mice and three GFAP-Cre/IDH2$^{R172K/wt}$ mice.

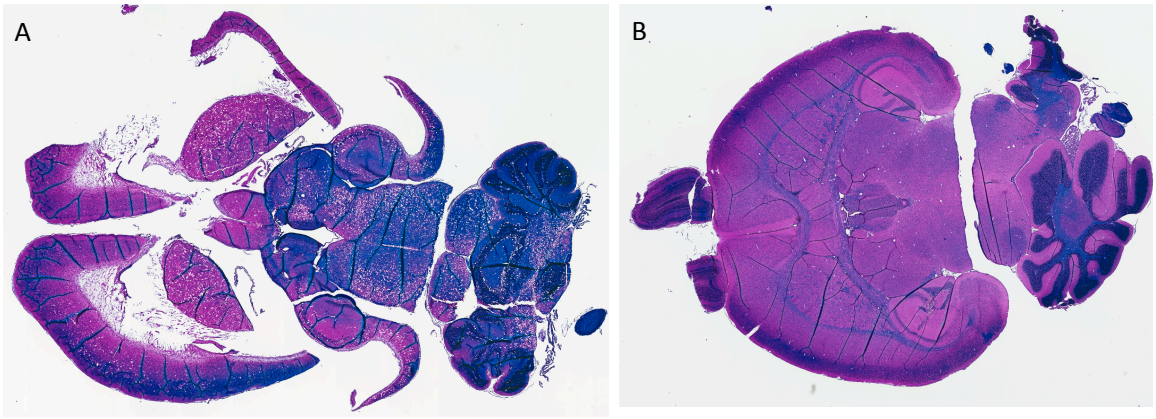

Figure 22: GFAP-Cre mice and brain histology. H&E with Luxol Fast Blue. A) GFAP-Cre/IDH2$^{R172K/wt}$ mouse, B) GFAP-Cre mouse.

A portion of GFAP-Cre/IDH2$^{R172K/wt}$ mice became symptomatic even prior to weaning. Symptoms included ataxia and head doming. The mice also had what could either be described as seizures or dystonic posturing. These mice demonstrated a several hundred-fold increase in 2-HG compared to GFAP-Cre littermates (Figure 21). Upon dissection, brains of GFAP-Cre/IDH2$^{R172K/wt}$ mice appeared to have enlarged lateral ventricles, as the brains collapsed inward bilaterally. H&E revealed brains with spongiform change throughout the parenchyma (Figure 22, Figure 23).

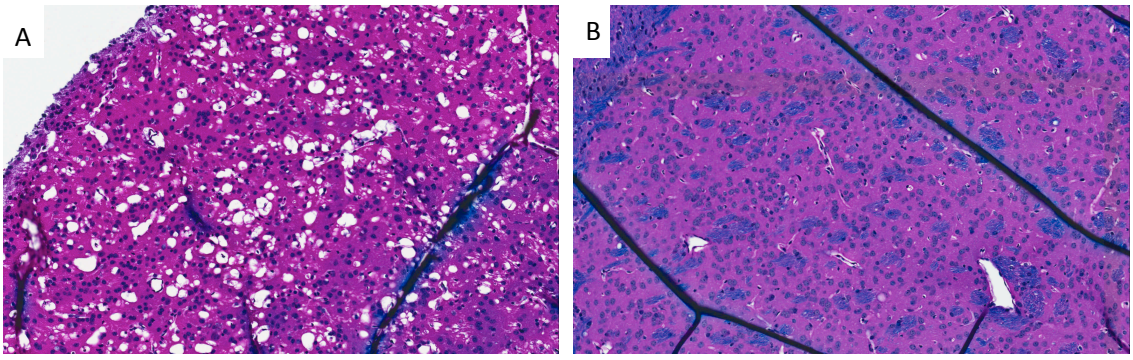

Figure 23: GFAP-Cre/IDH2$^{R172K/wt}$ and spongiform change. H&E with Luxol Fast Blue. 20x magnification vs. Fig.21. A) GFAP-Cre/IDH2$^{R172K/wt}$ mouse, B) GFAP-Cre mouse.

5.3.2. Verification of Nestin-CreER Mouse Model System

Nestin-CreER, because it requires tamoxifen for active Cre, and because Cre is only present in Nestin+ cells, does not lead to the same level of broad expression of Cre as does GFAP-Cre. To assess where cells with mutant enzyme would be present, we treated Nestin-CreER/Rosa-LacZ$^{+/-}$ with tamoxifen or corn oil at either E18.5 or P4 weeks of age. The greatest population of cells stained positive in mice treated at E18.5, with a smaller population affected in mice treated at P4 weeks of age. Of note, a small population of cells remained positive in untreated mice, suggesting some background "leakiness." The largest population of positive cells were present in the subventricular zone through the rostral migratory stream to the olfactory bulb. (Figure 24,Figure 25) Another population of cells was identified in the dentate gyrus of the hippocampus (Figure 26). Cells within the cerebellum also stained positive (not shown). In all treated mice, the brainstem demonstrated a greater degree of sporadically positive cells than the cortex (data not shown).

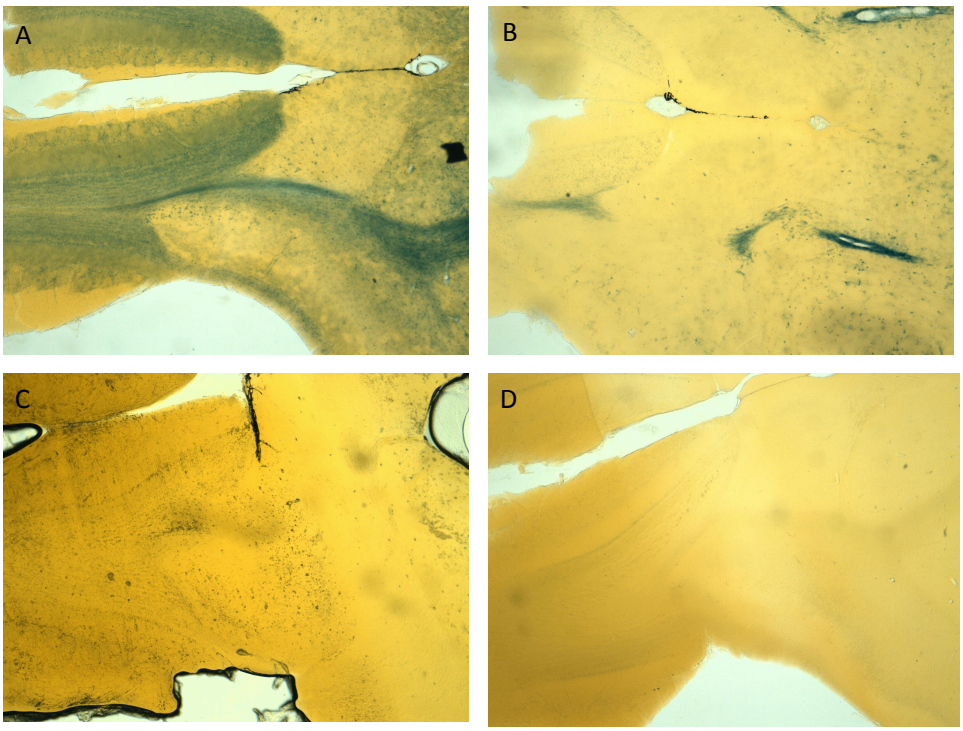

Figure 24: LacZ generation is induced in the subventricular zone and olfactory bulb of treated Nestin-CreER/Rosa-LacZ$^{+/-}$ mice. Horizontal view of rostral migratory stream going into the olfactory bulb on the left. A) E18.5-treated Nestin-CreER/Rosa-LacZ$^{mut/wt}$ mouse, B) P4 week-treated Nestin-CreER/Rosa-LacZ$^{+/-}$ mouse, C) corn oil-treated Nestin-CreER/Rosa-LacZ$^{+/-}$ mouse, D) E18.5-treated Rosa-LacZ$^{+/-}$ mouse.

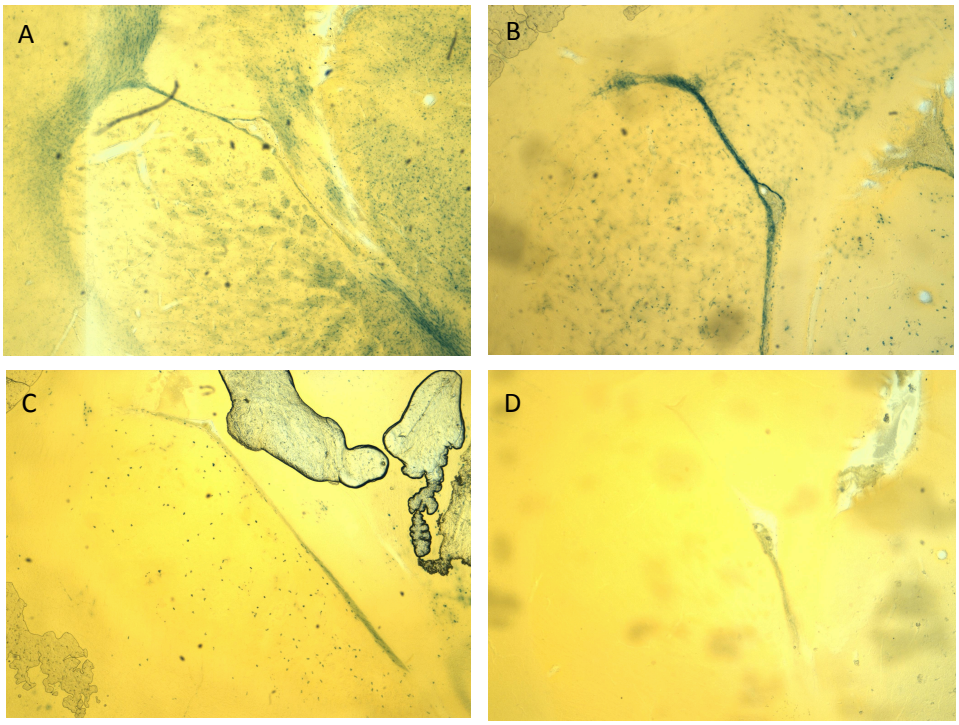

Figure 25: LacZ generation is induced in the SVZ of Nestin-CreER/Rosa-LacZ$^{+/-}$ mice. Horizontal view of SVZ , demonstrating increasing levels of positive following treatment with tamoxifen. A) E18.5-treated Nestin-CreER/Rosa-LacZ$^{+/-}$ mouse, B) P4 week-treated Nestin-CreER/Rosa-LacZ$^{+/-}$ mouse, C) corn oil-treated Nestin-CreER/Rosa-LacZ$^{+/-}$ mouse, D) E18.5-treated Rosa-LacZ$^{+/-}$ mouse.

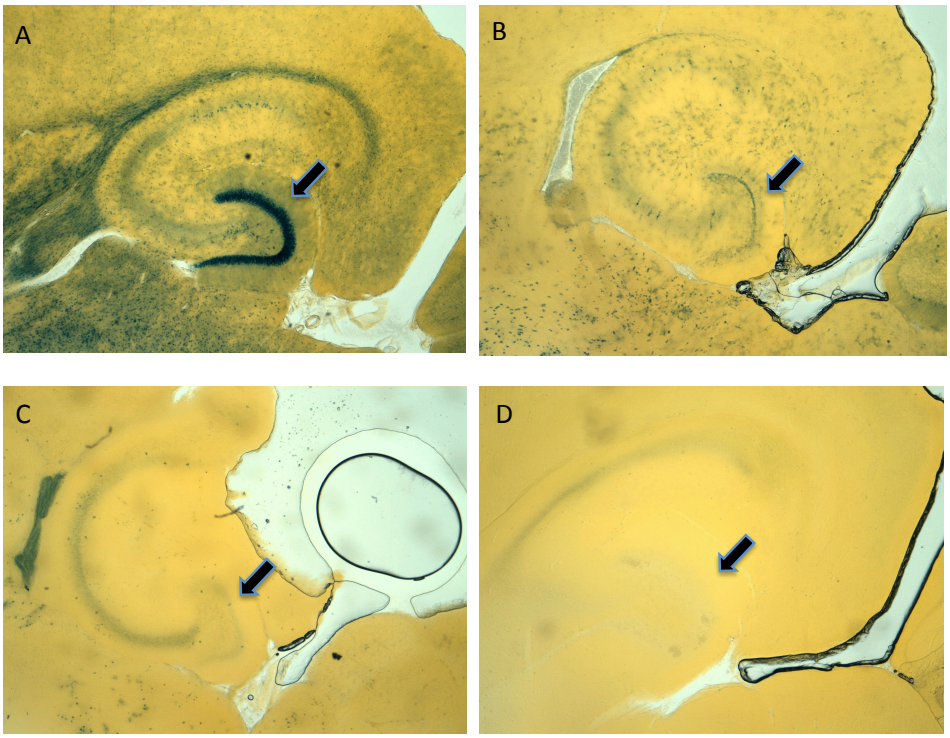

Figure 26: Active Cre is induced in the dentate gyrus of Nestin-CreER/Rosa-LacZ$^{+/-}$ mice following treatment with tamoxifen. Horizontal view of hippocampus, demonstrating increasing levels of positive staining in the dentate gyrus (arrow) following treatment with tamoxifen. A) E18.5-treated Nestin-CreER/Rosa-LacZ$^{+/-}$ mouse, B) P4 week-treated Nestin-CreER/Rosa-LacZ$^{+/-}$ mouse, C) corn oil treated-Nestin-CreER/Rosa-LacZ$^{+/-}$ mouse, D) E18.5-treated Rosa-LacZ$^{+/-}$ mouse.

5.3.3. Symptomatic Mice Have Increased 2-HG

To evaluate the changes in 2-HG under varying conditions, we measured 2-HG in mice with and without IDH2^{R172K} in varying scenarios. Mice without active IDH2$^{R172K/wt}$ demonstrated levels of 2-HG between 0-5μg/mL lysate. An asymptomatic E18.5-treated Nestin-CreER/IDH2$^{R172K/wt}$ mouse euthanized at the one-year time point demonstrated a >5-fold increase in 2-HG in the cortex compared to controls. Mice with neurological symptoms had a >200-fold increase in levels of 2-HG in their cortex compared to

controls. Some E18.5-treated Nestin-CreER/IDH2$^{R172K/wt}$/p53$^{fl/fl}$ mice developed flank tumors, which also demonstrated a >100-fold increase in 2-HG over that measured in the cortex of mice without mutant IDH2.

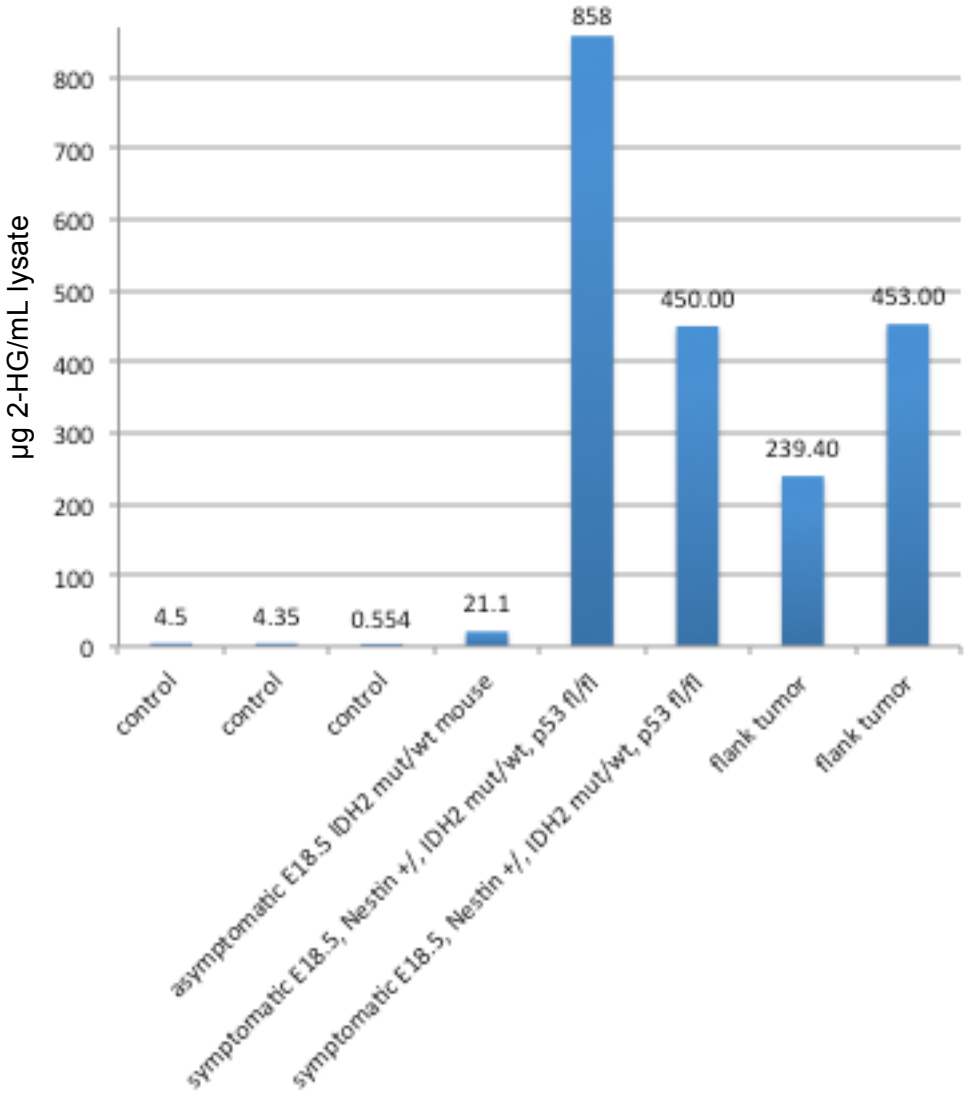

Figure 27: 2-HG is increased in symptomatic mice. Compared to control mice without IDH2 mut/wt, there is an increase in 2-HG in treated mice. Tissue analyzed is brain unless otherwise specified as a flank tumor.

5.3.4. Presence of Mutant IDH2 and/or p53 Deletion Impacts Survival

When treated embryonically at E18.5, Nestin-CreER/IDH2$^{R172K/wt}$/p53$^{fl/fl}$ mice (in red) demonstrated a significant difference in overall survival ($p<0.005$) compared to E18.5-treated Nestin-CreER/IDH2$^{R172K/wt}$ mice (in yellow) or Nestin-CreER/p53$^{fl/fl}$ mice (in orange) (Figure 28). While some mice treated at P4 weeks developed symptoms requiring euthanasia, the fraction of mice to become symptomatic was smaller compared to E18.5 (survival curves in Appendix Figure B- 6).

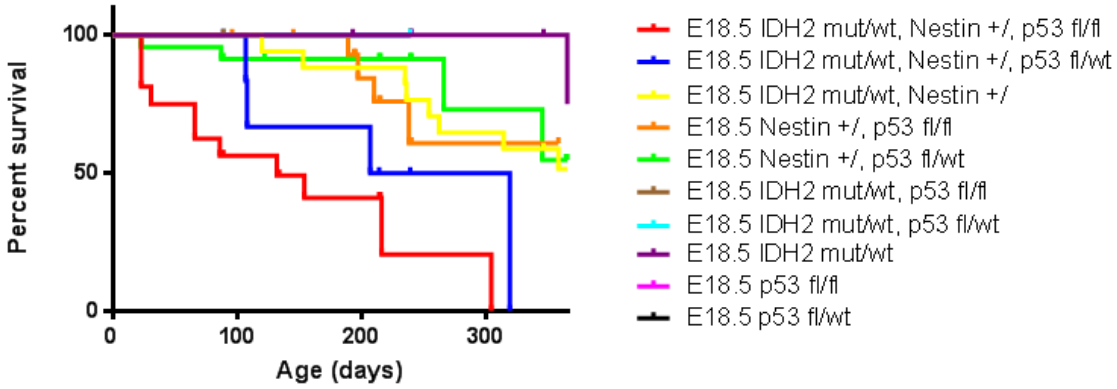

Figure 28: Presence of mutant IDH2 and/or p53 deletion impacts survival in Nestin-CreER mice induced at E18.5Colors/lines not visible did not have any deaths reported over the one year in which they were monitored.

None of the E18.5-treated Nestin-CreER/IDH2$^{R172K/wt}$/p53$^{fl/fl}$ mice or Nestin-CreER/IDH2$^{R172K/wt}$/p53$^{fl/wt}$ mice survived to one year, whereas a fraction of the mice in all other groups survived to one year (Figure B- 5).

(days)

5.3.5. Tumors in E18.5-treated Nestin-CreER/IDH2$^{R172K/wt}$/p53$^{fl/fl}$ Mice

An E18.5-treated Nestin-CreER/IDH2$^{R172K/wt}$/p53$^{fl/fl}$ developed head doming and difficulty with ambulation at 132 days of age. The mouse was euthanized as previously described and the brain formalin-fixed and paraffin-embedded. H&E analyses revealed a large central mass (Figure 29).

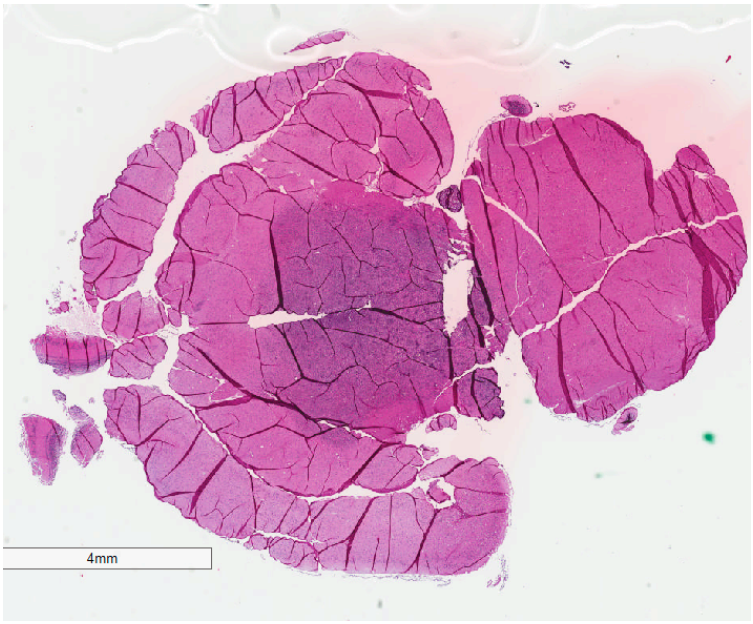

Figure 29: Tumor in E18.5-treated Nestin-CreER/IDH2$^{R172K/wt}$/p53$^{fl/fl}$ mouse.

Histological analyses revealed a migrating edge rather than pushing borders. Subarachnoid infiltration and peri-vascular infiltration were also present; additionally, 40-50% of tumor cells stained positive for Ki67 (Figure 30), a marker of proliferation. Immunohistochemical stains of the tumor were negative for staining utilizing anti-S-100, anti-GFAP, anti-CD45, and anti-pan-cytokeratin antibodies. S-100 positive reactive

astrocytes were present, as were some activated macrophages as identified through CD45 staining.

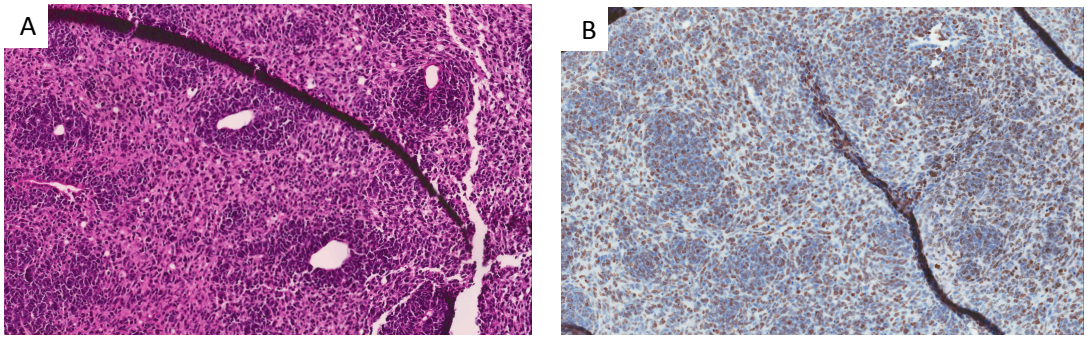

Figure 30: Staining reveals elevated Ki67 in brain tumor from E18.5-treated Nestin-CreER/IDH2$^{R172K/wt}$/p53$^{fl/fl}$ mouse. A) H&E stain, B) Ki67 stain.

Two E18.5-treated Nestin-CreER/IDH2$^{R172K/wt}$/p53$^{fl/fl}$ developed tumors on their flanks (one was euthanized at 304 days, while the other was euthanized at 154 days). Despite a lack of neurological symptoms, the presence of visible growth led to the decision to euthanize the mice. Both the tumors and brains from each mouse were paraffin-embedded. In one mouse, upon evaluation of the brain, we also identified tumor-like cells with an astrocytic appearance, fibrillar processes, and mucin in both olfactory bulbs (Figure 31). 25-30% of tumor cells stained positive for Ki67 (Figure 31). Tumor cells were focally positive for GFAP, and 20-30% of cells stained positive against S-100 (Figure B- 7).

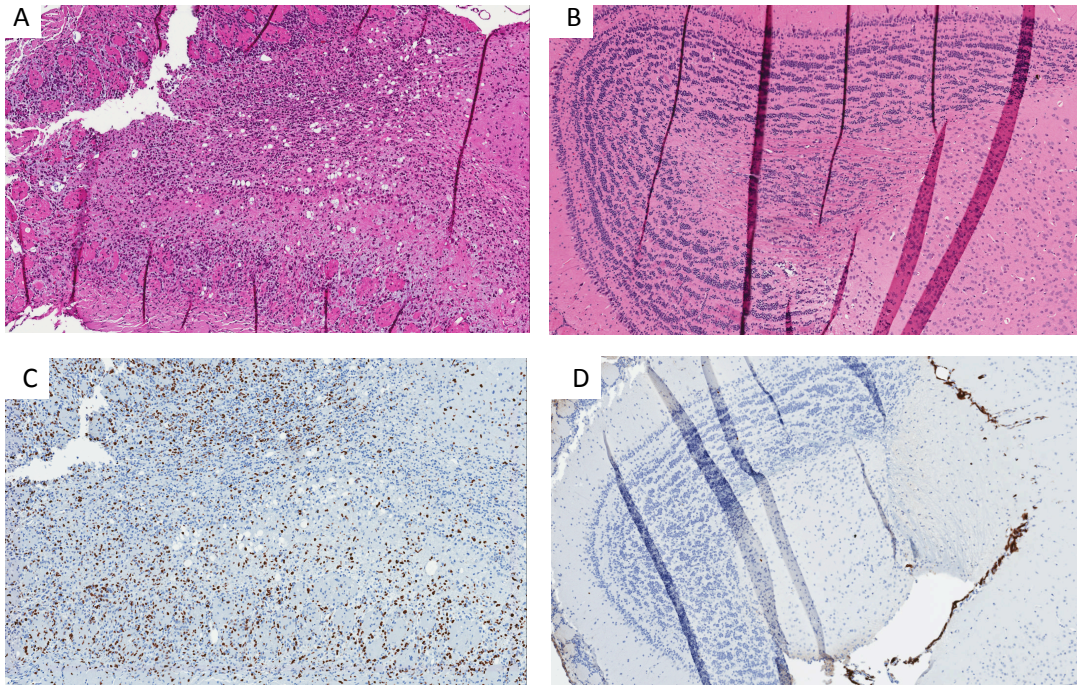

Figure 31: Disorganization and increased Ki67 in the OB of an E18.5-treated Nestin-Cre/IDH2$^{R172K/wt}$/p53$^{fl/fl}$ mouse. A,B) H&E stain, C,D) Ki67 stain. A,C) Experimental mouse. B,D) Control E18.5-treated IDH2$^{R172K/wt}$ mouse.

This same mouse was euthanized initially because of a tumor identified in the flank. Like the tumor in the olfactory bulb, the flank tumor was also focally S-100 positive (Figure B- 7). It had a higher Ki67, with 40-50% of cells staining positive (Figure 32). However, GFAP was negative (Figure B- 7).

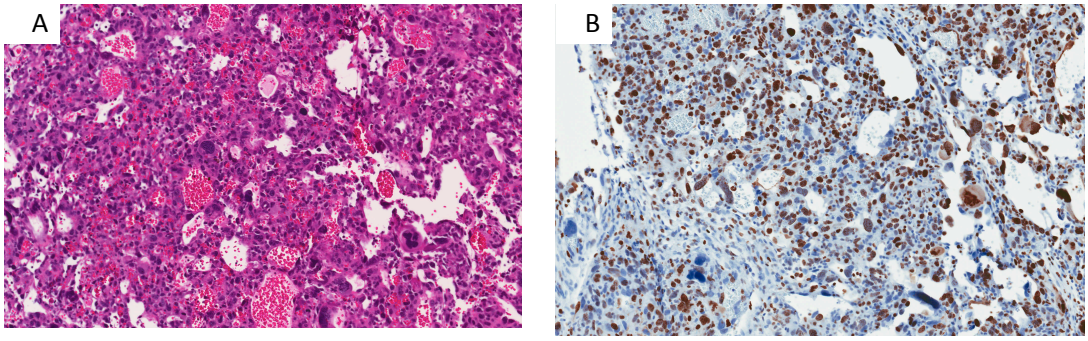

Figure 32: Flank tumor in E18.5-treated Nestin-CreER/IDH2$^{R172K/wt}$/p53$^{fl/f}$ mouse. A) H&E stain, B), Ki67 stain.

The second mouse to develop a flank tumor was also E18.5-treated Nestin-CreER/IDH2$^{R172K/wt}$/p53$^{fl/fl}$. The brain from this mouse appeared to be histologically normal. The flank tumor demonstrated pleiomorphic nuclei, carcinoma-like appearance, and Ki67 positivity in 25-30% of cells (Figure 33). GFAP and S-100 were negative (Figure B- 8)

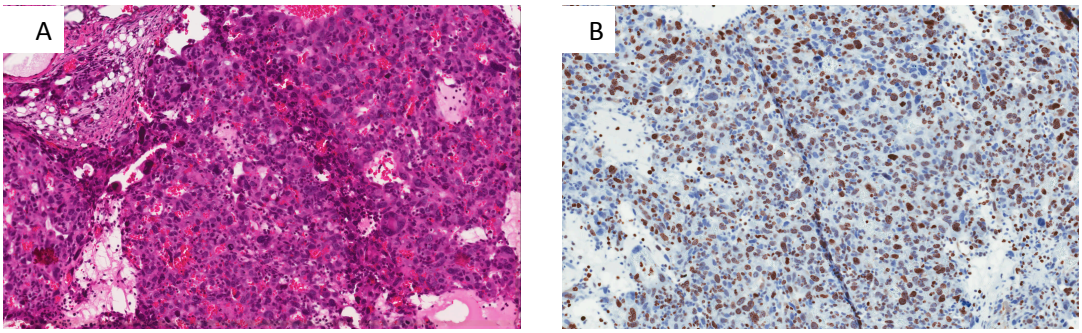

Figure 33: Flank tumor in E18.5-treated Nestin-CreER/IDH2$^{R172K/wt}$/p53$^{fl/fl}$ mouse. A) H&E stain, B), Ki67 stain.

5.4. Discussion

5.4.1. GFAP-Cre IDH2 Mice Have Severe Developmental Abnormalities

A recent study involving a conditional mutant IDH1^{R132H} explored the phenotypes that developed in the setting of mutant IDH1 under different drivers. When driven by Nestin-Cre, which leads to very broad expression, these mice developed hemorrhage and large cavities within the brain and died within a few days after birth.[121] GFAP-Cre/IDH1$^{R132H/wt}$ mice develop a milder phenotype, with some still exhibiting hemorrhage, but others surviving until adulthood.[121] Correspondingly, 2-HG levels in the brains of mice corresponded with the severity of the phenotype in the mice.[121]

We generated mice with GFAP-Cre driven IDH2^{R172K}. A fraction of the GFAP-Cre/IDH2$^{R172K/wt}$ mice developed severe ataxia and seizures. When 2-HG was measured in brains of these symptomatic mice, these mice had significant increases in 2-HG in the brains compared to baseline (Figure 21). Grossly, brains from these mice also developed large cavities, with hydrocephalus and enlarged lateral ventricles. Histologically, these brains exhibited spongiform change and encephalomalacia. However, despite these striking changes, there were no signs of tumors in GFAP-Cre/IDH2$^{R172K/wt}$ mice. It seems likely that the exceedingly high levels of IDH2 expression, and concomitant increase in 2-HG, led to neurological effects, such as those observed in patients with 2-hydroxyglutaric aciduria.[163] While no tumors were observed in the GFAP-Cre/IDH2$^{R172K/wt}$ mice, these findings do provide a unique opportunity with these mice. To our knowledge, there are currently no models of 2-hydroxyglutaric aciduria, and only one case report including a post-mortem analysis of histological

changes in the brain.[126] The changes observed in these mice, including hydrocephalus and encephalomalacia, appear to be consistent with what has been reported on MRI in humans with this disease.[123,125,129] This model could provide a means in which to better understand the neurological changes that occur in patients with mutant IDH2-based 2-hydroxyglutaric aciduria. An obvious alternative model is the generation of a mouse with germline expression of mutant IDH2 in all cells as are seen in some of these patients. However, in mouse models we generated, this is embryonic lethal (data not shown). To study 2-hydroxyglutaric aciduria with a viable model would require inducing the mutation later in life in all cells. Although this is certainly an important model and also one worth pursuing in the future, if any of the observed changes are a result of 2-HG early in life, they would be missed. Thus, GFAP-Cre/IDH$^{R172K/wt}$ mice may provide a means in which to better understand the neurological changes, and a system in which to begin to test potential treatments to either directly inhibit mutant IDH2 function or indirectly ameliorate some of the neurological symptoms.

5.4.2. Treated Nestin-CreER/IDH2$^{R172K/wt}$ Mice

In our continuing attempts to generate a model system for progressive gliomas, we then proceeded to generate Nestin-CreER/IDH2^{R172K} mice with and without other mutations observed in progressive gliomas. To our knowledge, these are the first mouse models generated in which there is expression of mutant IDH2.

To assess the effectiveness of treatment of our mice with one oral dose of tamoxifen at either E18.5 or P4 weeks of age, we utilized Nestin-CreER/Rosa-LacZ$^{+/-}$ mice treated at the aforementioned time points (Figure 20). Previous studies by other groups utilizing Nestin-CreER^{T2} reported that treatment of Nestin-CreER/Rosa-LacZ$^{+/-}$

mice leads to activation of Cre and subsequent recombination of cells largely within the subventricular zone (SVZ) and also to an extent with in the subgranular zone.[164] With time, the progeny of these cells become present in the olfactory bulb and the granule cell layer of the dentate gyrus.[164] Our findings were consistent with these results.

We treated Nestin-CreER/Rosa-LacZ$^{+/-}$ at either E18.5 or P4 weeks with tamoxifen, and sacrificed the mice at 7-9 weeks of age to assess activity using X-gal. Populations of positive cells were identified in the SVZ (Figure 25), with an additional population in the rostral migratory stream going into the olfactory bulb (Figure 24). Verification of expression in the subventricular zone was critical. Studies have identified that cells in the subventricular zone are more prone to malignant transformation than peripheral astrocytes.[165,166] There were additional populations identified in the dentate gyrus of the hippocampus (Figure 26). Positive cells were also identified in the cerebellum, with positive cells in the Purkinje layer with processes extending out into the molecular layer, consistent with Bergmann glia cells (data not shown), which have been reported in other models.[167] Of note, there was a dose-dependent increase in the number of positive cells. In E18.5-treated mice, cells in the corpus callosum were positive in addition to the aforementioned regions. In P4-treated mice, although cells were positive in all regions, there was a gross decrease in the degree in positivity. Of note, there is a degree of background leakiness, as sporadic positive cells were identified in the brains of mice treated with only corn oil. Thus, there is a theoretical potential for the development of symptoms in untreated mice due to the leakiness of Nestin-CreER at baseline. In a small cohort of mice of the experimental genotypes but treated with corn oil and monitored over one year, no deaths were observed (data not shown).

We were able to identify an increase in 2-HG in the brains of treated mice. Previous reports suggest that, in mice with mutant IDH1 expressed in the brain, severity of symptoms correlates with the levels of 2-HG measured in the brain.[121] We identified the strongest neurological symptoms in mice with GFAP-Cre/IDH2^{R172K}, which should have a broader expression than a system requiring induction for expression. We were uncertain if 2-HG levels would be detected in the brains of Nestin-CreER/IDH2$^{R172K/wt}$ mice, as only a small fraction of the cells in these brains would be generating 2-HG. In mice that developed neurological symptoms, we noted a several hundred-fold increase in the levels of 2-HG over that observed in mice without mutant IDH2. However, we questioned if this was an increase over the baseline in asymptomatic mice, which we had yet to measure. In other words, is 2-HG elevated in all treated Nestin-CreER mice with mutant IDH2 at all times, including asymptomatic mice, or does the fraction of IDH2^{R172K}-positive cells increase over time in some mice and lead to a corresponding increase in 2-HG and onset of symptoms? We measured 2-HG levels in an asymptomatic mouse with Nestin-CreER/IDH2$^{R172K/wt}$ that reached one year of age. Levels of 2-HG in the asymptomatic Nestin-CreER/IDH2$^{R172K/wt}$ were five-fold higher than levels of 2-HG in the brains of mice without IDH2. However, in symptomatic mice, the levels of 2-HG were over 100-fold higher. This would suggest that mice that become symptomatic either 1) have a larger mutant IDH2-positive population to begin with, eventually leading to neurological symptoms or 2) the mutant IDH2-postiive population in these mice increases over time, whether as a tumor or as an expansion of a population of cells normally present in the brain. As this was done with a small number of mice, more studies are needed to verify these observations, strengthen the correlation, and evaluate which hypothesis is more probable.

The presence of mutations in IDH2 or deletion of p53 appears to impact survival in E18.5-treated Nestin-CreER mice. The difference in survival was significant for E18.5-treated Nestin-CreER/IDH2$^{R172K/wt}$ mice vs. E18.5-treated Nestin-CreER/IDH2^{R172Kwt}/p53$^{fl/fl}$ at $p<0.005$ and for E18.5 Nestin-CreER/IDH2^{R172Kwt} mice vs. E18.5 Nestin-CreER/IDH2^{R172Kwt}/p53$^{fl/wt}$ at $p<0.05$. The difference in survival between E18.5 Nestin-CreER/IDH2^{R172Kwt}/p53$^{fl/fl}$ mice and E18.5 Nestin-CreER/IDH2^{R172Kwt}/p53$^{fl/wt}$ mice did not reach significance at $p<0.2$. Thus, the addition of p53 deletion, whether heterozygous or homozygous, to IDH2-mutated mice was correlated with a significant change in survival compared to mice with only mutant IDH2. Conversely, the addition of IDH2 to p53-homozygously deleted mice was also correlated with a significant difference in survival compared to mice with only p53 deletion. There was no significant difference in survival between those mice that had only mutation of IDH2 or only deletion of p53. It is worth noting that not all mice died of neurological causes. One mouse died from a GI obstruction, while another died from a renal obstruction, and yet another died from what might have been an inflammatory meningitis. For some mice, we were unable to determine the cause of death, and therefore could not rule in or rule out a brain tumor as a cause. For mice that were found dead, some of the brains were too degraded to interpret. Thus, to reflect this uncertainty, all survival curves refer to overall survival only. It is unclear if this difference in survival, therefore, is due solely to the presence of brain tumors, or if there is a non-CNS tumor pathology that is impacting the survival of the mice with both p53 deletion and IDH2 mutation more so than the mice with only one of these. Studies with a larger cohort of mice might help elucidate this.

We identified a tumor in the brain of an E18.5-treated Nestin-CreER/IDH2$^{R172K/wt}$/p53$^{fl/fl}$ mice. The central tumor demonstrated an invasive, migrating

edge. This tumor had an elevated Ki67, suggesting an aggressive tumor. However, this tumor did not stain positive for GFAP or S-100, which are often positive in glial tumors. Thus, it remains very possible that this is not a glial tumor, but rather a non-glial tumor driven by either mutant IDH2 or p53 deletion. Further stains are needed to characterize this tumor further.

Interestingly, two E18.5-treated Nestin-CreER/IDH2$^{R172K/wt}$/p53$^{fl/fl}$ mice developed flank tumors requiring euthanasia. One of these mice was also incidentally found to have a tumor in the olfactory bulb. However, the other mouse did not have any noticeable abnormalities in the brain. The tumor in the olfactory bulb, unlike the centrally-located tumor previously discussed, had a more astrocytic appearance, and was focally positive for both GFAP and S-100. Because the brain tumor and flank tumor in the one mouse shared some features, such as S-100 positivity, but did not share others, such as GFAP positivity, it is difficult to conclude one way or the other whether the two tumors are related to each other. It is possible that Nestin-CreER has leaky expression in tissues outside of the central nervous system. Knockout p53 mice develop other carcinomas and sarcomas, but do not develop brain tumors. Thus, we cannot rule out the possibility that leaky expression led to the development of a second tumor in the flank of the mouse that also had an olfactory bulb tumor. However, noting the presence of abnormalities in the olfactory bulb, which have also been identified in others of our mice, at least suggests the possibility of a tumor in the brain metastasizing elsewhere.

It is important to note that to date, no tumors have been identified in the brains of Nestin-CreER/IDH2$^{R172K/wt}$ mice without p53 deletion. This would suggest that IDH2 is at most a weak oncogenic driver. It is possible that mutations in IDH1/2 provide a cellular state in which other mutations are more easily able to promote tumorigenesis. It is

interesting to note that p53 knockout mice are not reported to form CNS tumors.[66-68] Likewise, to our knowledge there have been no reports of Nestin-CreER-driven p53 deletion leading to the development of brain tumors. The presence of two brain tumors and two flank tumors in the setting of both $IDH2^{R172K}$ and $p53^{fl/fl}$ is intriguing, but insufficient to draw large conclusions; more studies are needed to better understand the role of these mutations alone and in conjunction with each other. Studies involving a larger cohort of mice may allow us to identify more tumors and identify a trend in the types of tumors forming, as well as a more accurate evaluation of the rate of tumor formation. Other future studies include the use of different drivers, such as GFAP-CreER, to drive expression of mutant IDH2 and deletion of p53. The use of a different driver to induce these genetic alterations in slightly different cell types may impact the rate of tumor formation and the types of tumors formed. This may also provide insight as to the cell-of-origin for these tumors. Finally, future studies may include the generation of mice with additional mutations frequently observed in human gliomas. These studies may help in evaluating the roles of different mutations in gliomas. Additionally, gliomas with different mutations may respond differently to treatments. If they can be developed, mouse models reflecting the different genetic states of progressive gliomas in patients may allow for an improved ability to predict tumor response to various therapies.

We have identified that the presence of mutant IDH2 and p53 deletion in neural stem cells present at E18.5 and all their precursors is sufficient to impact survival in mice. We have identified four tumors in three E18.5-treated Nestin-CreER/$IDH2^{R172K/wt}$/$p53^{fl/fl}$ mice. Although it is not possible to draw definitely conclusions from these studies, they provide a basis upon which to build further studies. Further characterization of tumors in this mouse model is critical for evaluation of future utility of

the model system. This system holds the potential to provide a true in vivo mouse system, not requiring xenografts, in which to study tumors of the brain and mutant IDH2.

6. Summary and Future Directions

The identification of mutations in IDH1 and IDH2 in the vast majority of progressive gliomas led to a paradigm shift in the study of progressive gliomas. The field opened to include previously unidentified pathways as potentially playing a role in the development of progressive gliomas. The identification of a marked increase in 2-HG generation in the majority of progressive gliomas led to the coinage of the term "oncometabolite" to describe a compound that may be responsible for inducing tumorigenesis. However, the role that mutant IDH1/2 and 2-HG play in tumorigenesis in progressive gliomas is still unclear. Here, we completed a panel of studies involving patient samples, metabolic profiling of cell lines, and generation of mouse models to evaluate the role of these mutations in gliomas (Figure 34).

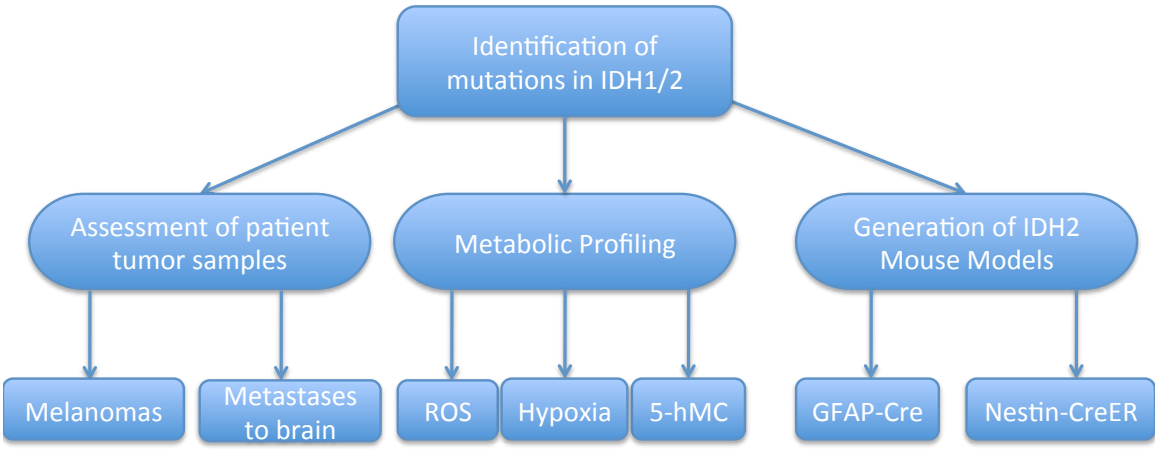

Figure 34: Overview of studies exploring and characterizing mutant IDH.

6.1. Assessment of Patient Tumor Samples

Through a series of studies on metastases to the brain, we attempted to ask whether these mutations worked to promote tumor growth in brain parenchyma in general, or worked to promote growth within a specific cell-of-origin within the brain. We did not find any mutations in IDH in tumor metastases to the brain from non-CNS tumors. Because mutations in IDH1/2 are among the earliest identified in gliomas, we propose that mutations in IDH1/2 may be necessary for tumor initiation when present in a specific cell-of-origin. Further studies, utilizing both patient samples and mouse models, may help to identify this specific cell-of-origin. Studies with patient samples, particularly of low-grade tumors, may identify key features of tumors that share similarity with certain cell types within the brain, such as neural stem cells or neural progenitor cells. Potential studies include immunohistochemical studies, methylation studies, and gene expression studies. Correlation to traits of specific normal cell types within the brain would be necessary to begin to be able to draw conclusions regarding a particular cell-of-origin.

6.2. Metabolic Profiling

Although the cell-of-origin for progressive gliomas has yet to be identified, we can begin to attempt to understand the role mutations in IDH1/2 play in gliomas by utilizing other model systems. Mutations in IDH1/2 are present at a high frequency in both astrocytomas and oligodendrogliomas, and are among the earliest identified mutations in both kinds of tumors. We propose that these mutations may occur in a common

precursor cell to both astrocytes and oligodendrocytes. Changes resulting from the presence of mutant IDH1/2 that impact a precursor cell may only be observed in vitro in studies on a cell line in a more undifferentiated state. Therefore, we utilized mouse ES cells with homologous recombination allowing for heterozygous expression of mutant IDH1 or mutant IDH2. A summary of our findings and potential implications are described in Figure 35. In our studies, we identified a decrease in 5-hydroxymethylcytosine in these cell lines in the presence of mutant IDH. This is an important finding, as levels of 5-hydroxymethylcytosine change in mouse ES cells during differentiation.[115,116] Additionally, a recent study identified that 5-hydroxymethylcytosine is likely to be decreased in human neural stem cells during development, with increased levels identified in adult brains.[160] Disappointingly, this same study did not identify any correlation between IDH1 mutation status and 5-hydroxymethylcytosine levels in the tumors evaluated.[160] Rather, 5-hydroxymethylcytosine status is associated with tumor grade, with the highest grade tumors demonstrating the lowest levels of 5-hydroxymethylcytosine, although this did not reach statistical significance.[160] However, this does not necessarily mean that mutations in IDH1/2 do not impact methylation. Rather, it suggests that if there are impacts on methylation, they may be more subtle than what has been identified with cell lines. Further study is needed to identify genes impacted by these mutations. Interesting future directions would involve study of the impact of mutant IDH1/2 on neural stem cells and their differentiation, a technically challenging, but not impossible endeavor. Novel model systems, such as the use of different drivers of mutant IDH1/2, may aid in these studies. The isolation of neural stem cells from genetically-engineered mouse models may be a method in which to accomplish these studies. Additionally, the utilization of 5-hydroxymethylcytosine or 5-

methylcytosine pull-down assays and mouse genome profiling on neural stem cells following induction of mutant IDH1/2 may allow for identification for genes that may be specifically altered as a result of the presence of these mutations. Clearly, more work is needed to understand the impacts of mutations in IDH1/2 on methylation and gene expression in tumor cells and potential cell-of-origin.

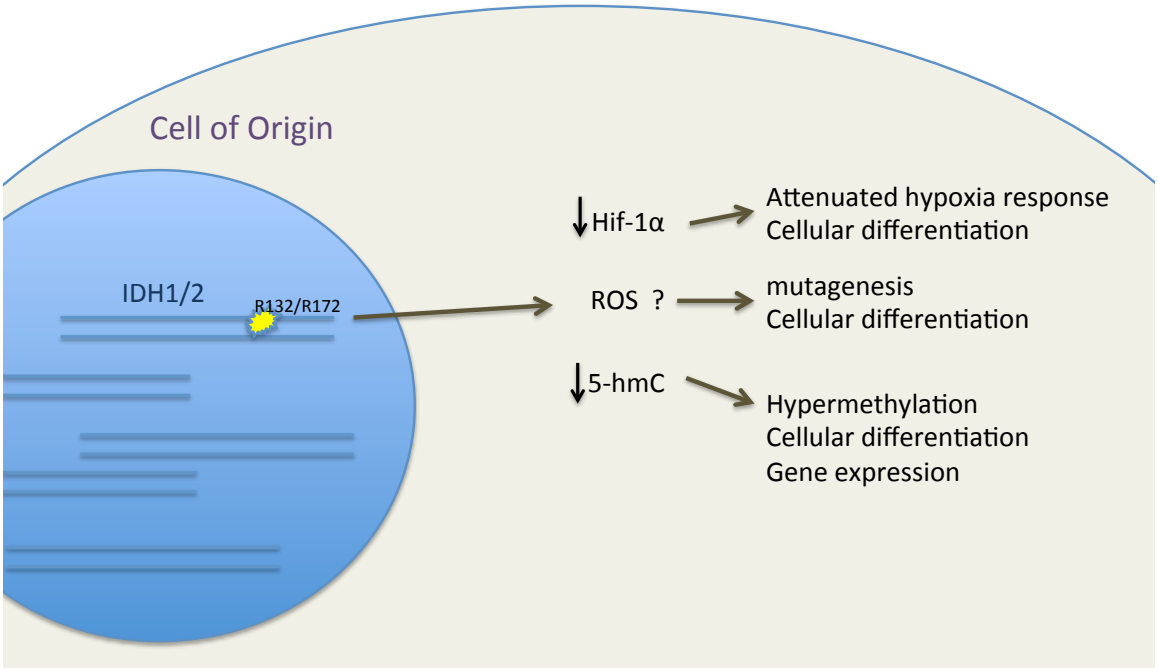

Figure 35: Potential changes results from presence of mutant IDH1/2.

6.3. Generation of IDH2 Mouse Models

Although much information can be gleaned from cell lines and in vitro studies, mouse model systems are critical to understanding the role of these mutations in vivo. Tumor cells do not exist on their own; they interact with their environment, the immune system, and surrounding cells. It is likely that the stem cell niche within the brain may play a role in providing a setting in which mutant IDH1/2 may promote tumorigenesis.

6.3.1. Mouse Models and 2-hydroxyglutaric aciduria

To study the role of mutant IDH2 in an in vivo system, we generated mice in which we could induce heterozygous expression of mutant $IDH2^{R172K}$ in a select population of cells within the brain. Broad expression led to severe neurological symptoms, including ataxia and seizures. Noting that neurological symptoms are frequent in patients with 2-hydroxyglutaric aciduria, this phenotype in our mice likely represents toxicity from elevated levels of 2-HG. This opens the opportunity for a unique model system in which to better understand the neurological implications of 2-hydroxyglutaric aciduria, a disease which is neurologically devastating in patients.

Future studies with this novel model system may involve correlating neurological effects with levels of 2-HG generation. Studies in mice with lower levels of 2-HG may identify areas that are particularly sensitive to the effects of 2-HG. Symptomatic mice with GFAP-Cre/$IDH2^{R172K/wt}$ demonstrated hydrocephalus, encephalomalacia, and significant spongiform change. Interestingly, about half of the E18.5-treated Nestin-CreER/$IDH2^{R172K/wt}$ mice evaluated by histology (regardless of p53 status) demonstrated some degree of spongiform change in either the hippocampus, near the lateral ventricles or in the front of the cortex, including the caudate putamen (data not shown). This evaluation only included euthanized and perfused mice, and did not include mice which were found dead and therefore had probable degradation between death and when the brains were dissected. Interestingly, these spongiform changes were not observed in any of the P4 week-treated Nestin-CreER/$IDH2^{R172K/wt}$ mice, regardless of p53 status. Our X-gal studies have identified that E18.5-treated mice have a greater fraction of cells expressing mutant IDH2 than P4-week treated mice. The areas with spongiform change appear to correlate with the areas of highest numbers of positive cells. It is tempting to

speculate that this may reflect a degree of 2-HG-related neurotoxicity within the E18.5-treated Nestin-CreER/IDH2$^{R172K/wt}$ mice. Interestingly, one study in patients comparing GBMs with and without mutant IDH1 found that tumors with *IDH1*$^{R132H/wt}$ were more likely to have a cystic component and be in contact with the ventricles than tumors with wild-type *IDH1*.[168] Directed studies correlating 2-HG levels and degree of spongiform change within the same brain are needed to verify these intriguing observations. This also provides a possible explanation for the decrease in survival observed among E18.5-treated Nestin-CreER/IDH2$^{R172K/wt}$ mice, and for the lack of obvious tumors in the majority of brains assessed by histology. If IDH2^{R172K} induced in neural stem cells present at E18.5 leads to neurotoxicity, this could decrease the lifespan of impacted mice.

6.3.2. Mouse Models and Tumors

To better study the role of mutant IDH2 in brain tumors, we expressed the mutant protein in a select population of neural stem cells and their progenitors. The cells induced were either 1) E18.5 neural stem cells and their progenitors, or 2) P4-week neural stem cells and their progenitors. Since p53 is also frequently mutated in progressive gliomas, we also induced heterozygous or homozygous deletion of p53 utilizing the same driver. No tumors were noted in mice with only mutant IDH2, regardless of when they were treated with tamoxifen. This would suggest the possibility that IDH2^{R172K} is at most weakly oncogenic, and not sufficient to lead to tumor formation in this model system. However, it is possible that we are not reaching the correct cell-of-origin, in which it might more rapidly form tumors. Thus, mouse studies utilizing different Cre drivers, such as GFAP-CreER (which would lead to induction of mutant IDH2 in

GFAP positive cells only following treatment with tamoxifen), or treatment with tamoxifen at different time points in either CreER system, may help clarify this further.

Tumors were identified in E18.5-treated mice that had IDH2 mutation and simultaneous deletion of p53. One mouse developed a tumor encompassing a large central portion of the brain. Two mice developed flank tumors; one of these mice was also found incidentally to have a tumor in the olfactory bulb. However, these tumors did not all share the histological features typically associated with astrocytomas or oligodendrogliomas. Further studies are needed to better characterize these tumors. Additionally, it is extremely challenging to draw large conclusions based on such a small number of tumors. These studies provide a base upon which to build our understanding of mutant IDH2 and progressive gliomas. The expansion of the number of mice with these genotypes may help us better understand these tumors by giving us a larger number to explore and characterize.

Genetically-engineered mouse model systems for the study of gliomas rarely demonstrate formation of tumors in the setting of only one genetic alteration. Mutations in IDH2 and p53 are not the only mutations observed in progressive gliomas. Further information on the roles of mutations in the development and progression of tumors may be yielded through the introduction of other commonly observed mutations in both progressive astrocytomas and oligodendrogliomas. These include alterations such as PDGFR overexpression, oncogenic PIK3CA mutation, or deletion of Rb, ATRX, ARF, CIC, or FUBP1. These studies will provide us not only with an insight into the impact different mutations have on the progression of gliomas, but also have the potential to provide unique, genetically-faithful model system in which to test therapies against this devastating disease.

Appendix A

Section 3 is based on an article published in *Biochemical and Biophysical Research Communications.* Per the journal at http://www.elsevier.com/wps/find/authorsview.authors/rights, the rights of the authors include “the right to include the journal article, in full or in part, in a thesis or dissertation.” For Section 4.2.5 and 4.3.5, which are in part from work in Koivunen, et al., Nature, 2012, data or protocols from that article were included based on the rights of authors as described in http://www.nature.com/reprints/permission-requests.html to “reproduce the Contribution in whole or in part in any printed volume (book or thesis) of which they are the author(s),” as long as the journal is acknowledged and referenced.

For Section 1, portions of that section are based on a review (López, G. Y., Cummings, T. J., Bigner, D. D. and McLendon, R. E. 2011. Brain Tumours. eLS.). Permission was received from Wiley for use of the material for this thesis.

Appendix B

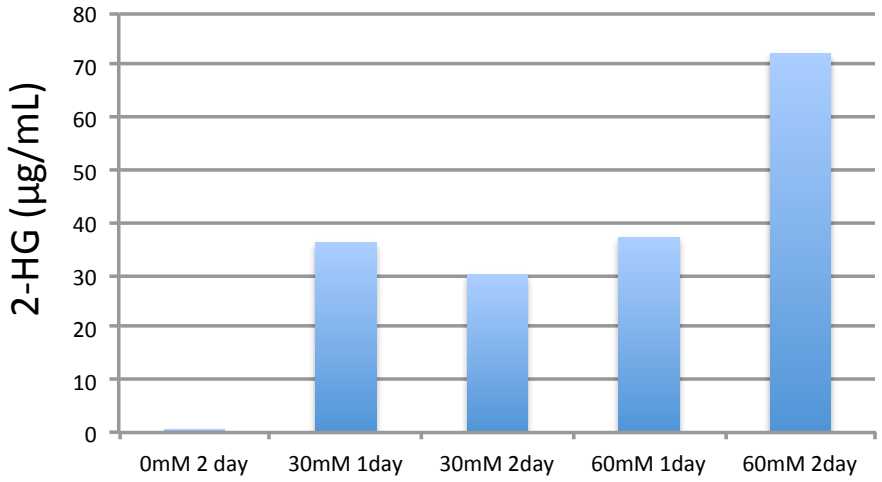

Figure B- 1: Measurable increase in 2-HG in cell lysates following exposure of wild-type mouse ES to 2-HG in cell culture media.

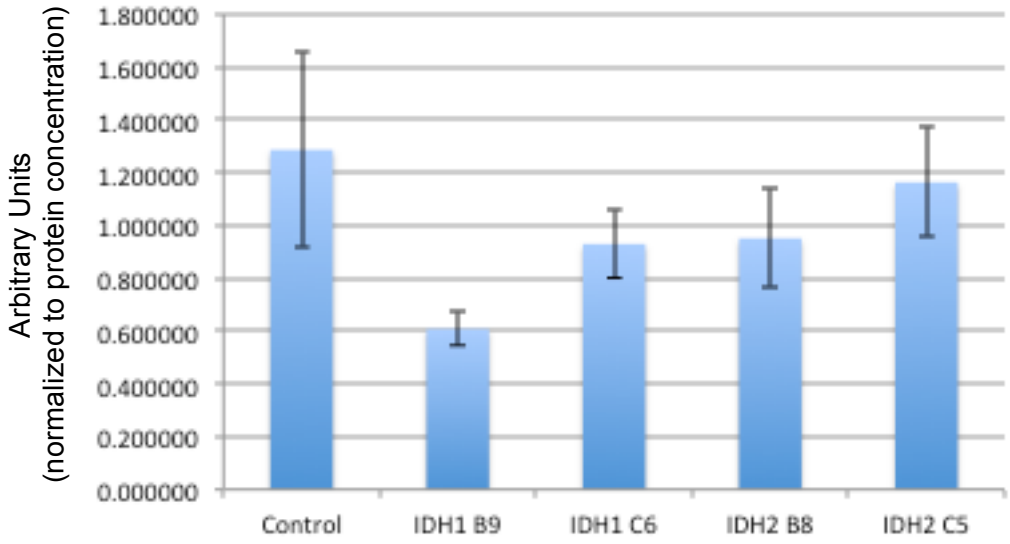

Figure B- 2: Glutamine is decreased in mouse ES cells with mutant IDH1/2. Each value represents measurements from five biological replicates. Error bars represent standard deviation. Difference from control only reached significance for IDH1 B9 at $P<0.05$

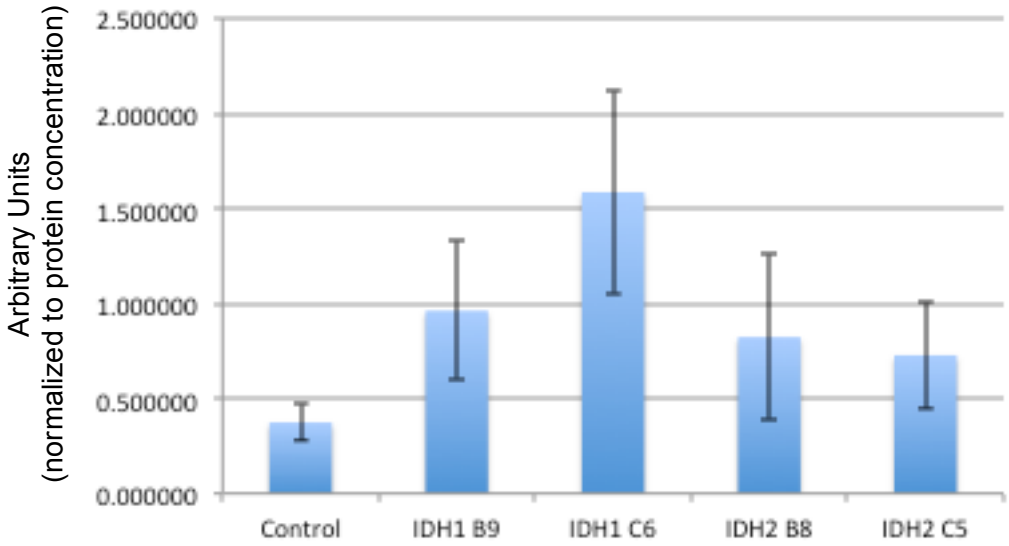

Figure B- 3: 2-aminobutyrate is increased in mouse ES cells with mutant IDH1/2. Each value represents measurements from five biological replicates. Error bars represent standard deviation. Difference from control was P<0.05 for IDH1 B9, IDH1 C6, and IDH2 C5.

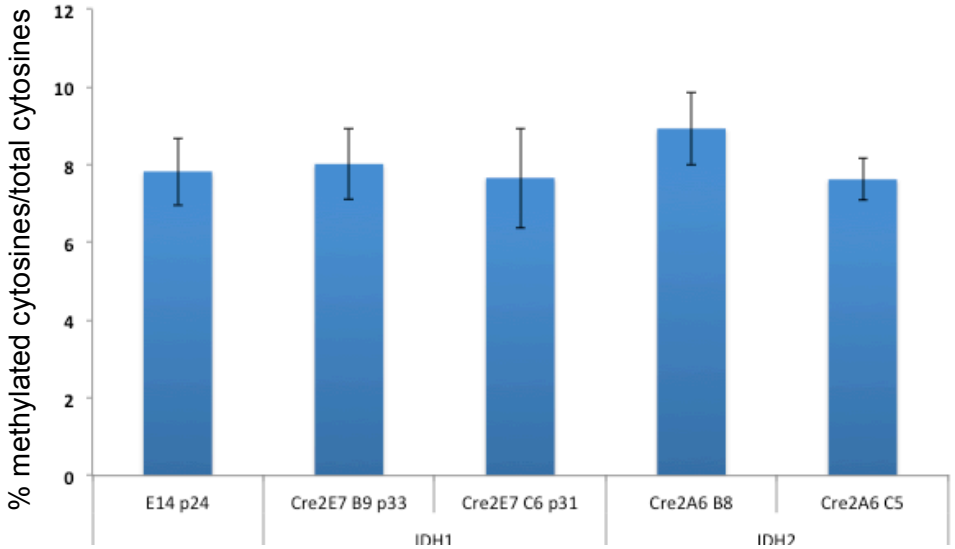

Figure B- 4: 5-methylcytosine is not significantly changed in mouse ES cells with mutant IDH1/2. Studies were completed in duplicate. Error bars represent standard deviation.

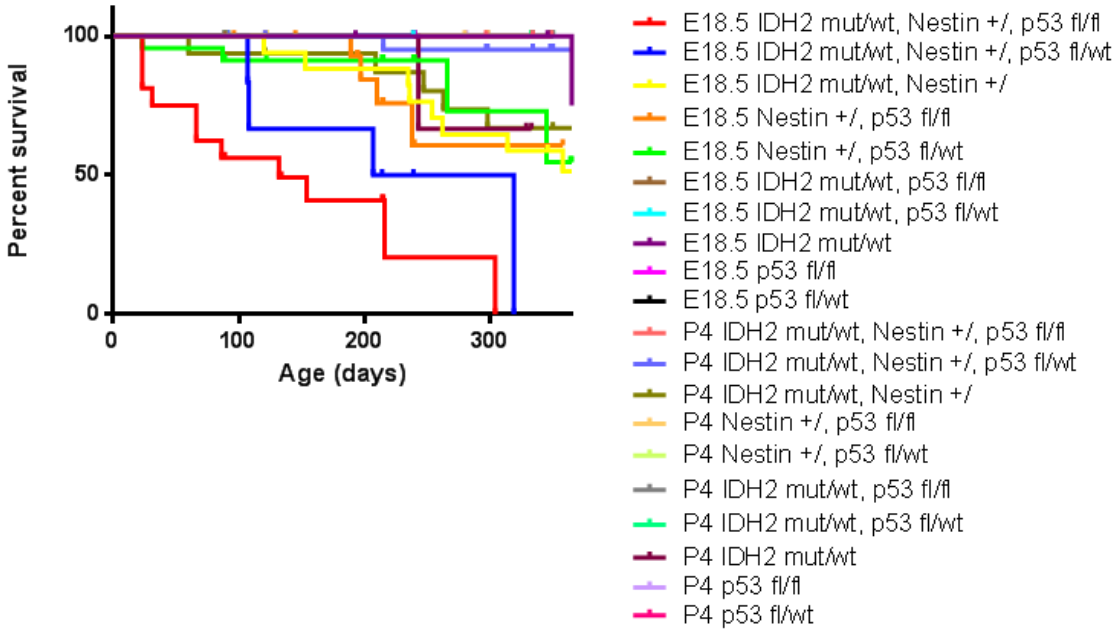

Figure B- 5: Survival among E18.5-treated and P4-week-treated mice.

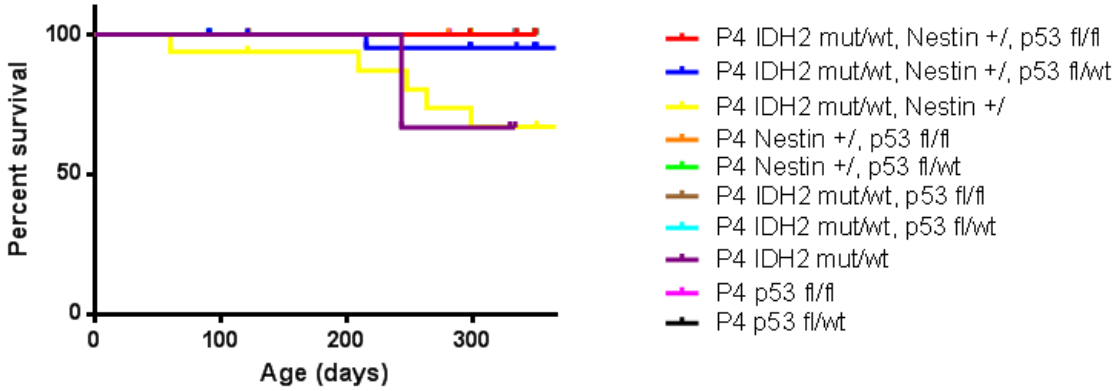

Figure B- 6: Survival in P4-week-treated mice.

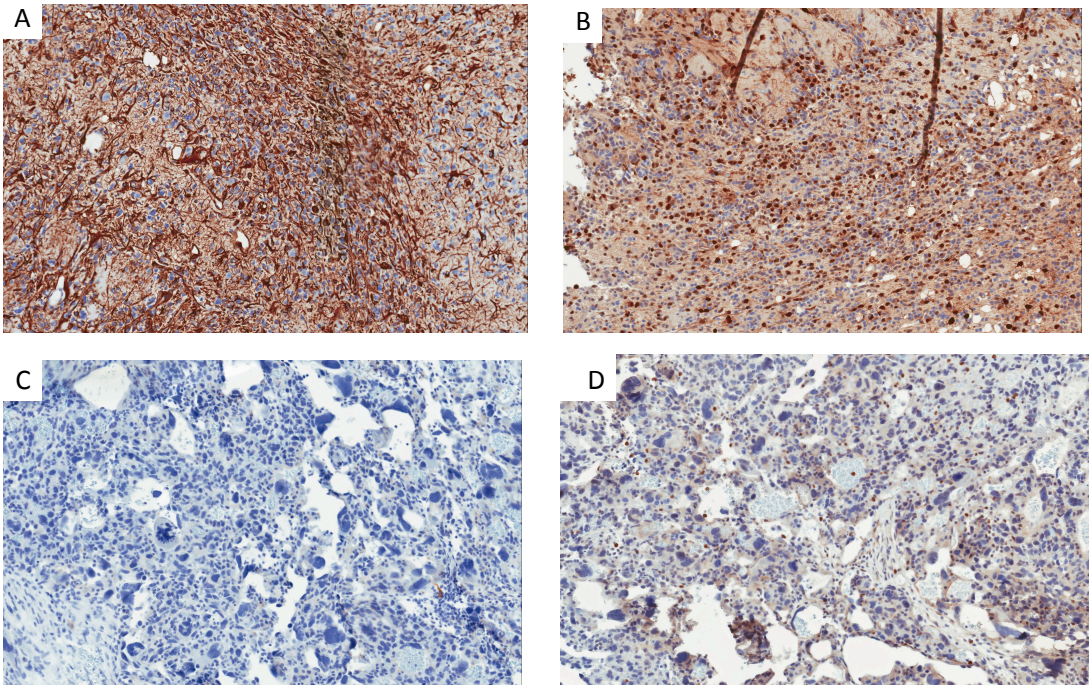

Figure B- 7: Immunohistochemistry on A,B) olfactory bulb tumor or C,D) flank tumor in E18.5-treated Nestin-CreER/IDH2$^{R172K/wt}$/p53$^{fl/fl}$ mouse. A,C) GFAP staining, B,D) S-100 staining.

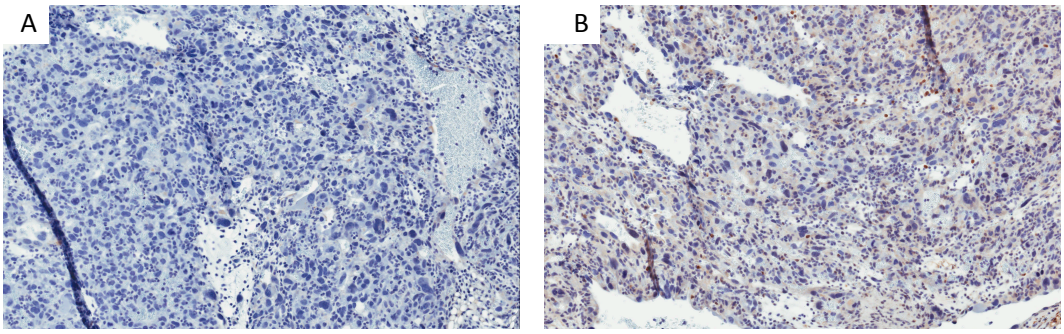

Figure B- 8: Immunohistochemical stains on flank tumor from E18.5-treated Nestin-CreER/IDH2$^{R172K/wt}$/p53$^{fl/fl}$ mouse. A) GFAP stain, B) S-100 stain.

Works Cited

1. Lopez, G.Y., *et al.* IDH1(R132) mutation identified in one human melanoma metastasis, but not correlated with metastases to the brain. *Biochemical and biophysical research communications* **398**, 585-587 (2010).

2. Koivunen, P., *et al.* Transformation by the (R)-enantiomer of 2-hydroxyglutarate linked to EGLN activation. *Nature* **483**, 484-488 (2012).

3. López, G.Y., Cummings, T.J., Bigner, D.D. & McLendon, R.E. Brain Tumours. in *eLS* (John Wiley & Sons, Ltd, 2011).

4. Louis, D.N., *et al.* The 2007 WHO classification of tumours of the central nervous system. *Acta neuropathologica* **114**, 97-109 (2007).

5. Bar, E.E., Lin, A., Tihan, T., Burger, P.C. & Eberhart, C.G. Frequent gains at chromosome 7q34 involving BRAF in pilocytic astrocytoma. *Journal of neuropathology and experimental neurology* **67**, 878-887 (2008).

6. Yu, J., *et al.* Alterations of BRAF and HIPK2 loci predominate in sporadic pilocytic astrocytoma. *Neurology* **73**, 1526-1531 (2009).

7. *WHO Classification of Tumours of the Central Nervous System*, (IARC, Lyon, 2007).

8. Ohgaki, H., *et al.* Genetic pathways to glioblastoma: a population-based study. *Cancer research* **64**, 6892-6899 (2004).

9. Nutt, C.L., *et al.* Gene expression-based classification of malignant gliomas correlates better with survival than histological classification. *Cancer research* **63**, 1602-1607 (2003).

10. Freije, W.A., *et al.* Gene expression profiling of gliomas strongly predicts survival. *Cancer research* **64**, 6503-6510 (2004).

11. Balss, J., *et al.* Analysis of the IDH1 codon 132 mutation in brain tumors. *Acta neuropathologica* **116**, 597-602 (2008).

12. Yan, H., *et al.* IDH1 and IDH2 Mutations in Gliomas. *New England Journal of Medicine* **360**, 765-773 (2009).

13. Ichimura, K., *et al.* IDH1 mutations are present in the majority of common adult gliomas but are rare in primary glioblastomas. *Neuro-oncology* (2009).

14. Korshunov, A., *et al.* Combined molecular analysis of BRAF and IDH1 distinguishes pilocytic astrocytoma from diffuse astrocytoma. *Acta neuropathologica* (2009).

15. Hartmann, C., *et al.* Type and frequency of IDH1 and IDH2 mutations are related to astrocytic and oligodendroglial differentiation and age: a study of 1,010 diffuse gliomas. *Acta neuropathologica* (2009).

16. Sanson, M., *et al.* Isocitrate Dehydrogenase 1 Codon 132 Mutation Is an Important Prognostic Biomarker in Gliomas. *J Clin Oncol* (2009).

17. Nobusawa, S., Watanabe, T., Kleihues, P. & Ohgaki, H. IDH1 mutations as molecular signature and predictive factor of secondary glioblastomas. *Clin Cancer Res* **15**, 6002-6007 (2009).

18. Sonoda, Y., *et al.* Analysis of IDH1 and IDH2 mutations in Japanese glioma patients. *Cancer science* **100**, 1996-1998 (2009).

19. Gravendeel, L.A., *et al.* Segregation of non-p.R132H mutations in IDH1 in distinct molecular subtypes of glioma. *Human mutation* **31**, E1186-1199 (2010).

20. Ichimura, K., *et al.* Deregulation of the p14ARF/MDM2/p53 pathway is a prerequisite for human astrocytic gliomas with G1-S transition control gene abnormalities. *Cancer research* **60**, 417-424 (2000).

21. Ichimura, K., Schmidt, E.E., Goike, H.M. & Collins, V.P. Human glioblastomas with no alterations of the CDKN2A (p16INK4A, MTS1) and CDK4 genes have frequent mutations of the retinoblastoma gene. *Oncogene* **13**, 1065-1072 (1996).

22. Schmidt, E.E., Ichimura, K., Reifenberger, G. & Collins, V.P. CDKN2 (p16/MTS1) gene deletion or CDK4 amplification occurs in the majority of glioblastomas. *Cancer research* **54**, 6321-6324 (1994).

23. Ueki, K., *et al.* CDKN2/p16 or RB alterations occur in the majority of glioblastomas and are inversely correlated. *Cancer research* **56**, 150-153 (1996).

24. The Cancer Genome Atlas Research, N. Comprehensive genomic characterization defines human glioblastoma genes and core pathways. *Nature* **455**, 1061-1068 (2008).

25. van den Boom, J., *et al.* Characterization of gene expression profiles associated with glioma progression using oligonucleotide-based microarray analysis and real-time reverse transcription-polymerase chain reaction. *The American journal of pathology* **163**, 1033-1043 (2003).

26. Henson, J.W., *et al.* The retinoblastoma gene is involved in malignant progression of astrocytomas. *Annals of neurology* **36**, 714-721 (1994).

27. Houillier, C., *et al.* Prognostic impact of molecular markers in a series of 220 primary glioblastomas. *Cancer* **106**, 2218-2223 (2006).

28. Korshunov, A., Sycheva, R. & Golanov, A. Genetically distinct and clinically relevant subtypes of glioblastoma defined by array-based comparative genomic hybridization (array-CGH). *Acta neuropathologica* **111**, 465-474 (2006).

29. Fults, D., Brockmeyer, D., Tullous, M.W., Pedone, C.A. & Cawthon, R.M. p53 mutation and loss of heterozygosity on chromosomes 17 and 10 during human astrocytoma progression. *Cancer research* **52**, 674-679 (1992).

30. Huang, H., *et al.* Gene expression profiling of low-grade diffuse astrocytomas by cDNA arrays. *Cancer research* **60**, 6868-6874 (2000).

31. Watanabe, K., *et al.* Overexpression of the EGF receptor and p53 mutations are mutually exclusive in the evolution of primary and secondary glioblastomas. *Brain pathology (Zurich, Switzerland)* **6**, 217-223; discussion 223-214 (1996).

32. Parsons, D.W., *et al.* An integrated genomic analysis of human glioblastoma multiforme. *Science (New York, N.Y* **321**, 1807-1812 (2008).

33. Hayashi, Y., *et al.* Association of EGFR gene amplification and CDKN2 (p16/MTS1) gene deletion in glioblastoma multiforme. *Brain pathology (Zurich, Switzerland)* **7**, 871-875 (1997).

34. Zheng, H., *et al.* p53 and Pten control neural and glioma stem/progenitor cell renewal and differentiation. *Nature* **455**, 1129-1133 (2008).

35. Schmidt, M.C., *et al.* Impact of genotype and morphology on the prognosis of glioblastoma. *Journal of neuropathology and experimental neurology* **61**, 321-328 (2002).

36. Hartmann, C., Bartels, G., Gehlhaar, C., Holtkamp, N. & von Deimling, A. PIK3CA mutations in glioblastoma multiforme. *Acta neuropathologica* **109**, 639-642 (2005).

37. Broderick, D.K., *et al.* Mutations of PIK3CA in anaplastic oligodendrogliomas, high-grade astrocytomas, and medulloblastomas. *Cancer research* **64**, 5048-5050 (2004).

38. Gallia, G.L., *et al.* PIK3CA gene mutations in pediatric and adult glioblastoma multiforme. *Mol Cancer Res* **4**, 709-714 (2006).

39. Mueller, W., *et al.* Mutations of the PIK3CA gene are rare in human glioblastoma. *Acta neuropathologica* **109**, 654-655 (2005).

40. Duerr, E.M., *et al.* PTEN mutations in gliomas and glioneuronal tumors. *Oncogene* **16**, 2259-2264 (1998).

41. Rasheed, B.K., *et al.* PTEN gene mutations are seen in high-grade but not in low-grade gliomas. *Cancer research* **57**, 4187-4190 (1997).

42. Heaphy, C.M., *et al.* Altered telomeres in tumors with ATRX and DAXX mutations. *Science (New York, N.Y* **333**, 425 (2011).

43. Jiao, Y., *et al.* Frequent ATRX, CIC, and FUBP1 mutations refine the classification of malignant gliomas. *Oncotarget* **3**, 709-722 (2012).

44. Liu, X.Y., *et al.* Frequent ATRX mutations and loss of expression in adult diffuse astrocytic tumors carrying IDH1/IDH2 and TP53 mutations. *Acta neuropathologica* (2012).

45. Schwartzentruber, J., *et al.* Driver mutations in histone H3.3 and chromatin remodelling genes in paediatric glioblastoma. *Nature* **482**, 226-231 (2012).

46. Martinho, O., *et al.* Expression, mutation and copy number analysis of platelet-derived growth factor receptor A (PDGFRA) and its ligand PDGFA in gliomas. *British journal of cancer* **101**, 973-982 (2009).

47. Lokker, N.A., Sullivan, C.M., Hollenbach, S.J., Israel, M.A. & Giese, N.A. Platelet-derived growth factor (PDGF) autocrine signaling regulates survival and mitogenic pathways in glioblastoma cells: evidence that the novel PDGF-C and PDGF-D ligands may play a role in the development of brain tumors. *Cancer research* **62**, 3729-3735 (2002).

48. Guha, A., Dashner, K., Black, P.M., Wagner, J.A. & Stiles, C.D. Expression of PDGF and PDGF receptors in human astrocytoma operation specimens supports the existence of an autocrine loop. *International journal of cancer* **60**, 168-173 (1995).

49. Varela, M., *et al.* EGF-R and PDGF-R, but not bcl-2, overexpression predict overall survival in patients with low-grade astrocytomas. *J Surg Oncol* **86**, 34-40 (2004).

50. Hermanson, M., *et al.* Platelet-derived growth factor and its receptors in human glioma tissue: expression of messenger RNA and protein suggests the presence of autocrine and paracrine loops. *Cancer research* **52**, 3213-3219 (1992).

51. Phillips, H.S., *et al.* Molecular subclasses of high-grade glioma predict prognosis, delineate a pattern of disease progression, and resemble stages in neurogenesis. *Cancer cell* **9**, 157-173 (2006).

52. Li, A., *et al.* Unsupervised analysis of transcriptomic profiles reveals six glioma subtypes. *Cancer research* **69**, 2091-2099 (2009).

53. Verhaak, R.G., *et al.* Integrated genomic analysis identifies clinically relevant subtypes of glioblastoma characterized by abnormalities in PDGFRA, IDH1, EGFR, and NF1. *Cancer cell* **17**, 98-110 (2010).

54. Reifenberger, G., Reifenberger, J., Ichimura, K., Meltzer, P.S. & Collins, V.P. Amplification of multiple genes from chromosomal region 12q13-14 in human malignant gliomas: preliminary mapping of the amplicons shows preferential involvement of CDK4, SAS, and MDM2. *Cancer research* **54**, 4299-4303 (1994).

55. Bigner, S.H., *et al.* Molecular genetic aspects of oligodendrogliomas including analysis by comparative genomic hybridization. *The American journal of pathology* **155**, 375-386 (1999).

56. Smith, J.S., *et al.* Alterations of chromosome arms 1p and 19q as predictors of survival in oligodendrogliomas, astrocytomas, and mixed oligoastrocytomas. *J Clin Oncol* **18**, 636-645 (2000).

57. Jenkins, R.B., *et al.* A t(1;19)(q10;p10) mediates the combined deletions of 1p and 19q and predicts a better prognosis of patients with oligodendroglioma. *Cancer research* **66**, 9852-9861 (2006).

58. Bettegowda, C., *et al.* Mutations in CIC and FUBP1 contribute to human oligodendroglioma. *Science (New York, N.Y* **333**, 1453-1455 (2011).

59. Sahm, F., *et al.* CIC and FUBP1 mutations in oligodendrogliomas, oligoastrocytomas and astrocytomas. *Acta neuropathologica* **123**, 853-860 (2012).

60. Yip, S., *et al.* Concurrent CIC mutations, IDH mutations, and 1p/19q loss distinguish oligodendrogliomas from other cancers. *The Journal of pathology* (2011).

61. Roch, F., Jimenez, G. & Casanova, J. EGFR signalling inhibits Capicua-dependent repression during specification of Drosophila wing veins. *Development* **129**, 993-1002 (2002).

62. Ajuria, L., *et al.* Capicua DNA-binding sites are general response elements for RTK signaling in Drosophila. *Development* **138**, 915-924 (2011).

63. Hsiao, H.H., *et al.* Quantitative characterization of the interactions among c-myc transcriptional regulators FUSE, FBP, and FIR. *Biochemistry* **49**, 4620-4634 (2010).

64. de Wilde, R.F., *et al.* Loss of ATRX or DAXX expression and concomitant acquisition of the alternative lengthening of telomeres phenotype are late events in a small subset of MEN-1 syndrome pancreatic neuroendocrine tumors. *Mod Pathol* **25**, 1033-1039 (2012).

65. Sasaki, H., *et al.* PTEN is a target of chromosome 10q loss in anaplastic oligodendrogliomas and PTEN alterations are associated with poor prognosis. *The American journal of pathology* **159**, 359-367 (2001).

66. Hede, S.M., *et al.* GFAP promoter driven transgenic expression of PDGFB in the mouse brain leads to glioblastoma in a Trp53 null background. *Glia* (2008).

67. Donehower, L.A., *et al.* Mice deficient for p53 are developmentally normal but susceptible to spontaneous tumours. *Nature* **356**, 215-221 (1992).

68. Hesselager, G., Uhrbom, L., Westermark, B. & Nister, M. Complementary effects of platelet-derived growth factor autocrine stimulation and p53 or Ink4a-Arf deletion in a mouse glioma model. *Cancer research* **63**, 4305-4309 (2003).

69. Assanah, M., *et al.* Glial progenitors in adult white matter are driven to form malignant gliomas by platelet-derived growth factor-expressing retroviruses. *J Neurosci* **26**, 6781-6790 (2006).

70. Reilly, K.M., Loisel, D.A., Bronson, R.T., McLaughlin, M.E. & Jacks, T. Nf1;Trp53 mutant mice develop glioblastoma with evidence of strain-specific effects. *Nature genetics* **26**, 109-113 (2000).

71. Zhu, Y., *et al.* Early inactivation of p53 tumor suppressor gene cooperating with NF1 loss induces malignant astrocytoma. *Cancer cell* **8**, 119-130 (2005).

72. Kwon, C.H., *et al.* Pten haploinsufficiency accelerates formation of high-grade astrocytomas. *Cancer research* **68**, 3286-3294 (2008).

73. Kang, M.R., *et al.* Mutational analysis of IDH1 codon 132 in glioblastomas and other common cancers. *International journal of cancer* **125**, 353-355 (2009).

74. Watanabe, T., Nobusawa, S., Kleihues, P. & Ohgaki, H. IDH1 mutations are early events in the development of astrocytomas and oligodendrogliomas. *The American journal of pathology* **174**, 1149-1153 (2009).

75. Geisbrecht, B.V. & Gould, S.J. The human PICD gene encodes a cytoplasmic and peroxisomal NADP(+)-dependent isocitrate dehydrogenase. *The Journal of biological chemistry* **274**, 30527-30533 (1999).

76. Henke, B., Girzalsky, W., Berteaux-Lecellier, V. & Erdmann, R. IDP3 encodes a peroxisomal NADP-dependent isocitrate dehydrogenase required for the beta-oxidation of unsaturated fatty acids. *The Journal of biological chemistry* **273**, 3702-3711 (1998).

77. Yoshihara, T., *et al.* Localization of cytosolic NADP-dependent isocitrate dehydrogenase in the peroxisomes of rat liver cells: biochemical and immunocytochemical studies. *J Histochem Cytochem* **49**, 1123-1131 (2001).

78. Nekrutenko, A., Hillis, D.M., Patton, J.C., Bradley, R.D. & Baker, R.J. Cytosolic isocitrate dehydrogenase in humans, mice, and voles and phylogenetic analysis of the enzyme family. *Molecular biology and evolution* **15**, 1674-1684 (1998).

79. Ceccarelli, C., Grodsky, N.B., Ariyaratne, N., Colman, R.F. & Bahnson, B.J. Crystal structure of porcine mitochondrial NADP+-dependent isocitrate dehydrogenase complexed with Mn2+ and isocitrate. Insights into the enzyme mechanism. *The Journal of biological chemistry* **277**, 43454-43462 (2002).

80. Dean, A.M. & Koshland, D.E., Jr. Kinetic mechanism of Escherichia coli isocitrate dehydrogenase. *Biochemistry* **32**, 9302-9309 (1993).

81. Xu, X., *et al.* Structures of human cytosolic NADP-dependent isocitrate dehydrogenase reveal a novel self-regulatory mechanism of activity. *The Journal of biological chemistry* **279**, 33946-33957 (2004).

82. Zhao, S., *et al.* Glioma-derived mutations in IDH1 dominantly inhibit IDH1 catalytic activity and induce HIF-1alpha. *Science (New York, N.Y* **324**, 261-265 (2009).

83. Ward, P.S., *et al.* The common feature of leukemia-associated IDH1 and IDH2 mutations is a neomorphic enzyme activity converting alpha-ketoglutarate to 2-hydroxyglutarate. *Cancer cell* **17**, 225-234 (2010).

84. Kil, I.S., Kim, S.Y., Lee, S.J. & Park, J.W. Small interfering RNA-mediated silencing of mitochondrial NADP+-dependent isocitrate dehydrogenase enhances the sensitivity of HeLa cells toward tumor necrosis factor-alpha and anticancer drugs. *Free radical biology & medicine* **43**, 1197-1207 (2007).

85. Dang, L., *et al.* Cancer-associated IDH1 mutations produce 2-hydroxyglutarate. *Nature* **462**, 739-744 (2009).

86. Mardis, E.R., *et al.* Recurring mutations found by sequencing an acute myeloid leukemia genome. *The New England journal of medicine* **361**, 1058-1066 (2009).

87. Figueroa, M.E., *et al.* Leukemic IDH1 and IDH2 mutations result in a hypermethylation phenotype, disrupt TET2 function, and impair hematopoietic differentiation. *Cancer cell* **18**, 553-567 (2010).

88. Sasaki, M., *et al.* IDH1(R132H) mutation increases murine haematopoietic progenitors and alters epigenetics. *Nature* **488**, 656-659 (2012).

89. Amary, M.F., *et al.* Ollier disease and Maffucci syndrome are caused by somatic mosaic mutations of IDH1 and IDH2. *Nature genetics* (2011).

90. Andrulis, M., *et al.* Detection of isocitrate dehydrogenase 1 mutation R132H in myelodysplastic syndrome by mutation-specific antibody and direct sequencing. *Leukemia research* **34**, 1091-1093 (2010).

91. Makishima, H., *et al.* CBL, CBLB, TET2, ASXL1, and IDH1/2 mutations and additional chromosomal aberrations constitute molecular events in chronic myelogenous leukemia. *Blood* **117**, e198-206 (2011).

92. Sjoblom, T., *et al.* The consensus coding sequences of human breast and colorectal cancers. *Science (New York, N.Y* **314**, 268-274 (2006).

93. Ang, D., *et al.* Biphasic Papillary and Lobular Breast Carcinoma With PIK3CA and IDH1 Mutations. *Diagn Mol Pathol* (2012).

94. Gaal, J., *et al.* Isocitrate dehydrogenase mutations are rare in pheochromocytomas and paragangliomas. *J Clin Endocrinol Metab* **95**, 1274-1278 (2010).

95. Minard, K.I. & McAlister-Henn, L. Dependence of peroxisomal beta-oxidation on cytosolic sources of NADPH. *The Journal of biological chemistry* **274**, 3402-3406 (1999).

96. Lee, S.M., *et al.* Cytosolic NADP(+)-dependent isocitrate dehydrogenase status modulates oxidative damage to cells. *Free radical biology & medicine* **32**, 1185-1196 (2002).

97. Ying, W. NAD+/NADH and NADP+/NADPH in cellular functions and cell death: regulation and biological consequences. *Antioxidants & redox signaling* **10**, 179-206 (2008).

98. Holmgren, A. Thioredoxin. *Annual review of biochemistry* **54**, 237-271 (1985).

99. Nakamura, H. Thioredoxin and its related molecules: update 2005. *Antioxidants & redox signaling* **7**, 823-828 (2005).

100. Ballatori, N., *et al.* Glutathione dysregulation and the etiology and progression of human diseases. *Biological chemistry* **390**, 191-214 (2009).

101. Kim, S.Y. & Park, J.W. Cellular defense against singlet oxygen-induced oxidative damage by cytosolic NADP+-dependent isocitrate dehydrogenase. *Free radical research* **37**, 309-316 (2003).

102. Kim, S.Y., *et al.* Regulation of singlet oxygen-induced apoptosis by cytosolic NADP+-dependent isocitrate dehydrogenase. *Molecular and cellular biochemistry* **302**, 27-34 (2007).

103. Maeng, O., *et al.* Cytosolic NADP(+)-dependent isocitrate dehydrogenase protects macrophages from LPS-induced nitric oxide and reactive oxygen species. *Biochemical and biophysical research communications* **317**, 558-564 (2004).

104. Lee, S.H., *et al.* Role of NADP+-dependent isocitrate dehydrogenase (NADP+-ICDH) on cellular defence against oxidative injury by gamma-rays. *International journal of radiation biology* **80**, 635-642 (2004).

105. Latini, A., *et al.* Mitochondrial energy metabolism is markedly impaired by D-2-hydroxyglutaric acid in rat tissues. *Mol Genet Metab* **86**, 188-199 (2005).

106. Xu, W., *et al.* Oncometabolite 2-hydroxyglutarate is a competitive inhibitor of alpha-ketoglutarate-dependent dioxygenases. *Cancer cell* **19**, 17-30 (2011).

107. Iyer, L.M., Tahiliani, M., Rao, A. & Aravind, L. Prediction of novel families of enzymes involved in oxidative and other complex modifications of bases in nucleic acids. *Cell cycle (Georgetown, Tex* **8**, 1698-1710 (2009).

108. Tahiliani, M., *et al.* Conversion of 5-methylcytosine to 5-hydroxymethylcytosine in mammalian DNA by MLL partner TET1. *Science (New York, N.Y* **324**, 930-935 (2009).

109. Christensen, B.C., *et al.* DNA methylation, isocitrate dehydrogenase mutation, and survival in glioma. *Journal of the National Cancer Institute* **103**, 143-153 (2011).

110. Noushmehr, H., *et al.* Identification of a CpG island methylator phenotype that defines a distinct subgroup of glioma. *Cancer cell* **17**, 510-522 (2010).

111. Chou, A.P., *et al.* Identification of Retinol Binding Protein 1 Promoter Hypermethylation in Isocitrate Dehydrogenase 1 and 2 Mutant Gliomas. *Journal of the National Cancer Institute* (2012).

112. Hartmann, C., *et al.* Patients with IDH1 wild type anaplastic astrocytomas exhibit worse prognosis than IDH1-mutated glioblastomas, and IDH1 mutation status accounts for the unfavorable prognostic effect of higher age: implications for classification of gliomas. *Acta neuropathologica* **120**, 707-718 (2010).

113. Mulholland, S., *et al.* MGMT CpG island is invariably methylated in adult astrocytic and oligodendroglial tumors with IDH1 or IDH2 mutations. *International journal of cancer* **131**, 1104-1113 (2012).

114. Nakamura, M., Watanabe, T., Yonekawa, Y., Kleihues, P. & Ohgaki, H. Promoter methylation of the DNA repair gene MGMT in astrocytomas is frequently associated with G:C --> A:T mutations of the TP53 tumor suppressor gene. *Carcinogenesis* **22**, 1715-1719 (2001).

115. Pastor, W.A., *et al.* Genome-wide mapping of 5-hydroxymethylcytosine in embryonic stem cells. *Nature* **473**, 394-397 (2011).

116. Ficz, G., *et al.* Dynamic regulation of 5-hydroxymethylcytosine in mouse ES cells and during differentiation. *Nature* (2011).

117. Ito, S., *et al.* Role of Tet proteins in 5mC to 5hmC conversion, ES-cell self-renewal and inner cell mass specification. *Nature* **466**, 1129-1133 (2010).

118. Majmundar, A.J., Wong, W.J. & Simon, M.C. Hypoxia-inducible factors and the response to hypoxic stress. *Mol Cell* **40**, 294-309 (2010).

119. Mailloux, R.J., Puiseux-Dao, S. & Appanna, V.D. Alpha-ketoglutarate abrogates the nuclear localization of HIF-1alpha in aluminum-exposed hepatocytes. *Biochimie* **91**, 408-415 (2009).

120. Williams, S.C., *et al.* R132H-mutation of isocitrate dehydrogenase-1 is not sufficient for HIF-1alpha upregulation in adult glioma. *Acta neuropathologica* **121**, 279-281 (2011).

121. Sasaki, M., *et al.* D-2-hydroxyglutarate produced by mutant IDH1 perturbs collagen maturation and basement membrane function. *Genes & development* **26**, 2038-2049 (2012).

122. Bajenaru, M.L., *et al.* Astrocyte-specific inactivation of the neurofibromatosis 1 gene (NF1) is insufficient for astrocytoma formation. *Molecular and cellular biology* **22**, 5100-5113 (2002).

123. Sugita, K., *et al.* Clinical and MRI findings in a case of D-2-hydroxyglutaric aciduria. *Brain Dev* **17**, 139-141; discussion 144-135 (1995).

124. Nyhan, W.L., *et al.* D-2-hydroxyglutaric aciduria. *J Child Neurol* **10**, 137-142 (1995).

125. Amiel, J., *et al.* Facial anomalies in D-2-hydroxyglutaric aciduria. *Am J Med Genet* **86**, 124-129 (1999).

126. Eeg-Olofsson, O., Zhang, W.W., Olsson, Y., Jagell, S. & Hagenfeldt, L. D-2-hydroxyglutaric aciduria with cerebral, vascular, and muscular abnormalities in a 14-year-old boy. *J Child Neurol* **15**, 488-492 (2000).

127. Struys, E.A., *et al.* Mutations in phenotypically mild D-2-hydroxyglutaric aciduria. *Annals of neurology* **58**, 626-630 (2005).

128. Struys, E.A., *et al.* Mutations in the D-2-hydroxyglutarate dehydrogenase gene cause D-2-hydroxyglutaric aciduria. *American journal of human genetics* **76**, 358-360 (2005).

129. Baker, N.S., *et al.* D-2-hydroxyglutaric aciduria: hypotonia, cortical blindness, seizures, cardiomyopathy, and cylindrical spirals in skeletal muscle. *J Child Neurol* **12**, 31-36 (1997).

130. Kolker, S., *et al.* NMDA receptor activation and respiratory chain complex V inhibition contribute to neurodegeneration in d-2-hydroxyglutaric aciduria. *The European journal of neuroscience* **16**, 21-28 (2002).

131. Patay, Z., *et al.* Cerebral neoplasms in L-2 hydroxyglutaric aciduria: 3 new cases and meta-analysis of literature data. *AJNR. American journal of neuroradiology* **33**, 940-943 (2012).

132. Matsunaga, H., *et al.* IDH1 and IDH2 have critical roles in 2-hydroxyglutarate production in D-2-hydroxyglutarate dehydrogenase depleted cells. *Biochemical and biophysical research communications* **423**, 553-556 (2012).

133. Kranendijk, M., *et al.* IDH2 mutations in patients with D-2-hydroxyglutaric aciduria. *Science (New York, N.Y* **330**, 336 (2010).

134. Kranendijk, M., *et al.* Evidence for genetic heterogeneity in D-2-hydroxyglutaric aciduria. *Human mutation* **31**, 279-283 (2010).

135. Ibrahim, N. & Haluska, F.G. Molecular pathogenesis of cutaneous melanocytic neoplasms. *Annual review of pathology* **4**, 551-579 (2009).

136. Bleeker, F.E., *et al.* IDH1 mutations at residue p.R132 (IDH1(R132)) occur frequently in high-grade gliomas but not in other solid tumors. *Human mutation* **30**, 7-11 (2009).

137. Wan, P.T., *et al.* Mechanism of activation of the RAF-ERK signaling pathway by oncogenic mutations of B-RAF. *Cell* **116**, 855-867 (2004).

138. Dhomen, N., *et al.* Oncogenic Braf induces melanocyte senescence and melanoma in mice. *Cancer cell* **15**, 294-303 (2009).

139. Amary, M.F., *et al.* IDH1 and IDH2 mutations are frequent events in central chondrosarcoma and central and periosteal chondromas but not in other mesenchymal tumours. *The Journal of pathology* **224**, 334-343 (2011).

140. Warburg, O., Wind, F. & Negelein, E. The Metabolism of Tumors in the Body. *The Journal of general physiology* **8**, 519-530 (1927).

141. Vander Heiden, M.G., Cantley, L.C. & Thompson, C.B. Understanding the Warburg effect: the metabolic requirements of cell proliferation. *Science (New York, N.Y* **324**, 1029-1033 (2009).

142. Thompson, C. Metabolic Enzymes as Oncogenes or Tumor Suppressors. *New England Journal of Medicine* **360**, 813-815 (2009).

143. DeBerardinis, R.J., *et al.* Beyond aerobic glycolysis: transformed cells can engage in glutamine metabolism that exceeds the requirement for protein and nucleotide synthesis. *Proceedings of the National Academy of Sciences of the United States of America* **104**, 19345-19350 (2007).

144. Meissner, A., *et al.* Genome-scale DNA methylation maps of pluripotent and differentiated cells. *Nature* **454**, 766-770 (2008).

145. Jin, G., *et al.* 2-hydroxyglutarate production, but not dominant negative function, is conferred by glioma-derived NADP-dependent isocitrate dehydrogenase mutations. *PLoS One* **6**, e16812 (2011).

146. Struys, E.A., Jansen, E.E., Verhoeven, N.M. & Jakobs, C. Measurement of urinary D- and L-2-hydroxyglutarate enantiomers by stable-isotope-dilution liquid chromatography-tandem mass spectrometry after derivatization with diacetyl-L-tartaric anhydride. *Clin Chem* **50**, 1391-1395 (2004).

147. Lawton, K.A., *et al.* Analysis of the adult human plasma metabolome. *Pharmacogenomics* **9**, 383-397 (2008).

148. Ryals, J., Lawton, K., Stevens, D. & Milburn, M. Metabolon, Inc. *Pharmacogenomics* **8**, 863-866 (2007).

149. Evans, A.M., DeHaven, C.D., Barrett, T., Mitchell, M. & Milgram, E. Integrated, nontargeted ultrahigh performance liquid chromatography/electrospray ionization tandem mass spectrometry platform for the identification and relative quantification of the small-molecule complement of biological systems. *Anal Chem* **81**, 6656-6667 (2009).

150. Reitman, Z.J., *et al.* Profiling the effects of isocitrate dehydrogenase 1 and 2 mutations on the cellular metabolome. *Proceedings of the National Academy of Sciences of the United States of America* **108**, 3270-3275 (2011).

151. Duncan, C.G., *et al.* A heterozygous IDH1R132H/WT mutation induces genome-wide alterations in DNA methylation. *Genome research* (2012).

152. Song, C.X., *et al.* Selective chemical labeling reveals the genome-wide distribution of 5-hydroxymethylcytosine. *Nat Biotechnol* **29**, 68-72 (2011).

153. Soga, T., *et al.* Differential metabolomics reveals ophthalmic acid as an oxidative stress biomarker indicating hepatic glutathione consumption. *The Journal of biological chemistry* **281**, 16768-16776 (2006).

154. Abbas, R., *et al.* The dynamics of glutathione species and ophthalmate concentrations in plasma from the VX2 rabbit model of secondary liver tumors. *HPB Surg* **2011**, 709052 (2011).

155. Andres Ibarra, R., *et al.* Disturbances in the glutathione/ophthalmate redox buffer system in the woodchuck model of hepatitis virus-induced hepatocellular carcinoma. *HPB Surg* **2011**, 789323 (2011).

156. Latini, A., *et al.* D-2-hydroxyglutaric acid induces oxidative stress in cerebral cortex of young rats. *The European journal of neuroscience* **17**, 2017-2022 (2003).

157. Chowdhury, R., *et al.* The oncometabolite 2-hydroxyglutarate inhibits histone lysine demethylases. *EMBO Rep* **12**, 463-469 (2011).

158. Blouw, B., *et al.* The hypoxic response of tumors is dependent on their microenvironment. *Cancer cell* **4**, 133-146 (2003).

159. Ko, M., *et al.* Impaired hydroxylation of 5-methylcytosine in myeloid cancers with mutant TET2. *Nature* **468**, 839-843 (2010).

160. Orr, B.A., Haffner, M.C., Nelson, W.G., Yegnasubramanian, S. & Eberhart, C.G. Decreased 5-hydroxymethylcytosine is associated with neural progenitor phenotype in normal brain and shorter survival in malignant glioma. *PLoS One* **7**, e41036 (2012).

161. Balordi, F. & Fishell, G. Mosaic removal of hedgehog signaling in the adult SVZ reveals that the residual wild-type stem cells have a limited capacity for self-renewal. *J Neurosci* **27**, 14248-14259 (2007).

162. Burns, K.A., Murphy, B., Danzer, S.C. & Kuan, C.Y. Developmental and post-injury cortical gliogenesis: a genetic fate-mapping study with Nestin-CreER mice. *Glia* **57**, 1115-1129 (2009).

163. Kranendijk, M., Struys, E.A., Salomons, G.S., Van der Knaap, M.S. & Jakobs, C. Progress in understanding 2-hydroxyglutaric acidurias. *J Inherit Metab Dis* **35**, 571-587 (2012).

164. Lagace, D.C., *et al.* Dynamic contribution of nestin-expressing stem cells to adult neurogenesis. *J Neurosci* **27**, 12623-12629 (2007).

165. Jacques, T.S., *et al.* Combinations of genetic mutations in the adult neural stem cell compartment determine brain tumour phenotypes. *The EMBO journal* **29**, 222-235 (2010).

166. Alcantara Llaguno, S., *et al.* Malignant astrocytomas originate from neural stem/progenitor cells in a somatic tumor suppressor mouse model. *Cancer cell* **15**, 45-56 (2009).

167. Chow, L.M., Zhang, J. & Baker, S.J. Inducible Cre recombinase activity in mouse mature astrocytes and adult neural precursor cells. *Transgenic Res* **17**, 919-928 (2008).

168. Lai, A., *et al.* Evidence for Sequenced Molecular Evolution of IDH1 Mutant Glioblastoma From a Distinct Cell of Origin. *J Clin Oncol* (2011).

Biography

Giselle Yvette López was born in Clinton, Maryland, on May 18, 1983. She graduated from the University of Maryland-College Park in May 2005 with a Bachelor of Science in Physiology and Neurobiology with High Honors in Biochemistry, and a Bachelor of Arts in Spanish Language and Literature with Honors in Spanish. She entered the Medical Scientist Training Program at Duke University in 2005. In 2007 she joined the Cell and Molecular Biology Program as a graduate student, and in 2008 she joined the Department of Pathology as a graduate student and formally joined the lab of Hai Yan. From 2006-2007 she served on the North Carolina Medical Society's Ethical and Judicial Affairs Committee. Giselle is an Associate Member of the American Association for Cancer Research (AACR). In 2011 she was named an AACR Minority Scholar in Cancer Research. She has served as a delegate at state-level and national-level medical society meetings. She has presented abstracts at two national scientific conferences.

Caldovic L, Morizono H, Panglao MG, **López GY**, Shi D, Summar ML, Tuchman M. Late onset N-acetylglutamate synthase deficiency caused by hypomorphic alleles. *Hum Mutat*. 2005;25:293-298.

Caldovic L, **López GY**, Haskins N, Panglao M, Shi D, Morizono H, Tuchman M. Biochemical properties of recombinant human and mouse N-acetylglutamate synthase. *Mol Genet Metab*. 2006;87:226-232.

Degan S, **López GY**, Kevill K, Sunday ME. Gastrin-releasing peptide, immune responses, and lung disease. *Ann NY Acad Sci*. 2008;1144:136-147.

López GY, Reitman ZJ, Solomon D, Waldman T, Bigner DD, McLendon R, Rosenberg SA, Samuels Y, Yan H. IDH1 mutation identified in one human melanoma metastasis, but not correlated with metastases to the brain. *Biochem Biophys Res Commun*. 2010;298:585-587.

López GY, Cummings TJ, Bigner DD, McLendon RE. Brain Tumours. In: Encyclopedia of Life Sciences. John Wiley & Sons, Ltd: Chichester. DOI: 10.1002/9780470015902.a0006111.pub2. March 2011.

Guo C, Pirozzi CJ, **López GY**, Yan H. Isocitrate dehydrogenase mutations in gliomas: mechanisms, biomarkers, and therapeutic target. *Curr Opin Neurol*. 2011;24:648-652.

Koivunen P, Lee S, Duncan CG, **López G**, Lu G, Ramkissoon S, Losman JA, Joensuu P, Bergmann U, Gross S, Travins J, Weiss S, Looper R, Ligon KL, Verhaak RGW, Yan H, Kaelin WG. Transformation by the (*R*)-enantiomer of 2-hydroxyglutarate linked to EGLN activation. *Nature*. 2012; 483(7390):484-488.

Heibel SK, **Lopez GY**, Panglao M, Sodha S, Mariño-Ramírez L, Tuchman M, Caldovic L. Transcriptional regulation of N-acetylglutamate synthase. *PLoS One*. 2012;7(2):e29527. Epub 2012 Feb 27.

Jiao Y, Killela PJ, Reitman ZJ, Rasheed AB, Heaphy CM, de Wilde RF, Rodriguez FJ, Rosemberg S, Oba-Shinjo SM, Marie SK, Bettegowda C, Agrawal N, Lipp E, Pirozzi C, **Lopez G**, He Y, Friedman H, Friedman AH, Riggins GJ, Holdhoff M, Burger P, McLendon R, Bigner DD, Vogelstein BK, Meeker AK, Kinzler KW, Papadopoulos N, Diaz LA, Yan H. Frequent ATRX, CIC, and FUBP1 mutations refine the classification of malignant gliomas. *Oncotarget*. 2012; 3(7):709-722.

Jin G, Pirozzi CJ, Chen LH, **Lopez GY**, Duncan CG, Feng J, Spasojevic I, Bigner DD, He Y, Yan H. Mutant IDH1 is required for IDH1 mutated tumor cell growth. *Oncotarget*. 2012;3(8):774-782.

López GY, Samsky M, Jones R, Adamson DC, Yan HY. Brain cancers. *Systems Biology of Cancer*, Sam Thiagalingam, Ed. Cambridge University Press. In press, 2012.